2006

STATISTICAL MODELS AND ANALYSIS TECHNIQUES FOR LEARNING IN RELATIONAL DATA

Jennifer Neville
University of Massachusetts Amherst

STATISTICAL MODELS AND ANALYSIS TECHNIQUES FOR LEARNING IN RELATIONAL DATA

A Dissertation Presented

by

JENNIFER NEVILLE

Submitted to the Graduate School of the
University of Massachusetts Amherst in partial fulfillment
of the requirements for the degree of

DOCTOR OF PHILOSOPHY

September 2006

Computer Science

STATISTICAL MODELS AND ANALYSIS TECHNIQUES FOR LEARNING IN RELATIONAL DATA

A Dissertation Presented

by

JENNIFER NEVILLE

Approved as to style and content by:

David Jensen, Chair

Andrew Barto, Member

Andrew McCallum, Member

Foster Provost, Member

John Staudenmayer, Member

W. Bruce Croft, Department Chair
Computer Science

To the one who didn't see the beginning, the one who didn't see the end, and the one who was there for me throughout.

ACKNOWLEDGMENTS

First, I would like to express my deepest gratitude to my advisor, David Jensen. I cannot thank him enough for introducing me to the exciting world of research—it certainly has changed my life. Working with David has always been a delightful, rewarding experience. He provided a research environment in which I could thrive—where the pursuit of discovery was fostered through collaborative exploration rather than competitive isolation. During my tenure at UMass, David has imparted innumerable lessons, ranging from invaluable advice on the intangible art of science, to practical instruction on research, writing, and presentation, to insightful guidance on academia and politics. Without his support, encouragement, and tutelage, I would certainly not be where I am today. He is more than just a great advisor, he is a friend, and that combination has made the past six years seem more like six months. It's hard to believe it's coming to an end.

I would also like to thank the other members of my committee: Andy Barto, Andrew McCallum, Foster Provost, and John Staudenmayer. Their helpful comments and technical guidance facilitated the process, especially in light of my simultaneous two-body search. Moreover, I greatly appreciate the assistance that Foster and Andrew have offered throughout the years, even before I started my thesis. Exposure to their supplementary views helped to broaden and deepen my sense of research and academia in general and statistical relational learning in particular.

During my internship at AT&T Labs, working with Daryl Pregibon and Chris Volinsky, I developed an appreciation for real-world applications and massive datasets. This interest underlies much of the work in this thesis, in that efficient algorithms and understandable models are two key components of applied data mining research.

In addition, Daryl and Chris have been wonderful mentors, both officially and unofficially. Daryl cultivated my interdisciplinary nature—as he continually questioned the modeling choices of computer scientists and the computation choices of statisticians. I hope to live up to his example as I start my joint appointment in CS and Statistics and I will always think of him when I can't remember what temporary data is stored in my files named *t*, *tt*, and *ttt*.

I would like to express my appreciation to my collaborators at NASD: John Komoroske, Henry Goldberg, and Kelly Palmer. The NASD fraud detection task is a fascinating real-world problem, which has been a continual source of motivation and often a harsh reality check. My work on the NASD project reminded me how inspiring real-world applications can be. In addition, I am indebted to them for providing such a compelling example for use throughout this thesis.

The work in this thesis has been directly impacted by my many collaborations in the Knowledge Discovery Laboratory. I would like to thank Hannah Blau, Andy Fast, Ross Fairgrieve, Lisa Friedland, Brian Gallagher, Amy McGovern, Michael Hay, Matt Rattigan, and Özgür Şimşek for their excellent input and feedback. I am also indebted to the invaluable assistance of the KDL technical staff: Matt Cornell, Cindy Loiselle, and Agustin Schapira. All the members of KDL have been both friends and colleagues. They made my graduate life not only bearable, but also rewarding and fun—as we saw each other through arduous paper deadlines, frustrating database problems, puzzling research findings, marathon pair-programming sessions, and countless practice talks.

Next, there are the friends who helped me maintain my sanity through the difficult coursework, research plateaus, and emotional challenges that inevitably occur during graduate school. I couldn't have done it without Özgür Şimşek and Pippin Wolfe—they were always willing to offer insightful research advice and unquestioning moral support. And what can I say to the other good friends I made at UMass? Brian Gallagher, Kat Hanna, Michael Hay, Brent Heeringa, Amy McGovern, Nandini

Natarajan, Matt Rattigan, Agustin Schapira and David Stracuzzi—thanks for all the cube-side discussions, Rao's coffee breaks, campus walks, and conference beers.

I owe an enormous amount to my family who set the foundation for this work. To my father, who taught me how to ask *why* and to my mother, who listened patiently to all my wonderings thereafter. To my stepdaughters Naomi and Kristin, who willingly endured all my hours in front of the computer and never-ending bowls of noodles when we were too busy to cook. To my son Jackson, who slept enough over the past two months to give me time to finish writing. And to my husband Jim, for being my joy, my strength, and my continuity.

Lastly, this work was supported by a National Science Foundation Graduate Research Fellowship, an AT&T Labs Graduate Research Fellowship, and by DARPA and AFRL under contract numbers HR0011-04-1-0013 and F30602-01-2-0566.

ABSTRACT

STATISTICAL MODELS AND ANALYSIS TECHNIQUES FOR LEARNING IN RELATIONAL DATA

SEPTEMBER 2006

JENNIFER NEVILLE

Ph.D., UNIVERSITY OF MASSACHUSETTS AMHERST

Directed by: Professor David Jensen

Many data sets routinely captured by organizations are relational in nature—from marketing and sales transactions, to scientific observations and medical records. Relational data record characteristics of heterogeneous objects and persistent relationships among those objects (e.g., citation graphs, the World Wide Web, genomic structures). These data offer unique opportunities to improve model accuracy, and thereby decision-making, if machine learning techniques can effectively exploit the relational information.

This work focuses on how to learn accurate statistical models of complex, relational data sets and develops two novel probabilistic models to represent, learn, and reason about statistical dependencies in these data. *Relational dependency networks* are the first relational model capable of learning general autocorrelation dependencies, an important class of statistical dependencies that are ubiquitous in relational data. *Latent group models* are the first relational model to generalize about the properties of underlying group structures to improve inference accuracy and efficiency. Not only do

these two models offer performance gains over current relational models, but they also offer efficiency gains which will make relational modeling feasible for large, relational datasets where current methods are computationally intensive, if not intractable.

We also formulate of a novel analysis framework to analyze relational model performance and ascribe errors to model learning and inference procedures. Within this framework, we explore the effects of data characteristics and representation choices on inference accuracy and investigate the mechanisms behind model performance. In particular, we show that the inference process in relational models can be a significant source of error and that relative model performance varies significantly across different types of relational data.

TABLE OF CONTENTS

LIST OF TABLES

Table **Page**

LIST OF FIGURES

Figure **Page**

CHAPTER 1

INTRODUCTION

Many data sets routinely captured by businesses and organizations are relational in nature—from marketing and sales transactions, to scientific observations and medical records. Relational data record characteristics of heterogeneous objects (e.g., people, places, and things) and persistent relationships among those objects. Examples of relational data include citation graphs, the World Wide Web, genomic structures, epidemiology data, and data on interrelated people, places, and events extracted from text documents.

For example, consider the National Association of Securities Dealers' (NASD) Central Registration Depository system (CRD©).[1] The system contains data on approximately 3.4 million securities brokers, 360,000 branches, 25,000 firms, and 550,000 disclosure events, which record disciplinary information on brokers from customer complaints to termination actions. Figure 1.1 shows the data schematically, including frequency counts and example attributes for both entities and relations in a sample of the CRD data. Relational data such as these are often stored in multiple tables, with separate tables recording the attributes of different object types (e.g., brokers, branches) and the relationships among objects (e.g., located-at).

In contrast, propositional data record characteristics of a single set of homogeneous objects. Propositional data are often stored in a single database table, with each row corresponding to a separate object (e.g. broker) and each column recording an

[1] See http://www.nasdbrokercheck.com.

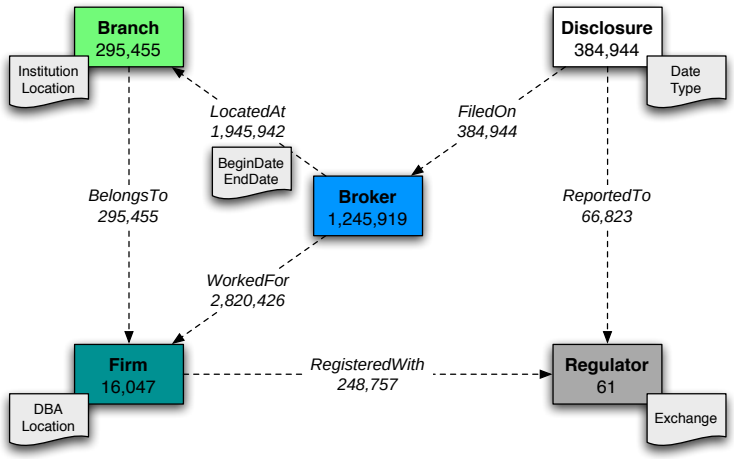

Figure 1.1. NASD relational data schema.

attribute of the objects (e.g. age). For example, Figure 1.2 depicts a propositional table with hypothetical broker information.

Consider the task of identifying brokers involved in securities fraud faced by the NASD [66]. NASD is the world's largest private-sector securities regulator, with responsibility for preventing and discovering misconduct among brokers such as fraud and other violations of securities regulations. NASD currently identifies *higher-risk* brokers using a set of handcrafted rules. However, we are interested in using *supervised learning* techniques to automatically induce a predictive model of broker risk to use to target NASD's limited regulatory resources on brokers who are most likely to engage in fraudulent behavior.

Supervised learning techniques are methods for automatically inducing a predictive model from a set of training data. Over the past two decades, most machine learning research focused on induction algorithms for propositional datasets. Propositional training data consist of pairs of class labels Y (e.g., is-higher-risk) and attribute vectors $\mathbf{X} = \{X_1, X_2, ..., X_m\}$ (e.g., {age, start-year}). The task is to estimate

IsHigher Risk	Age	StartYear	CollegeDeg	Series7	...
+	25	1997	N	Y	...
-	32	1982	N	N	...
-	24	2000	Y	N	...
-	28	1995	Y	Y	...
...	...	...	...	...	...

Figure 1.2. Example NASD database table.

a function, given data from a number of training examples, that predicts a class label value for any input attribute vector (i.e., $f(\mathbf{x}) \rightarrow y$).

Algorithms for modeling propositional data assume that the training examples are recorded in homogeneous structures (e.g., rows in a table, see Figure 1.2) but relational data are usually more varied and complex. For example, consider the relational data graph in Figure 1.3. Each broker has a different number of related objects, resulting in diverse structures—some brokers have no disclosures while others have many; some have few coworkers while others have many. Algorithms for propositional data also assume the examples are independent and identically distributed (i.i.d.) but relational data violate this assumption—the data have dependencies both as a result of direct relations and through chaining multiple relations together. For example, in Figure 1.3 brokers are not independent, they are related through the branches where they work.

Relational data offer unique opportunities to boost model accuracy and to improve decision-making quality if the algorithms can learn effectively from the additional information the relationships provide. The power of relational data lies in combining intrinsic information about objects in isolation with information about related objects and the connections among those objects. For example, relational information is often central to the task of fraud detection because fraud and malfeasance are social

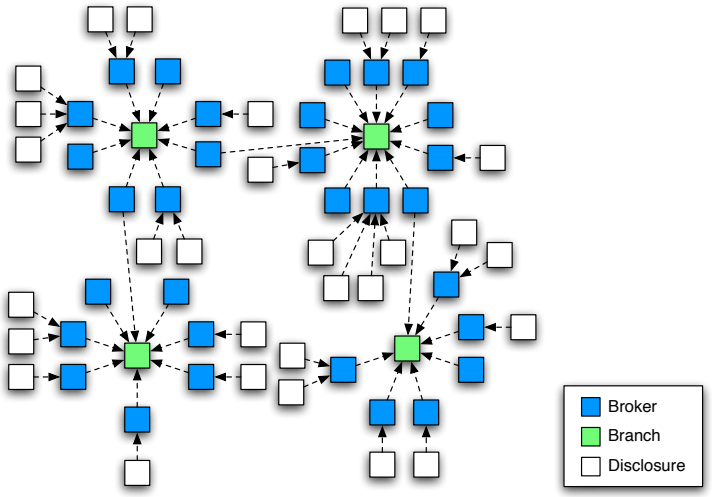

Figure 1.3. Example NASD database fragment.

phenomena, communicated and encouraged by the presence of other individuals who also wish to commit fraud (e.g., [11]).

In particular, the presence of *autocorrelation* provides a strong motivation for using relational techniques for learning and inference. Autocorrelation is a statistical dependency between the values of the same variable on related entities, which is a nearly ubiquitous characteristic of relational datasets.[2] For example, pairs of brokers working at the same branch are more likely to share the same fraud status than randomly selected pairs of brokers.

A number of widely occurring phenomena give rise to autocorrelation dependencies. A hidden condition or event, whose influence is correlated among instances that are closely located in time or space, can result in autocorrelated observations [63, 1]. Social phenomena, including social influence [57], diffusion [19], and homophily [61], can also cause autocorrelated observations through their influence on social interactions that govern the data generation process. Relational data often record information about people (e.g., organizational structure, email transactions) or about

[2]See Section 2.2 for a more formal definition of relational autocorrelation.

artifacts created by people (e.g., citation networks, World Wide Web) so it is likely that these social phenomena will contribute to autocorrelated observations in relational domains.

Recent research has advocated the utility of modeling autocorrelation in relational domains [89, 2, 56]. The presence of autocorrelation offers a unique opportunity to improve model performance because inferences about one object can be used to improve inferences about related objects. For example, when broker fraud status exhibits autocorrelation, if we know one broker is involved in fraudulent activity, then his coworkers have increased likelihood of being engaged in misconduct as well. Indeed, recent work in relational domains has shown that *collective inference* over an entire dataset can result in more accurate predictions than conditional inference for each instance independently [9, 67, 90, 76, 54] and that the gains over conditional models increase as autocorrelation increases [42].

In this work, we focus on the development and analysis of supervised learning techniques for relational data, moving beyond the conventional analysis of entities in isolation to analyze networks of interconnected entities. We aim to develop models to represent and reason with relational dependencies in general, and autocorrelation dependencies in particular, to improve inference performance in relational domains. More specifically, when inducing a predictive model for relational data, instead of estimating a function to map the intrinsic attributes $\mathbf{X}$ of an object to a class label Y, we aim to estimate a function that maps both the attributes intrinsic to the object and the attributes of its *related* neighbors $\{\mathbf{X_R}, \mathbf{Y_R}\}$ to a class label Y. We focus on autocorrelation as a simple, understandable form of dependence that exemplifies the characteristics of general relational dependencies. In particular, relational autocorrelation dependencies exhibit the full range of complexities involved in modeling relational data, including heterogeneity, cyclic dependencies, redundant forms of representation, and long-ranging correlation structure.

In this thesis, we investigate the following hypothesis: **Data characteristics and representation choices interact to affect relational model performance through their impact on learning and inference error.** In particular, we evaluate different approaches to representing autocorrelation, explore the effects of attribute and link structure on prediction accuracy, and investigate the mechanisms behind model performance.

The contributions of this thesis include (1) the development of two novel *probabilistic relational models* (PRMs)[3] to represent arbitrary autocorrelation dependencies and algorithms to learn these dependencies, and (2) the formulation of a novel analysis framework to analyze model performance and ascribe errors to model learning and inference procedures.

First, we present relational dependency networks (RDNs), an undirected graphical model that can be used to represent and reason with cyclic dependencies in a relational setting. RDNs use *pseudolikelihood* learning techniques to estimate an efficient approximation of the full joint distribution of the attribute values in a relational dataset.[4] RDNs are the first PRM capable of *learning* autocorrelation dependencies. RDNs also offer a relatively simple method for structure learning and parameter estimation, which can result in models that are easier to understand and interpret.

Next, we present latent group models (LGMs), a directed graphical model that models both the attribute and link structure in relational datasets. LGMs posit groups of objects in the data—membership in these groups influences the observed attributes of the objects, as well as the existence of relations among the objects. LGMs are the first PRM to *generalize* about latent group properties and take advantage of those properties to improve inference accuracy.

---

[3]Several previous papers (e.g., [26, 29]) use the term *probabilistic relational model* to refer to a specific model that is now often called a *relational Bayesian network* (Koller, personal communication). In this thesis, we use PRM in its more recent and general sense.

[4]See Section 3.2.2 for a formal definition of pseudolikelihood estimation.

Finally, we develop a novel bias/variance analysis framework to explore the mechanisms underlying model performance in relational domains. Conventional bias/variance analysis associates model errors with aspects of the *learning* process. However, in relational applications, the use of collective inference techniques introduces an additional source of error—both through the use of approximate inference algorithms and through variation in the availability of test set information. We account for this source of error in a decomposition that associates error with aspects of both *learning* and *inference* processes, showing that inference can be a significant source of error and that models exhibit different types of errors as data characteristics are varied.

1.1 Contributions

This thesis investigates the connections between autocorrelation and improvements in inference due to the use of probabilistic relational models and collective inference procedures.

The primary contributions of this thesis are two-fold. First, a thorough investigation of autocorrelation and its impact on relational learning has improved our understanding of the range and applicability of relational models. We compare the performance of models that represent autocorrelation indirectly (i.e., LGMs) to the performance of models that represent the observed autocorrelation directly (i.e., RDNs) and show that representation choices interact with dataset characteristics and algorithm execution to affect performance. This indicates that properties other than attribute correlation structure should be considered when choosing a model for relational datasets.

Second, this work has improved the overall performance of relational models, increasing both inference performance and model efficiency. In small datasets, where we have the computational resources to apply current learning and inference techniques, a better understanding of the effects of data characteristics on model performance can

increase the accuracy of the models. More specifically, we show that graph structure, autocorrelation dependencies, and amount of test set labeling, affect relative model performance. In larger datasets, where current learning and inference techniques are computationally intensive, if not intractable, the efficiency gains offered by *RDN*s and *LGM*s can make relational modeling both practical and feasible.

This thesis makes a number of theoretical and empirical contributions that we outline below:

- Theoretical
  - Development of *relational dependency networks*, a novel probabilistic relational model to efficiently learn arbitrary autocorrelation dependencies
    - Proof of correspondence between consistent *RDN*s and relational Markov networks[5]
    - Proof of asymptotic properties of pseudolikelihood estimation in *RDN*s
  - Development of *latent group models*, a novel probabilistic relational model to generalize about latent group structures to improve inference accuracy
  - Creation of novel bias/variance framework that decomposes relational model errors into learning and inference components
- Empirical
  - Validation of *RDN*s and *LGM*s on several real-world domains, including a dataset of scientific papers, a collection of webpages, and data for a fraud detection task
  - Illustration of effects of representation choices on model performance using synthetic datasets

[5]See Section 3.4.1 for a description of relational Markov networks (*RMN*s) [89].

– Illustration of effects of data characteristics on model performance using synthetic datasets

– Investigation of errors introduced by collective inference processes using synthetic datasets

1.2 Thesis Outline

There are three components to the thesis. In the first component, we develop a probabilistic relation model capable of modeling arbitrary autocorrelation dependencies. In the second component, we develop a probabilistic relational model that incorporates group structure in a tractable manner to model observed autocorrelation. In the third component, we propose a bias/variance analysis framework to evaluate the effects of model representation and data characteristics on performance.

The remainder of this thesis is organized as follows. Chapter 2 reviews relevant background material on relational data, tasks, and models. Chapter 3 describes relational dependency networks (RDNs), outlines the RDN learning and inference procedures, and presents empirical results on both real-world and synthetic datasets. Chapter 4 describes latent group models (LGMs), outlines a learning and inference procedure for a specific form of LGMs, and presents empirical results on both real-world and synthetic datasets. Chapter 5 outlines a bias/variance framework for relational models and presents empirical experiments on synthetic data, which explore the mechanisms underlying model performance. Finally, we conclude in Chapter 6 with a review of the main contributions of the thesis and a discussion of extensions and future work.

Some of this material has appeared previously in workshop and conference papers. The work on RDNs in Chapter 3 first appeared in Neville and Jensen [69]. It later appeared in Neville and Jensen [70] and Neville and Jensen [74]. The work on LGMs in Chapter 4 first appeared in Neville and Jensen [71], and later in Neville

and Jensen [72]. The bias/variance framework in Chapter 5 first appeared in Neville and Jensen [73].

CHAPTER 2

MODELING RELATIONAL DATA

2.1 Relational Data

There are three nearly equivalent representations for relational datasets:

- Graphs—A directed, attributed hypergraph with V nodes representing objects and E hyperedges representing relations, with one or more connected components.
- Relational databases—A set of database tables with entities E and relations R. Items of a common type are stored in a separate database table with one field for each attribute.
- First-order logic knowledge bases—A set of first-order logic statements.

This work considers relational data represented as a typed, attributed data graph $G_D = (V_D, E_D)$. To simplify discussion we will restrict our attention to binary links, however the models and algorithms are applicable to more general hypergraphs.[1] For example, consider the data graph in Figure 1.3. The nodes V_D represent objects in the data (e.g., people, organizations, events) and the edges E_D represent relations among the objects (e.g., works-for, located-at). We use rectangles to represent objects and dashed lines to represent relations.[2]

[1]The limitations imposed by binary links can usually by avoided by creating objects to represent more complex relations such as events [14].

[2]Later, we will use circles to represent random variables and solid lines to represent probabilistic dependencies in graphical representations of PRMs.

Each node $v_i \in V_D$ and edge $e_j \in E_D$ are associated with a type $T(v_i) = t_{v_i},\ T(e_j) = t_{e_j}$. This is depicted by node color in Figure 1.3. For example, blue nodes represent *people* and green nodes represent *organizations*. Each item type $t \in T$ has a number of associated attributes $\mathbf{X^t} = (X_1^t, ..., X_m^t)$ (e.g., age, gender).[3] Consequently, each object v and link e are associated with a set of attribute values determined by their type $\mathbf{X_v^{t_v}} = (X_{v1}^{t_v}, ..., X_{vm}^{t_v})$, $\mathbf{X_e^{t_e}} = (X_{e1}^{t_e}, ..., X_{em'}^{t_e})$.

Relational data often have irregular structures and complex dependencies that contradict the assumptions of conventional machine learning techniques. Algorithms for propositional data assume that the data instances are recorded in homogeneous structures (i.e., a fixed set of fields for each object), but relational data instances are usually more varied and complex. For example, organizations each employ a different number of people and customers each purchase a different number of products. The ability to generalize across heterogeneous data instances is a defining characteristic of relational learning algorithms. Algorithms designed for propositional data also assume data instances are i.i.d.. Relational data, on the other hand, have dependencies both as a result of direct relations (e.g., company subsidiaries) and through chaining of multiple relations (e.g., employees at the same firm).

2.2 Relational Autocorrelation

Relational autocorrelation refers to a statistical dependency between values of the same variable on related objects.[4] More formally, we define relational autocorrelation with respect to a set of *related* instance pairs P_R related through paths of length l in a set of edges E_R: $P_R = \{(v_i, v_j) : e_{ik_1}, e_{k_1k_2}, ..., e_{k_lj} \in E_R\},\ where\ E_R = \{e_{ij}\} \subseteq E.$

[3] We use the generic term "item" to refer to objects or links.

[4] We use the term *autocorrelation* in a more general sense than past work in econometrics (e.g., [63]) and spatial statistics (e.g., [13]). In this work, we use autocorrelation to refer to *autodependence* among the values of a variable on related instances, including non-linear correlation among continuous variables and dependence among discrete variables.

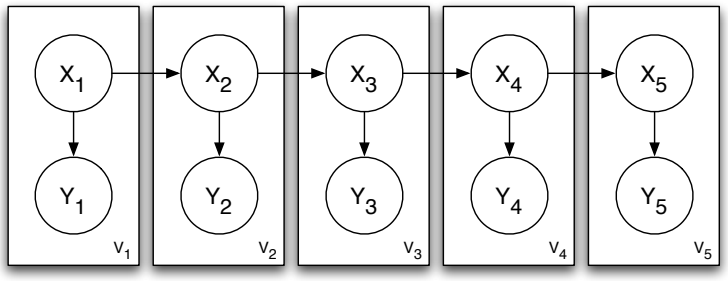

Figure 2.1. Time series autocorrelation example.

Relational autocorrelation measures the dependence among the values of a variable X defined on the instance pairs P_R. It is the correlation between the values of X on all pairs of related instances in P_R (i.e., (x_i, x_j) such that $(v_i, v_j) \in P_R$). Any traditional measure of association, such as the chi-square statistic or information gain, can be used to assess the association between these pairs of values of X.

For example, consider the time series in Figure 2.1 with five objects V, each with attributes X and Y. Each object is related to the object in the following time step (i.e., V_i is related to V_{i+1}). One measure of the autocorrelation of X is the correlation between the values of X on pairs of instances V that are one time step apart (i.e., X_i and X_{i+1}):

$$r_{ac} = \frac{\sum_{i=1}^{4}(X_i - \bar{X})(X_{i+1} - \bar{X})}{\sum_{i=1}^{5}(X_i - \bar{X})^2}$$

In arbitrary relational datasets, the set of instance pairs can be related in myriad ways, either by direct links (e.g., corporate subsidiaries) or by indirect chaining through a path of relations (e.g., brokers that work at the same branch). Given a set of related pairs P_R, we can measure the autocorrelation of a continuous variable X as the correlation between related X_i and X_j:

$$r_{ac} = \frac{\sum_{ij\ s.t.(v_i,v_j)\in P_R}(X_i - \bar{X})(X_j - \bar{X})}{\sum_{i\ s.t.(v_i,.)\vee(.,v_i)\in P_R}(X_i - \bar{X})^2}$$

Alternatively for a binary variable X, we can measure the autocorrelation between related X_i and X_j using Pearson's contingency coefficient [84]:

$$r_{ac} = \sqrt{\frac{\chi^2}{(N+\chi^2)}} = \sqrt{\frac{\frac{(n_{00}n_{11}-n_{01}n_{10})^2 \cdot N}{(n_{00}+n_{01})(n_{10}+n_{11})(n_{01}+n_{11})(n_{00}+n_{10})}}{(N+\frac{(n_{00}n_{11}-n_{01}n_{10})^2 \cdot N}{(n_{00}+n_{01})(n_{10}+n_{11})(n_{01}+n_{11})(n_{00}+n_{10})})}}$$

where $n_{ab} = |(x_i, x_j) : x_i = a, x_j = b, (v_i, v_j) \in P_R|$ and N is the total number of instances in P_R.

A number of widely occurring phenomena give rise to autocorrelation dependencies. Temporal and spatial locality often result in autocorrelated observations, due to temporal or spatial dependence of measurement errors, or to the existence of a variable whose influence is correlated among instances that are closely located in time or space [63, 1]. Social phenomena such as social influence [57], diffusion processes [19], and the principle of homophily [61] give rise to autocorrelated observations as well, through their influence on social interactions that govern the data generation process.

Autocorrelation is a nearly ubiquitous characteristic of relational datasets. For example, recent analysis of relational datasets has reported autocorrelation in the following variables:

- Topics of hyperlinked web pages [9, 89]
- Industry categorization of corporations that share board members [67]
- Fraud status of cellular customers who call common numbers [22, 11]
- Topics of coreferent scientific papers [90, 69]
- Functions of colocated proteins in a cell [68]
- Box-office receipts of movies made by the same studio [40]
- Industry categorization of corporations that co-occur in news stories [2]

- Tuberculosis infection among people in close contact [29]
- Product/service adoption among customers in close communication [18, 35]

If a dataset exhibits high autocorrelation, then we can exploit the autocorrelation dependencies and improve overall predictions for X by collectively inferring values over the entire set of instances. For example, Figure 2.2 depicts a fragment of the NASD database, where brokers are labeled to indicate their fraud status—fraudulent broker are labeled with $+$, lawful brokers are labeled with $-$. Notice that the fraud status of co-workers is correlated—fraudulent brokers are clustered at the top-left and bottom-right of the graph. When such autocorrelation is present, the inferences about one object can be used to improve the inferences about other related objects—if we know one broker is fraudulent, then his coworkers have higher likelihood of being engaged in fraud as well.

The presence of autocorrelation is a strong motivation for use of relational learning and inference techniques. Recent work has shown that in relational domains, collective inference over an entire dataset often results in more accurate predictions than conditional inference for each instance independently [9, 67, 89, 95, 54, 55, 69]. Furthermore, we have demonstrated that the gains over conditional models increase as autocorrelation increases [42]—illustrating that autocorrelation is the mechanism by which inferences about one object can improve inferences about related objects.

In this thesis, we focus on autocorrelation as an archetype of relational dependence. Autocorrelation is a simple, understandable form of dependence, which is prevalent in relational datasets and exhibits the full range of complexities involved in modeling relational dependencies. First, in order to represent autocorrelation, models must be able to tie parameters across heterogeneous structures (e.g., a broker's fraud status depends on the fraud status of a variable number of other brokers, depending on how many brokers work at the same branch). Second, it is beneficial for models to be able to represent cyclic dependencies. While domain knowledge can sometimes

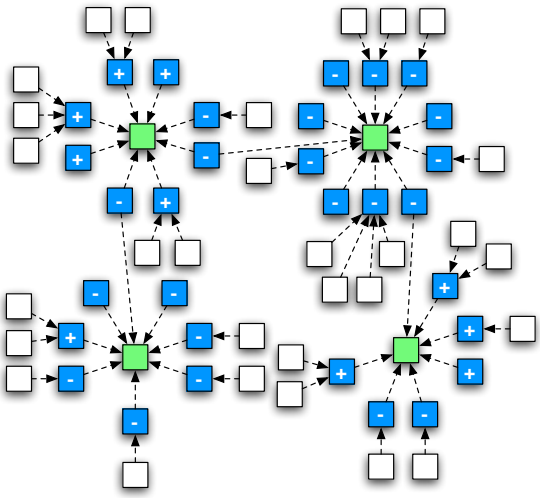

Figure 2.2. Example NASD database fragment with broker fraud labels.

be used to determine the causal direction of autocorrelation dependencies, and thus structure them in an acyclic manner, often we can only represent an undirected correlation between the attributes of related objects. Third, it is helpful if models are be able to exploit long-ranging correlation structures. If two objects are not directly related, but they are close neighbors in the relational data graph, and the data exhibit autocorrelation, there may be indirect dependencies among their attributes values. Finally, there are a number of ways to represent autocorrelation in relational models and the choice of representation can affect model performance. For example, autocorrelation can be modeled directly through the dependencies among class labels of related instances, or indirectly through the association between the class label and the observed attributes of related instances.

2.3 Tasks

This work is concerned with two modeling tasks for relational datasets. The first task is *relational knowledge discovery*. Knowledge discovery is the process of identifying valid, novel, potentially useful, and ultimately understandable patterns

in data [23]. One way of identifying useful patterns in data is to estimate a joint distribution for a set of m attributes $\mathbf{X} = \{X_1, X_2, ..., X_m\}$. In propositional datasets, the joint distribution is estimated for the attributes of a single instance:

$$p(\mathbf{x}) = p(x_1, x_2, ..., x_m)$$

In relational datasets, the joint distribution is estimated for the m attributes of *all* n instances, $\mathbf{X^n} = \{X_1^1, X_2^1, ..., X_m^1, \ ... \ , X_1^n, X_2^n, ..., X_m^n\}$. We use superscripts to refer to instance numbers and subscripts to refer to attribute numbers:

$$p(\mathbf{x^n}) = p(x_1^1, x_2^1, ..., x_m^1, \ ... \ , x_1^n, x_2^n, ..., x_m^n)$$

If the learning process uses feature selection to determine which of the $O(m^2)$ possible pairwise attribute dependencies are reflected in the data, then the model may identify useful patterns in the data. If, in addition, the model has an understandable knowledge representation (e.g., decision trees, Bayesian networks) then the patterns may be useful for knowledge discovery in the domain of interest.

The second task is *conditional modeling*. This involves estimating a conditional distribution for a single attribute Y, given other attributes $\mathbf{X}$. In propositional datasets, the conditional distribution is estimated for the attributes of a single instance:

$$p(y|\mathbf{x}) = p(y|x_1, x_2, ..., x_m)$$

In relational datasets, the distribution is also conditioned on the attributes of *related* instances. One technique for estimating conditional distributions in relational data assumes that the class labels are conditionally independent given the attributes of related instances:

$$p(y^i|\mathbf{x}^i, \mathbf{x}^r, \mathbf{y}^r) = p(y^i|\mathbf{x}^i, \mathbf{x}^r) = p(y^i|x_1^i, x_2^i, ..., x_m^i, x_1^1, x_2^1, ..., x_m^1, \ ...x_1^r, x_2^r, ..., x_m^r)$$

where instances 1 through r are related to instance i. We will refer to methods that use this approach as *individual inference* techniques. An alternative approach models the influences of *both* the attributes and the class labels of related instances:

$$p(y^i|\mathbf{x}^i, \mathbf{x}^r, \mathbf{y}^r) = p(y^i|x^i_1, x^i_2, ..., x^i_m, x^1_1, x^1_2, ..., x^1_m, \ ... \ x^r_1, x^r_2, ..., x^r_m, y^1, y^2, ..., y^r)$$

We will refer to methods that use this approach as *collective inference* techniques. When inferring the values of y^i for a number of instances, some of the values of $\mathbf{y}^r$ may be unknown (if the related objects' class labels are to be inferred as well), thus the y^i must be inferred *collectively*. Collective inference may also be used in *joint modeling* tasks, where a number of different variables are inferred for a set of related instances (e.g., $\mathbf{y}$ and $\mathbf{x_1}$) but we restrict our consideration to conditional modeling tasks in this work.

2.4 Sampling

In order to accurately estimate the generalization performance of machine learning algorithms, sampling procedures are applied to split datasets into separate *training* and *test* sets. The learning algorithms are used to estimate models from the training set, then the learned models are applied to the test set and inference performance is evaluated with standard measures such as accuracy, squared loss, and area under the ROC curve (AUC) [21]. Separate training and test sets are used because measurements of performance are generally biased when they are assessed on the dataset used for training.

Most sampling methods assume that the instances are i.i.d. so that disjoint training and tests can be constructed by randomly sampling instances from the data. If random sampling is applied to relational datasets, relations between instances can produce dependencies between the training and test sets. This can cause traditional methods of evaluation to overestimate the generalization performance of induced models for *independent samples* [39].

Methods for sampling dependent relational data are not well understood. However, there are two primary approaches in current use that we outline below. We

discuss the approaches in the context of sampling instances into a training set A and test set B.

The first approach we will refer to as *independent sampling*. This approach does not allow dependencies between the training and test set. From a relational data graph, we sample N_A and N_B instances to form *disjoint* training and test sets. When independent sampling is used for evaluation, the assumption is that the model will be learned from, and applied to, separate networks, or that the model will be learned from a labeled subgraph within a larger network. In the later case, the subgraph is nearly disjoint from the unlabeled instances in the larger network so dependencies between A and B will be minimal. In the former case, the assumption is that the separate networks are drawn from the same distribution, so the model learned on the training network will accurately reflect the attribute dependencies and link structure of the test network.

The second approach we will refer to as *interdependent sampling*. This approach allows dependencies between the training and test set. From a relational data graph, we sample N_A instances for the training set and N_B instances for the test set. Links from A to B are removed during learning so that A and B are disjoint. However, during inference, when testing the learned model on B, links from A to B are not removed—the learned model can access objects and attribute information in A that are linked to objects in B. When interdependent sampling is used for evaluation, the assumption is that the model will be learned from a partially labeled network, and then applied to the same network to infer the remaining labels. For example, in relational data with a temporal ordering, we can learn a model on all data up to time t, then apply the model to the same dataset at time $t+x$, inferring class values for the objects that appeared after t. In these situations, we expect the model will always be able to access the training set during inference, so the dependencies between A and B will not bias our measurement of generalization performance.

2.5 Models

2.5.1 Individual Inference Models

There are a number of relational models that are used for individual inference, where inferences about one instance are not used to inform the inference of related instances (e.g., [20, 75, 76, 79, 82, 80]). These approaches model relational instances as independent, disconnected subgraphs (e.g., molecules). The models can represent the complex relational structure around a single instance, but they do not attempt to model the relational structure among instances—thus removing the need (and the opportunity) for collective inference.

Individual inference models typically transform relational data into a form where conventional machine learning techniques (or slightly modified versions) can be applied. Transforming relational data to propositional form through flattening is by far the most common technique. One method of transforming heterogeneous data into homogenous records uses aggregation to map multiple values into a single value (e.g. average co-worker age) and duplication to share values across records (e.g. firm location is repeated across all associated brokers). Examples of models that use these types of transformations include: relational Bayesian classifiers (*RBC*s) [76], relational probability trees (*RPT*s) [75], and *ACORA* [79, 80]. An alternative method uses relational learners to construct conjunctive features that represent various characteristics of the instances [49]. Structured instances are then transformed into homogenous sets of relational features. Any conventional machine learning technique can be applied to the flattened set of features. Examples of this technique include: inductive logic programming extensions [20], first-order Bayesian classifiers [24], and structural logistic regression [82].

2.5.2 Collective Inference Models

Collective inference models exploit autocorrelation dependencies in a network of objects to improve predictions. For example, consider the problem of automatically predicting the topic of a scientific paper (e.g., neural networks, genetic algorithms). One method for predicting topics could look at papers in the context of their citation graphs. It is possible to predict a given paper's topic with high accuracy based on the topics of its neighboring papers because there is high autocorrelation in the citation graph (i.e., papers tend to cite other papers with the same topic).

An ad-hoc approach to collective inference combines locally-learned individual inference models (e.g., RBCs) with a joint inference procedure (e.g., relaxation labeling). Examples of this type of approach include: iterative classification models [67], link-based classification models [54], and probabilistic relational neighbor models [55, 56].

Joint relational models model the dependencies among attributes of related instances. These approaches are able to exploit autocorrelation by estimating joint probability distributions over the attributes in the entire data graph and jointly inferring the labels of related instances.

Probabilistic relational models are one class of joint models used for density estimation and inference in relational datasets. These models extend graphical model formalisms to relational domains by *upgrading* [45] them to a first-order logic representation with an entity-relationship model. Examples of PRMs include: relational Bayesian networks[5] (RBNs) [29] and relational Markov networks (RMNs) [89]. We discuss the general characteristics of PRMs below and outline the details of RBNs and RMN in Section 3.4.1.

[5]We use the term relational Bayesian network to refer to Bayesian networks that have been upgraded to model relational databases. The term has also been used by Jaeger [38] to refer to Bayesian networks where the nodes correspond to relations and their values represent possible interpretations of those relations in a specific domain.

Probabilistic logic models (PLMs) are another class of joint models used for density estimation and inference in relational datasets. PLMs extend conventional logic programming models to support probabilistic reasoning in first-order logic environments. Examples of PLMs include Bayesian logic programs [46] and Markov logic networks [83].

PLMs represent a joint probability distribution over the ground atoms of a first-order knowledge base. The first-order knowledge base contains a set of first-order formulae, and the PLM associates a set of weights/probabilities with each of the formulae. Combined with a set of constants representing objects in the domain, PLMs specify a probability distribution over possible truth assignments to ground atoms of the first-order formulae. Learning a PLM consists of two tasks: generating the relevant first-order clauses, and estimating the weights/probabilities associated with each clause.

2.5.3 Probabilistic Relational Models

PRMs represent a joint probability distribution over the attributes of a relational dataset. When modeling propositional data with a graphical model, there is a single graph G that that comprises the model. In contrast, there are three graphs associated with models of relational data: the *data graph* G_D, the *model graph* G_M, and the *inference graph* G_I. These correspond to the *skeleton*, *model*, and *ground graph* as outlined in Heckerman et al. [34].

First, the relational dataset is represented as a typed, attributed data graph $G_D = (V_D, E_D)$. For example, consider the data graph in Figure 2.3a. The nodes V_D represent objects in the data (e.g., authors, papers) and the edges E_D represent relations among the objects (e.g., author-of, cites).[6] Each node $v_i \in V_D$ and edge $e_j \in$

[6]We use rectangles to represent objects, circles to represent random variables, dashed lines to represent relations, and solid lines to represent probabilistic dependencies.

E_D is associated with a type, $T(v_i) = t_{v_i}$ and $T(e_j) = t_{e_j}$ (e.g., paper, cited-by). Each item type $t \in T$ has a number of associated attributes $\mathbf{X^t} = (X_1^t, ..., X_m^t)$ (e.g., topic, year). Consequently, each object v_i and link e_j is associated with a set of attribute values determined by their type, $\mathbf{X_{v_i}^{t_{v_i}}} = (X_{v_i 1}^{t_{v_i}}, ..., X_{v_i m}^{t_{v_i}})$ and $\mathbf{X_{e_j}^{t_{e_j}}} = (X_{e_j 1}^{t_{e_j}}, ..., X_{e_j m'}^{t_{e_j}})$. A PRM represents a joint distribution over the values of the attributes in the data graph, $\mathbf{x} = \{\mathbf{x_{v_i}^{t_{v_i}}} : v_i \in V \; s.t. \; T(v_i) = t_{v_i}\} \cup \{\mathbf{x_{e_j}^{t_{e_j}}} : e_j \in E \; s.t. \; T(e_j) = t_{e_j}\}$.

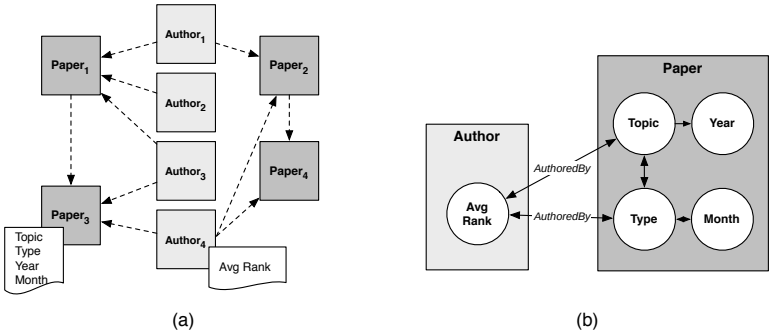

Figure 2.3. Example PRM (a) data graph and (b) model graph.

Next, the dependencies among attributes are represented in the model graph $G_M = (V_M, E_M)$. Attributes of an item can depend probabilistically on other attributes of the same item, as well as on attributes of other related objects or links in G_D. For example, the topic of a paper may be influenced by attributes of the authors that wrote the paper. Instead of defining the dependency structure over attributes of specific objects, PRMs define a generic dependency structure at the level of item types. Each node $v \in V_M$ corresponds to an X_k^t, where $t \in T \; \wedge \; X_k^t \in \mathbf{X^t}$. The set of variables $\mathbf{X_k^t} = (X_{ik}^t : (v_i \in V \; \vee \; e_i \in E) \; \wedge \; T(i) = t)$ is tied together and modeled as a single variable. This approach of typing items and tying parameters across items of the same type is an essential component of PRM learning. It enables generalization from a *single* instance (i.e., one data graph) by decomposing the data graph into *multiple* examples of each item type (e.g., all paper objects), and building a joint model of dependencies between and among attributes of each type. The relations in G_D are

used to limit the search for possible statistical dependencies, thus they constrain the set of edges that can appear in G_M. However, note that a relationship between two objects in G_D does not necessarily imply a probabilistic dependence between their attributes in G_M.

As in conventional graphical models, each node is associated with a probability distribution conditioned on the other variables. Parents of X_k^t are either: (1) other attributes associated with items of type t_k (e.g., paper *topic* depends on paper *type*), or (2) attributes associated with items of type t_j where items t_j are related to items t_k in G_D (e.g., paper *topic* depends on author *rank*). For the latter type of dependency, if the relation between t_k and t_j is one-to-many, the parent consists of a set of attribute values (e.g., author ranks). In this situation, current PRMs use aggregation functions to generalize across heterogeneous attribute sets (e.g., one paper may have two authors while another may have five). Aggregation functions are used either to map sets of values into single values, or to combine a set of probability distributions into a single distribution.

Consider the model graph G_M in Figure 2.3b.[7] It models the data in Figure 2.3a, which has two object types: paper and author. In G_M, each item type is represented by a plate [43], and each attribute of each item type is represented as a node. Edges characterize the dependencies among the attributes at the type level. The representation uses a modified plate notation—dependencies among attributes of the same object are contained inside the rectangle and arcs that cross the boundary of the rectangle represent dependencies among attributes of related objects. For example,

[7]For clarity, we omit cyclic autocorrelation dependencies in this example. See Section 3.3.2 for more complex model graphs.

$month_i$ depends on $type_i$, while $avgrank_j$ depends on the $type_k$ and $topic_k$ for all papers k written by author j in G_D.[8]

There is a nearly limitless range of dependencies that could be considered by algorithms for learning PRMs. In propositional data, learners model a fixed set of attributes intrinsic to each object. In contrast, in relational data, learners must decide how much to model (i.e., how much of the relational neighborhood around an item can influence the probability distribution of a item's attributes). For example, a paper's topic may depend of the topics of other papers written by its authors—but what about the topics of the references in those papers or the topics of other papers written by coauthors of those papers? Two common approaches to limiting search in the space of relational dependencies are: (1) exhaustive search of all dependencies within a fixed-distance neighborhood (e.g., attributes of items up to k links away), or (2) greedy iterative-deepening search, expanding the search in directions where the dependencies improve the likelihood.

Finally, during inference, a PRM uses a model graph G_M and a data graph G_D to instantiate an inference graph $G_I = (V_I, V_E)$ in a process sometimes called "roll out." The roll out procedure used by PRMs to produce G_I is nearly identical to the process used to instantiate sequence models such as hidden Markov models. G_I represents the probabilistic dependencies among all the variables in a single test set (here G_D is different from G'_D used for training, see Section 2.3 for more detail). The structure of G_I is determined by both G_D and G_M—each item-attribute pair in G_D gets a separate, local copy of the appropriate CPD from G_M. The relations in G_D determine the way that G_M is rolled out to form G_I. PRMs can produce inference graphs with wide variation in overall and local structure because the structure of G_I is

[8]Author rank records ordering in paper authorship (e.g., first author, second author). Paper type records category information (e.g., PhD thesis, technical report); topic records content information (e.g., genetic algorithms, reinforcement learning); year and month record publication dates.

determined by the specific data graph, which typically has non-uniform structure. For example, Figure 2.4 shows the model from Figure 2.3b rolled out over the dataset in Figure 2.3a. Notice that the number of authors per paper varies. This illustrates why current PRMs use aggregation in their CPDs—for example, the CPD for paper-type must be able to utilize a variable number of author ranks.

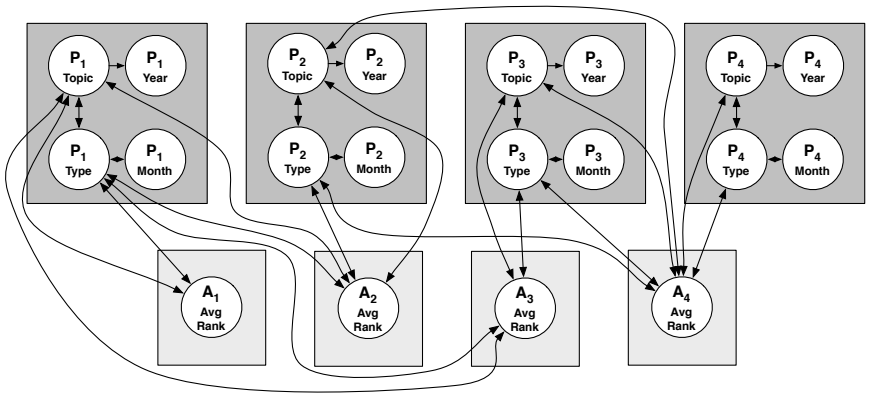

Figure 2.4. Example PRM inference graph.

All PRMs model data that can be represented as a graph (i.e., G_D). PRMs use different approximation techniques for inference in G_I (e.g., Gibbs sampling [65], loopy belief propagation [64]), but they all use a similar process for rolling out an inference graph G_I. Consequently, PRMs differ primarily with respect to the representation of the model graph G_M, how that model is learned, and how inference is conducted. We discuss the details of relational Bayesian networks and relational Markov networks in the context of RDNs in Section 3.4.1.

CHAPTER 3

RELATIONAL DEPENDENCY NETWORKS

Joint relational models are able to exploit autocorrelation by estimating a joint probability distribution over an entire relational dataset and collectively inferring the labels of related instances. Recent research has produced several novel PRMs for estimating joint probability distributions for relational data that consist of non-independent and heterogeneous instances [29, 85, 18, 51, 89]. PRMs extend traditional graphical models such as Bayesian networks to relational domains, removing the assumption of i.i.d. instances that underlies propositional learning techniques. PRMs have been successfully evaluated in several domains, including the World Wide Web, genomic data, and scientific literature.

Directed PRMs, such as relational Bayesian networks (RBNs) [29], can model autocorrelation dependencies if they are structured in a manner that respects the acyclicity constraint of the model. While domain knowledge can sometimes be used to structure the autocorrelation dependencies in an acyclic manner, often an acyclic ordering is unknown or does not exist. For example, in genetic pedigree analysis there is autocorrelation among the genes of relatives [52]. In this domain, the casual relationship is from ancestor to descendent so we can use the temporal parent-child relationship to structure the dependencies in an acyclic manner (i.e., parents' genes will never be influenced by the genes of their children). However, given a set of hyperlinked web pages, there is little information to use to determine the causal direction of the dependency between their topics. In this case, we can only represent an (undirected) correlation between the topics of two pages, not a (directed) causal

relationship. The acyclicity constraint of directed PRMs precludes the learning of arbitrary autocorrelation dependencies and thus severely limits the applicability of these models in relational domains.

Undirected PRMs, such as relational Markov networks (RMNs) [89], can represent arbitrary forms of autocorrelation. However, research on these models focused primarily on parameter estimation and inference procedures. Current implementations of RMNs do not select features—model structure must be pre-specified by the user. While, in principle, it is possible for RMN techniques to learn cyclic autocorrelation dependencies, inefficient parameter estimation makes this difficult in practice. Because parameter estimation requires multiple rounds of inference over the entire dataset, it is impractical to incorporate it as a subcomponent of feature selection. Recent work on conditional random fields for sequence analysis includes a feature selection algorithm [58] that could be extended for RMNs. However, the algorithm abandons estimation of the full joint distribution during the inner loop of feature selection and uses an approximation instead, which makes the approach tractable but removes some of the advantages of reasoning with the full joint distribution.

In this chapter, we describe relational dependency networks (RDNs), an extension of dependency networks [33] for relational data. RDNs can represent the cyclic dependencies required to express and exploit autocorrelation during collective inference. In this regard, they share certain advantages of RMNs and other undirected models of relational data [9, 18, 83]. To our knowledge, RDNs are the first PRM capable of *learning* cyclic autocorrelation dependencies. RDNs also offer a relatively simple method for structure learning and parameter estimation, which results in models that are easier to understand and interpret. In this regard, they share certain advantages of RBNs and other directed models [85, 34]. The primary distinction between RDNs and other existing PRMs is that RDNs are an approximate model. RDNs approximate the full joint distribution and thus are not guaranteed to specify a *consistent*

probability distribution, where each CPD can be derived from the joint distribution using the rules of probability.[1] The quality of the approximation will be determined by the data available for learning—if the models are learned from large datasets, and combined with Monte Carlo inference techniques, the approximation should be sufficiently accurate.

We start by reviewing the details of dependency networks for propositional data. Then we discuss the specifics of *RDN* learning and inference procedures. We evaluate *RDN* learning and inference on synthetic datasets, showing that *RDN* learning is accurate for large to moderate-size datasets and that *RDN* inference is comparable, or superior, to *RMN* inference over a range of data conditions. In addition, we evaluate *RDN*s on five real-world datasets, presenting learned *RDN*s for subjective evaluation. Of particular note, all the real-world datasets exhibit multiple autocorrelation dependencies that were automatically discovered by the *RDN* learning algorithm. We evaluate the learned models in a prediction context, where only a single attribute is unobserved, and show that the models outperform conventional conditional models on all five tasks. Finally, we discuss related work and conclude.

3.1 Dependency Networks

Graphical models represent a joint distribution over a set of variables. The primary distinction between Bayesian networks, Markov networks, and dependency networks (*DN*s) is that dependency networks are an approximate representation. *DN*s approximate the joint distribution with a set of conditional probability distributions (CPDs) that are learned independently. This approach to learning results in significant efficiency gains over models that estimate the joint distribution explicitly. However, because the CPDs are learned independently, *DN*s are not guaranteed to

[1] In this work, we use the term *consistent* to refer to the consistency of the individual CPDs (as Heckerman et al. [33]), rather than the asymptotic properties of a statistical estimator.

specify a consistent joint distribution from which each CPD can be derived using the rules of probability. This limits the applicability of exact inference techniques. In addition, the correlational DN representation precludes DNs from being used to infer causal relationships. Nevertheless, DNs can encode predictive relationships (i.e., dependence and independence) and Gibbs sampling inference techniques (e.g., [65]) can be used to recover a full joint distribution, regardless of the consistency of the local CPDs. We begin by reviewing traditional graphical models and then outline the details of dependency networks in this context.

Consider the set of random variables $\mathbf{X} = (X_1, ..., X_n)$ over which we would like to model the joint distribution $p(\mathbf{x}) = p(x_1, ..., x_n)$. We use upper case letters to refer to random variables and lower case letters to refer to an assignment of values to the variables.

A Bayesian network for $\mathbf{X}$ uses a directed acyclic graph $G = (V, E)$ and a set of conditional probability distributions P to represent the joint distribution over $\mathbf{X}$. Each node $v \in V$ corresponds to an $X_i \in \mathbf{X}$. The edges of the graph encode statistical dependencies among the variables and can be used to infer conditional independence among variables using notions of d-separation. The parents of node X_i, denoted PA_i, are the set of $v_j \in V$ such that $(v_j, v_i) \in E$. The set P contains a conditional probability distribution for each variable given its parents, $p(x_i|pa_i)$. The acyclicity constraint on G ensures that the CPDs in P factor the joint distribution into the formula below. A directed graph is acyclic if there is no directed path that starts and ends at the same variable. More specifically, there can be no self-loops from a variable to itself. Given (G, P), the joint probability for a set of values $\mathbf{x}$ is computed with the formula:

$$p(\mathbf{x}) = \prod_{i=1}^{n} p(x_i|pa_i)$$

A Markov network for $\mathbf{X}$ uses an undirected graph $U = (V, E)$ and a set of potential functions Φ to represent the joint distribution over $\mathbf{X}$. Again, each node $v \in V$

corresponds to an $X_i \in \mathbf{X}$ and the edges of the graph encode conditional independence assumptions. However, with undirected graphs, conditional independence can be inferred using simple graph separation. Let $C(U)$ be the set of cliques in the graph U. Then each clique $c \in C(U)$ is associated with a set of variables X_c and a clique potential $\phi_c(x_c)$ which is a non-negative function over the possible values for x_c. Given (U, Φ), the joint probability for a set of values $\mathbf{x}$ is computed with the formula:

$$p(\mathbf{x}) = \frac{1}{Z} \prod_{i=1}^{c} \phi_i(x_{c_i})$$

where $Z = \sum_X \prod_{i=1}^{c} \phi_i(x_{c_i})$ is a *normalizing constant*, which sums over all possible instantiations of $\mathbf{x}$ to ensure that $p(\mathbf{x})$ is a valid probability distribution.

3.1.1 DN Representation

Dependency networks are an alternative form of graphical model that approximates the full joint distribution with a set of conditional probability distributions that are each learned independently. A DN encodes probabilistic relationships among a set of variables $\mathbf{X}$ in a manner that combines characteristics of both undirected and directed graphical models. Dependencies among variables are represented with a directed graph $G = (V, E)$, where conditional independence is interpreted using graph separation, as with undirected models. However, as with directed models, dependencies are quantified with a set of conditional probability distributions P. Each node $v_i \in V$ corresponds to an $X_i \in \mathbf{X}$ and is associated with a probability distribution conditioned on the other variables, $P(v_i) = p(x_i|\mathbf{x} - \{x_i\})$. The parents of node i are the set of variables that render X_i conditionally independent of the other variables ($p(x_i|pa_i) = p(x_i|\mathbf{x} - \{x_i\})$), and G contains a directed edge from each parent node v_j to each child node v_i ($(v_j, v_i) \in E$ iff $X_j \in pa_i$). The CPDs in P do not necessarily factor the joint distribution so we cannot compute the joint probability for a set of values $\mathbf{x}$ directly. However, given G and P, a joint distribution can be recovered

through Gibbs sampling (see Section 3.2.3 for details). From the joint distribution, we can extract any probabilities of interest.

For example, the DN in Figure 3.1 models the set of variables: $\mathbf{X} = \{X_1, X_2, X_3, X_4, X_5\}$. Each node is conditionally independent of the other nodes in the graph given its immediate neighbors (e.g., X_1 is conditionally independent of $\{X_2, X_4\}$ given $\{X_3, X_5\}$). Each node contains a CPD, which specifies a probability distribution over its possible values, given the values of its parents.

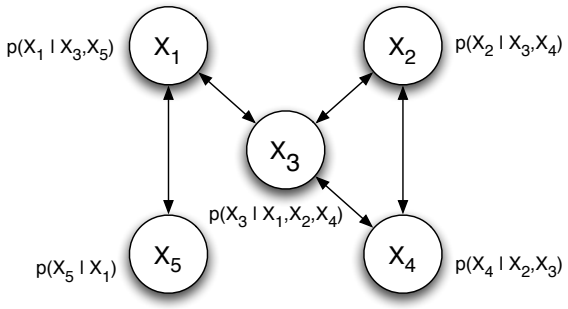

Figure 3.1. Example DN.

3.1.2 DN Learning

Both the structure and parameters of DNs are determined through learning the local CPDs. The DN learning algorithm learns a separate distribution for each variable X_i, conditioned on the other variables in the data (i.e., $\mathbf{X} - \{X_i\}$). Any conditional learner can be used for this task (e.g., logistic regression, decision trees). The CPD is included in the model as $P(v_i)$ and the variables selected by the conditional learner form the parents of X_i (e.g., if $p(x_i|\{\mathbf{x} - x_i\}) = \alpha x_j + \beta x_k$ then $PA_i = \{x_j, x_k\}$). The parents are then reflected in the edges of G appropriately. If the conditional learner is not selective (i.e., the algorithm does not select a subset of the features), the DN will be fully connected (i.e., $PA_i = \mathbf{x} - \{x_i\}$). In order to build understandable DNs,

it is desirable to use a selective learner that will learn CPDs that use a subset of all available variables.

3.1.3 DN Inference

Although the DN approach to structure learning is simple and efficient, it can result in an inconsistent network, both structurally and numerically. In other words, there may be no joint distribution from which each of the CPDs can be obtained using the rules of probability. Learning the CPDs independently with a selective conditional learner can result in a network that contains a directed edge from X_i to X_j, but not from X_j to X_i. This is a structural inconsistency—X_i and X_j are dependent but X_j is not represented in the CPD for X_i. In addition, learning the CPDs independently from finite samples may result in numerical inconsistencies in the parameter estimates. If this is the case, the joint distribution derived numerically from the CPDs will not sum to one. However, when a DN is inconsistent, approximate inference techniques can still be used to estimate a full joint distribution and extract probabilities of interest. Gibbs sampling can be used to recover a full joint distribution, regardless of the consistency of the local CPDs, provided that each X_i is discrete and its CPD is positive [33]. In practice, Heckerman et al. [33] show that DNs are nearly consistent if learned from large datasets because the data serve a coordinating function to ensure some degree of consistency among the CPDs.

3.2 Relational Dependency Networks

Several characteristics of DNs are particularly desirable for modeling relational data. First, learning a collection of conditional models offers significant efficiency gains over learning a full joint model. This is generally true, but it is even more pertinent to relational settings where the feature space is very large. Second, networks that are easy to interpret and understand aid analysts' assessment of the utility

of the relational information. Third, the ability to represent cycles in a network facilitates reasoning with autocorrelation, a common characteristic of relational data. In addition, whereas the need for approximate inference is a disadvantage of DNs for propositional data, due to the complexity of relational model graphs in practice, all PRMs use approximate inference.

Relational dependency networks extend DNs to work with relational data in much the same way that RBNs extend Bayesian networks and RMNs extend Markov networks. We describe the characteristics of RDNs within the PRM framework described in Section 2.5.

3.2.1 RDN Representation

Relational dependency networks encode probabilistic relationships in a similar manner to DNs, extending the representation to a relational setting. RDNs define a generic dependency structure at the level of item types, using a directed model graph G_M and a set of conditional probability distributions P. Each node $v_i \in V_M$ corresponds to an $X_k^t \in \mathbf{X^t}$, $t \in T$. The set of variables $\mathbf{X_k^t} = (X_{ik}^t : (v_i \in V_D \ \vee \ e_i \in E_D) \wedge T(i) = t)$ is tied together and modeled as a single variable X_k^t, with an associated conditional distribution $p(x_k^t \mid pa_{x_k^t})$.

Figure 2.3b illustrates an example RDN model graph for the data graph in Figure 2.3a. The graphical representation illustrates the qualitative component (G_D) of the RDN—it does not depict the quantitative component (P) of the model, which consists of CPDs that use aggregation functions. Although conditional independence is inferred using an undirected view of the graph, directed edges are useful for representing the set of variables in each CPD. For example, in Figure 2.3b the CPD for *year* contains *topic* but the CPD for *topic* does not contain *year*. This represents inconsistencies that may result from the RDN learning technique.

A *consistent RDN* specifies a joint probability distribution $p(\mathbf{x})$ over the attribute values of a relational dataset from which each CPD $\in P$ can be derived using the rules of probability. There is a direct correspondence between consistent *RDN*s and relational Markov networks. It is similar to the correspondence between consistent *DN*s and Markov networks [33], but the correspondence is defined with respect to the template model graphs G_M and U_M.

Theorem 1. *The set of positive distributions that can be encoded by a consistent RDN* (G_M, P) *is equal to the set of positive distributions that can be encoded by an* $RMN(U_M, \Phi)$ *provided (1)* $G_M = U_M$*, and (2)* P *and* Φ *use the same aggregations functions.*

Proof. Let p be a positive distribution defined by an RMN (U_M, Φ) for G_D. First, we construct a Markov network with tied clique potentials by rolling out the RMN inference graph U_I over the data graph G_D. By Theorem 1 of [33], which uses the Hammersley-Clifford theorem [3], there is a corresponding dependency network that represents the same distribution p as the Markov network U_I. Since the conditional probability distribution for each occurrence of an attribute k of a given type t (i.e., $\forall i\ (v_i \in V_D \vee e_i \in E_D) \wedge T(i) = t\ p(x_{ik}^t|\mathbf{x})$) is derived from the Markov network, we know that the resulting CPDs will be identical—the nodes adjacent to each occurrence are equivalent by definition, thus by the global Markov property the derived CPDs will be identical. From this dependency network we can construct a consistent RDN (G_M, P) by first setting $G_M = U_M$. Next, we compute from U_I the CPDs for the attributes of each item type: $p(x_k^t|\mathbf{x} - \{x_k^t\})$ for $t \in T, X_k^t \in \mathbf{X^t}$. To derive the CPDs for P, the CPDs must utilize the same aggregation functions as the potentials in Φ. Since the adjacencies in the RDN model graph are the same as those in the RMN model graph, and there is a correspondence between the rolled out DN and MN, the distribution encoded by the RDN is p.

Next let p be a positive distribution defined by an RDN (G_M, P) for G_D. First, we construct a dependency network with tied CPDs by rolling out the RDN inference graph G_I over the data graph G_D. Again, by Theorem 1 of [33], there is a corresponding Markov network that represents the same distribution p as the dependency network G_I. Of the valid Markov networks representing p, there will exist a network where the potentials are tied across occurrences of the same clique template (i.e., $\forall c_i \in C \quad \phi_C(x_C)$). This follows from the first part of the proof, which shows that each RMN with tied clique potentials can be transformed to an RDN with tied CPDs. From this Markov network we can construct an RMN (U_M, Φ) by setting $U_M = G_M$ and grouping the set of clique template potentials in Φ. Since the adjacencies in the RMN model graph are the same as those in the RDN model graph, and since there is a correspondence between the rolled out MN and DN, the distribution encoded by the RMN is p. □

This proof shows an exact correspondence between *consistent* RDNs and RMNs. We cannot show the same correspondence for general RDNs. However, we show in Section 3.2.3 that Gibbs sampling can be used to extract a unique joint distribution, regardless of the consistency of the model.

3.2.2 RDN Learning

Learning a PRM consists of two tasks: learning the dependency structure among the attributes of each object type, and estimating the parameters of the local probability models for an attribute given its parents. Relatively efficient techniques exist for learning both the structure and parameters of RBNs. However, these techniques exploit the requirement that the CPDs *factor* the full distribution—a requirement that imposes acyclicity constraints on the model and precludes the learning of arbitrary autocorrelation dependencies. On the other hand, although, in principle, it is possible for RMN techniques to learn cyclic autocorrelation dependencies, inef-

ficiencies due to calculating the normalizing constant Z in undirected models make this difficult in practice. Calculation of Z requires a summation over all possible states $\mathbf{x}$. When modeling the joint distribution of propositional data, the number of states is exponential in the number of attributes (i.e., $O(2^m)$). When modeling the joint distribution of relational data, the number of states is exponential in the number of attributes and *the number of instances*. If there are N objects, each with m attributes, then the total number of states is $O(2^{Nm})$. For any reasonable-size dataset, a single calculation of Z is an enormous computational burden. Feature selection generally requires repeated parameter estimation while measuring the change in likelihood affected by each attribute, which would require recalculation of Z on each iteration.

The *RDN* learning algorithm uses a more efficient alternative—estimating the set of conditional distributions independently rather than jointly. This approach is based on *pseudolikelihood* techniques [4], which were developed for modeling spatial datasets with similar autocorrelation dependencies. The pseudolikelihood for data graph G_D is computed as a product over the item types T, the attributes of that type X^t, and the items of that type v, e:

$$PL(G_D;\theta) = \prod_{t \in T} \prod_{X_i^t \in X^t} \prod_{v:T(v)=t} p(x_{vi}^t | pa_{x_{vi}^t};\theta) \prod_{e:T(e)=t} p(x_{ei}^t | pa_{x_{ei}^t};\theta) \tag{3.1}$$

On the surface, Equation 3.1 may appear similar to a likelihood that specifies a joint distribution of an *RBN*. However, the CPDs in the *RDN* pseudolikelihood are not required to factor the joint distribution of G_D. More specifically, when we consider the variable X_{vi}^t, we condition on the values of the parents $PA_{X_{vi}^t}$ regardless of whether the estimation of CPDs for variables in $PA_{X_{vi}^t}$ was conditioned on X_{vi}^t. The parents of X_{vi}^t may include other variables on the same item (e.g., $X_{vi'}^t$ such that $i' \neq i$), the same variable on related items (e.g., $X_{v'i}^t$ such that $v' \neq v$), or other variables on related items (e.g., $X_{v'i'}^{t'}$ such that $v' \neq v$ and $i' \neq i$).

Pseudolikelihood estimation avoids the complexities of estimating Z and the requirement of acyclicity. Instead of optimizing the log-likelihood of the full joint distribution, we optimize the pseudo-loglikelihood. The contribution for each variable is conditioned on all other attribute values in the data, thus we can maximize the pseudo-loglikelihood for each variable independently:

$$log\ PL(G_D;\theta) = \sum_{t\in T} \sum_{X_i^t \in X^t} \sum_{v:T(v)=t} log\ p(x_{vi}^t | pa_{x_{vi}^t};\theta) + \sum_{e:T(e)=t} log\ p(x_{ei}^t | pa_{x_{ei}^t};\theta)$$

In addition, this approach can utilize existing techniques for learning conditional probability distributions of relational data such as first-order Bayesian classifiers [24], structural logistic regression [82], or *ACORA* [79].

Maximizing the pseudolikelihood function gives the maximum pseudolikelihood estimate (MPLE) of θ. To estimate the parameters we need to solve the following pseudolikelihood equation:

$$\frac{\partial}{\partial\theta} PL(G_D;\theta) = 0 \tag{3.2}$$

With this approach, we lose the asymptotic efficiency properties of maximum likelihood estimators. However, under some general conditions the asymptotic properties of the MPLE can be established. In particular, in the limit as sample size grows, the MPLE will be an unbiased estimate of the true parameter θ_0 and it will be normally distributed. Geman and Graffine [28] established the first proof of the properties of maximum pseudolikelihood estimators of fully observed data. Gidas [31] gives an alternative proof and Comets [10] establishes a more general proof that does not require finite state space $\mathbf{x}$ or stationarity of the true distribution P_{θ_0}.

Theorem 2. *Assuming the following regularity conditions*[2] *are satisfied for an RDN:*

1. *The model is identifiable, that is if* $\theta \neq \theta'$, *then* $PL(G_D;\theta) \neq PL(G_D;\theta')$.

[2]These are the standard regularity conditions (e.g., [8]) used to prove asymptotic properties of estimators, which are usually satisfied in most reasonable problems.

2. *The distributions $PL(G_D;\theta)$ have common support and are differentiable with respect to θ.*

3. *The parameter space Ω contains an open set ω of which the true parameter θ_0 is an interior point.*

In addition, assuming the pseudolikelihood equation (3.2) has a unique solution in ω almost surely as $|G_D| \to \infty$, then, provided that G_D is of bounded degree, the MPLE $\tilde{\theta}$ converges in probability to the true value θ_0 as $|G_D| \to \infty$.

Proof. Provided the size of the *RDN* model graph does not grow as the size of the dataset grows (i.e., $|P|$ remains constant as $|G_D| \to \infty$) and G_D is of bounded degree, then previous proofs apply. We provide the intuition for the proof here and refer the reader to [10, 93, 53] for details. Let $\tilde{\theta}$ be the maximum pseudolikelihood estimate that maximizes $PL(G_D;\theta)$. As $|G_D| \to \infty$, the data will consist of all possible data configurations for each CPD $\in P$ (assuming bounded degree structure in G_D). As such, the pseudolikelihood function will converge to its expectation, $PL(G_D;\theta) \to E(PL(G_D;\theta))$. The expectation is maximized by the true parameter θ_0 because the expectation is taken with respect to all possible data configurations. Therefore as $|G_D| \to \infty$, the MPLE converges to the true parameter (i.e., $\tilde{\theta} - \theta_0 \to 0$). □

The *RDN* learning algorithm is similar to the *DN* learning algorithm, except we use a relational probability estimation algorithm to learn the set of conditional models, maximizing pseudolikelihood for each variable separately. The algorithm input consists of: (1) G_D: a relational data graph, (2) R: a conditional relational learner, and (3) $\mathbf{Q^t}$: a set of queries[3] that specify the relational neighborhood considered in R for each type T.

[3]Our implementation utilizes a set of user-specified queries to limit the search space considered during learning. However, a simple depth limit (e.g., ≤ 2 links away in the data graph) can be used to limit the search space as well.

Table 1 outlines the learning algorithm in pseudocode. It cycles over each attribute of each item type and learns a separate CPD, conditioned on the other values in the training data. We discuss details of the subcomponents (querying and relational learners) in the sections below.

Quantifying the asymptotic complexity of PRM learners is difficult due to the use of heuristic search and numerical optimization techniques. The asymptotic complexity of RDN learning is $O(|\mathbf{X}| \cdot |PA_X| \cdot N)$, where $|\mathbf{X}|$ is the number of CPDs to be estimated, $|PA_X|$ is the number of attributes, and N is the number of instances, used to estimate the CPD for X.[4] RBN learning requires multiple rounds of parameter estimation during the algorithm's heuristic search through the model space, and each round of parameter estimation has the same complexity as RDN learning, thus RBN learning will generally require more time. For RMN learning, there is no closed-form parameter estimation technique. Instead, the models are trained using conjugate gradient, where each iteration requires approximate inference over the unrolled Markov network. In general this RMN nested loop of optimization and approximation will require more time to learn than an RBN [89]. Therefore, given equivalent search spaces, RMN learning is generally more complex than RBN learning, and RBN learning is generally more complex than RDN learning.

3.2.2.1 Conditional Relational Learners

The conditional relational learner R is used for both parameter estimation and structure learning in RDNs. The variables selected by R are reflected in the edges of G_M appropriately. If R selects all of the available attributes, the RDN will be fully connected.

---

[4]This assumes the complexity of the relational learner R is $O(|PA_X| \cdot N)$, which is true for the conditional relational learners considered in this work (i.e., RBCs and RPTs).

Learn RDN $(G_D, R, \mathbf{Q^t})$:
$P \leftarrow \emptyset$
For each $t \in T$:
  For each $X_k^t \in \mathbf{X^t}$:
    Use R to learn a CPD for X_k^t given the attributes in the relational neighborhood defined by Q^t.
    $P \leftarrow P \cup CPD_{X_k^t}$
Use P to form G_M.

Table 3.1. *RDN* learning algorithm.

In principle, any conditional relational learner can be used as a subcomponent to learn the individual CPDs provided that it can closely approximate CPDs consistent with the joint distribution. In this chapter, we discuss the use of two different conditional models—relational Bayesian classifiers (*RBC*s) [76] and relational probability trees (*RPT*s) [75].

Relational Bayesian Classifiers

*RBC*s extend naive Bayesian classifiers to a relational setting. *RBC*s treat heterogeneous relational subgraphs as a homogenous set of attribute multisets. For example, when considering the references of a single paper, the publication dates of those references form multisets of varying size (e.g., {1995, 1995, 1996}, {1975, 1986, 1998, 1998}). The *RBC* assumes each value of a multiset is independently drawn from the same multinomial distribution.[5] This approach is designed to mirror the independence assumption of the naive Bayesian classifier. In addition to the conventional assumption of attribute independence, the *RBC* also assumes attribute value independence within each multiset.

[5]Alternative constructions are possible but prior work [76] has shown this approach achieves superior performance over a wide range of conditions.

For a given item type $t \in T$, the query scope specifies the set of item types $\mathbf{T_R}$ that form the relevant relational neighborhood for t. Note that $\mathbf{T_R}$ does not necessarily contain all item types in the database and the query may also dynamically introduce new types in the returned view of the database (e.g., papers → papers *and* references). For example, in Figure 3.3a, $t = paper$ and $\mathbf{T_R} = \{paper, author, reference, authorof, cites\}$. To estimate the CPD for attribute X on items t (e.g., paper topic), the *RBC* considers all the attributes associated with the types in $\mathbf{T_R}$. *RBC*s are non-selective models, thus all attributes are included as parents:

$$p(x|pa_x) \propto \prod_{t' \in \mathbf{T_R}} \prod_{X_i^{t'} \in X^{t'}} \prod_{v \in T_R(x)} p(x_{vi}^{t'}|x) \;\; p(x)$$

Relational Probability Trees

*RPT*s are selective models that extend classification trees to a relational setting. *RPT*s also treat heterogeneous relational subgraphs as a set of attribute multisets, but instead of modeling the multisets as independent values drawn from a multinomial, the *RPT* algorithm uses aggregation functions to map a set of values into a single feature value. For example, when considering the publication dates on references of a research paper, the *RPT* could construct a feature that tests whether the *average* publication date was after 1995. Figure 3.2 provides an example *RPT* learned on citation data.[6]

The *RPT* algorithm automatically constructs and searches over aggregated relational features to model the distribution of the target variable X on items of type t. The algorithm constructs features from the attributes associated with the types $\mathbf{T_R}$ specified in the query for t. The algorithm considers four classes of aggregation functions to group multiset values: *mode, count, proportion, and degree*. For discrete

[6]The leaves of the tree represent probability distributions over the class label values graphically, with each color corresponding to a class label value.

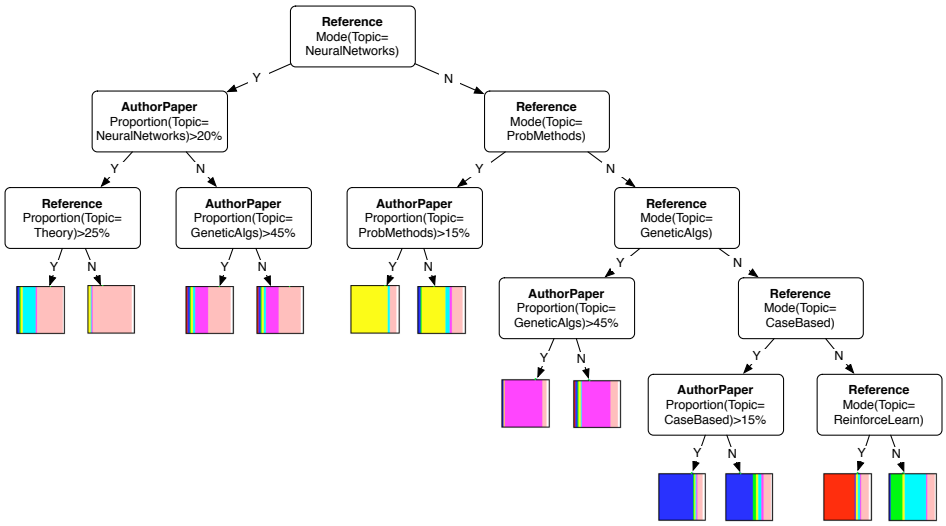

Figure 3.2. Example *RPT* to predict machine-learning paper topic.

attributes, the algorithm constructs features for all unique values of an attribute. For continuous attributes, the algorithm constructs aggregate features for a number of different discretizations, first binning the values by frequency (e.g., $year > 1992$). Count, proportion, and degree features consider a number of different thresholds (e.g., $proportion(A) > 10\%$). All experiments reported herein considered 10 thresholds and discretizations per feature.

The *RPT* algorithm uses recursive greedy partitioning, splitting on the feature that maximizes the correlation between the feature and the class. Feature scores are calculated using the chi-square statistic and the algorithm uses pre-pruning in the form of a p-value cutoff and a depth cutoff to limit tree size and overfitting. All experiments reported herein used *p-value cutoff*=$0.05/|attributes|$, *depth cutoff*=7. Although the objective function does not optimize pseudolikelihood directly, probability estimation trees can be used effectively to approximate CPDs consistent with the underlying joint distribution [33].

The *RPT* learning algorithm adjusts for biases towards particular features due to degree disparity and autocorrelation in relational data [40, 41]. We have shown that

*RPT*s build significantly smaller trees than other conditional models and achieve equivalent, or better, performance [75]. These characteristics of *RPT*s are crucial for learning understandable *RDN*s and have a direct impact on inference efficiency because smaller trees limit the size of the final inference graph.

3.2.2.2 Queries

In our implementation, we utilize user-specified queries to limit the relational neighborhoods that will be considered by the conditional learner R. The queries' structures define a typing over instances in the database. Subgraphs are extracted from a larger graph database using the visual query language QGraph [5]. Queries allow for variation in the number and types of objects and links that form the subgraphs and return collections of all matching subgraphs from the database.

For example, consider the query in Figure 3.3a.[7] The query specifies match criteria for a target item (paper) and its local relational neighborhood (authors and references). The example query matches all research papers that were published in 1995 and returns for each paper a subgraph that includes all authors and references associated with the paper. Textual annotations specify match conditions on attribute values; numerical annotations (e.g., [0..]) specify constraints on the cardinality of matched objects (e.g., zero or more authors). Note the constraint on paper ID in the lower left corner—this ensures that the target paper does not match as a reference in the resulting subgraphs. Figure 3.3b shows a hypothetical match to this query: a paper with two authors and seven references.

The query defines a typing over the objects of the database (e.g., people that have authored a paper are categorized as *authors*) and specifies the relevant relational context for the target item type in the model. For example, given this query the

[7]We have modified QGraph's visual representation to conform to our convention of using rectangles to represent objects and dashed lines to represent relations.

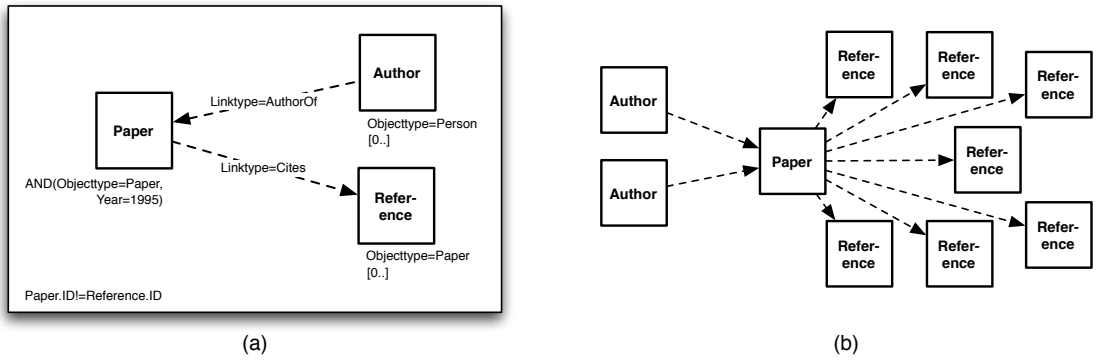

Figure 3.3. (a) Example QGraph query, and (b) matching subgraph.

learner R would model the distribution of a paper's attributes given the attributes of the paper itself and the attributes of its related authors and references. The queries are a means of restricting model search. Instead of setting a simple depth limit on the extent of the search, the analyst has a more flexible means with which to limit the search (e.g., we can consider other papers written by the paper's authors but not other authors of the paper's references, both at the same depth).

3.2.3 RDN Inference

The *RDN* inference graph G_I is potentially much larger than the original data graph. To model the full joint distribution there must be a separate node (and CPD) for each attribute value in G_D. To construct G_I, the set of template CPDs in P is rolled out over the test-set data graph. Each item-attribute pair gets a separate, local copy of the appropriate CPD. Consequently, the total number of nodes in the inference graph will be $\sum_{v \in V_D} |\mathbf{X}^{\mathbf{T(v)}}| + \sum_{e \in E_D} |\mathbf{X}^{\mathbf{T(e)}}|$. Roll out facilitates generalization across data graphs of varying size—we can learn the CPD templates from one data graph and apply the model to a second data graph with a different number of objects by rolling out more CPD copies. This approach is analogous to other graphical models that tie distributions across the network and roll out copies of model templates (e.g., hidden Markov models, conditional random fields [51]).

We use randomly ordered Gibbs samplers (e.g., [65]) for inference in *RDN*s. This refers to a procedure where a random ordering of the variables is selected; each variable is initialized to an arbitrary value; and then each variable is visited (repeatedly) in order, where its value is resampled according to its conditional distribution. Gibbs sampling can be used to extract a unique joint distribution, regardless of the consistency of the model.

Theorem 3. *The procedure of a randomly ordered Gibbs sampler applied to an RDN* (G, P)*, where each* X_i *is discrete and each local distribution in* P *is positive, defines a Markov chain with a unique stationary joint distribution* $\tilde{\pi}$ *for* $\mathbf{X}$ *that can be reached from any initial state of the chain.*

Proof. The proof that Gibbs sampling can be used to estimate the joint distribution of a dependency network [33] applies to rolled out *RDN*s as well. We restate the proof here for completeness.

Let $\mathbf{x}^t$ be the sample of $\mathbf{x}$ after the t^{th} iteration of the Gibbs sampler. The sequence $\mathbf{x}^1, \mathbf{x}^2, ...$ can be viewed as samples drawn from a homogeneous Markov chain with transition matrix $\tilde{\mathbf{P}}$, where $\tilde{\mathbf{P}}_{ij} = p(\mathbf{x}^{t+1} = j | \mathbf{x}^t = i)$. The matrix $\tilde{\mathbf{P}}$ is the product $\tilde{\mathbf{P}}^1 \cdot \tilde{\mathbf{P}}^2 \cdot ... \cdot \tilde{\mathbf{P}}^n$, where $\tilde{\mathbf{P}}^k$ is the *local* transition matrix describing the resampling of X^k according to the local distribution of $p(x_k | \mathbf{pa}_k)$. The positivity of the local distributions guarantees the positivity of $\tilde{\mathbf{P}}$. The positivity of $\tilde{\mathbf{P}}$ in turn guarantees that the Markov chain is irreducible and aperiodic. Consequently there exists a unique joint distribution that is stationary with respect to $\tilde{\mathbf{P}}$, and this stationary distribution can be reached from any starting point. □

This shows that an ordered Gibbs sampling procedure can be used with an *RDN* to recover samples from a unique stationary distribution $\tilde{\pi}$, but how close will this distribution be to the true distribution π? Small perturbations in the local CPDs could propagate in the Gibbs sampling procedure to produce large deviations in the

stationary distribution. Heckerman et al. [33] provide some initial theoretical analysis that suggests that Markov chains with good convergence properties will be insensitive to deviations in the transition matrix. This implies that when Gibbs sampling is effective (i.e., converges), then $\tilde{\pi}$ will be close to π and the RDN will be a close approximation to the full joint distribution.

Table 2 outlines the inference algorithm. To estimate a joint distribution, we start by rolling out the model G_M onto the target dataset G_D and forming the inference graph G_I. The values of all unobserved variables are initialized to values drawn from their prior distributions. Gibbs sampling then iteratively relabels each unobserved variable by drawing from its local conditional distribution, given the current state of the rest of the graph. After a sufficient number of iterations (*burn in*), the values will be drawn from a stationary distribution and we can use the samples to estimate probabilities of interest.

For prediction tasks, we are often interested in the marginal probabilities associated with a single variable X (e.g., paper topic). Although Gibbs sampling may be a relatively inefficient approach to estimating the probability associated with a joint assignment of values of X (e.g., when $|X|$ is large), it is often reasonably fast to use Gibbs sampling to estimate the marginal probabilities for each X.

There are many implementation issues that can improve the estimates obtained from a Gibbs sampling chain, such as length of burn-in and number of samples. For the experiments reported in this work, we used fixed-length chains of 2000 samples (each iteration re-labels every value sequentially) with burn-in set at 100. Empirical inspection indicated that the majority of chains had converged by 500 samples. Section 3.3.1 includes convergence graphs for synthetic data experiments.

Infer RDN $(G_D, G_M, P, iter, burnin)$:

$G_I(V_I, E_I) \leftarrow (\emptyset, \emptyset)$ \\ *form* G_I *from* G_D *and* G_M
For each $t \in T$ *in* G_M:
  For each $X_k^t \in \mathbf{X^t}$ *in* G_M:
    For each $v_i \in V_D$ *s.t.* $T(v_i) = t$ and $e_i \in E_D$ *s.t.* $T(e_i) = t$:
      $V_I \leftarrow V_I \cup \{X_{ik}^t\}$
    For each $v_i \in V_D$ *s.t.* $T(v_i) = t$ and $e_i \in E_D$ *s.t.* $T(e_i) = t$:
      For each $v_j \in V_D$ *s.t.* $X_{v_j} \in pa_{X_{ik}^t}$ and each $e_j \in E_D$ *s.t.* $X_{e_j} \in pa_{X_{ik}^t}$:
        $E_I \leftarrow E_I \cup \{e_{ij}\}$

For each $v \in V_I$: \\ *initialize Gibbs sampling*
  Randomly initialize x_v to value drawn from prior distribution $p(x_v)$

$S \leftarrow \emptyset$ \\ *Gibbs sampling procedure*
Choose a random ordering over V_I
For $i \in iter$:
  For each $v \in V_I$, in random order:
    Resample x'_v from $p(x_v|\mathbf{x} - \{x_v\})$
    $x_v \leftarrow x'_v$
    If $i > burnin$:
      $S \leftarrow S \cup \{\mathbf{x}\}$:
Use samples S to estimate probabilities of interest

Table 3.2. *RDN* inference algorithm.

3.3 Experimental Evaluation

The experiments in this section demonstrate the utility of RDNs as a joint model of relational data. First, we use synthetic data to assess the impact of training-set size and autocorrelation on RDN learning and inference, showing that accurate models can be learned with reasonable dataset sizes and that RDN learning is robust to varying levels of autocorrelation. In addition, to assess the quality of the RDN approximation for inference, we compare RDNs to RMNs, showing that RDNs achieve equivalent or better performance over a range of datasets. Next, we learn RDNs of five real-world datasets to illustrate the types of domain knowledge that the models discover automatically. In addition, we evaluate RDNs in a prediction context, where only a single attribute is unobserved in the test set, and report significant performance gains compared to two individual models.

3.3.1 Synthetic Data Experiments

To explore the effects of training-set size and autocorrelation on RDN learning and inference, we generated homogeneous data graphs with an autocorrelated class label and linkage due to an underlying (hidden) group structure. Each object has four boolean attributes: X_1, X_2, X_3, and X_4. See appendix A.1.1 for a detailed description of the data generation process.

We compare two different RDNs, learning models with queries that include all neighbors one link away in the data graph. The RDN_{RBC} uses RBCs for the component learner R; the RDN_{RPT} uses RPTs for R. The RPT performs feature selection, which may result in structural inconsistencies in the learned RDN. The RBC does not use feature selection so any deviation from the true model is due to parameter inconsistencies alone. Note that the two models do not consider identical feature spaces so we can only roughly assess the impact of feature selection by comparing RDN_{RBC} and RDN_{RPT} results.

3.3.1.1 RDN Learning

The first set of synthetic experiments examines the effectiveness of the *RDN* learning algorithm. Our theoretical analysis indicates that, in the limit, the true parameters will maximize the pseudolikelihood function. This implies that the pseudolikelihood function, evaluated at the learned parameters, will be no greater than the pseudolikelihood of the true model (on average). To evaluate the quality of the *RDN* parameter estimates, we calculated the pseudolikelihood of the test-set data using both the true model (used to generate the data) and the learned models. If the pseudolikelihood given the learned parameters approaches the pseudolikelihood given the true parameters, then we can conclude that parameter estimation is successful. We also measured the standard error of the pseudolikelihood estimate for a single test-set using learned models from 10 different training sets. This illustrates the amount of variance due to parameter estimation.

Figure 3.4 graphs the pseudo-loglikelihood of learned models as a function of training-set size for three levels of autocorrelation. Training-set size was varied at the levels $\{50, 100, 250, 500, 1000, 5000\}$. We varied $p(X_1|\mathbf{X}_{\mathbf{1}R}, X_2)$ to generate data with approximate levels of autocorrelation corresponding to $\{0.25, 0.50, 0.75\}$. At each training set size (and autocorrelation level), we generated 10 test sets. For each test set, we generated 10 training sets and learned *RDN*s. Using each learned model, we measured the pseudolikelihood of the test set (size 250) and averaged the results over the 10 models. We plot the mean pseudolikelihood for both the learned models and the *RDN* used for data generation, which we refer to as *True Model*. The top row reports experiments with data generated from an RDN_{RPT} where we learned an RDN_{RPT}. The bottom row reports experiments with data generated from an RDN_{RBC}, where we learned an RDN_{RBC}.

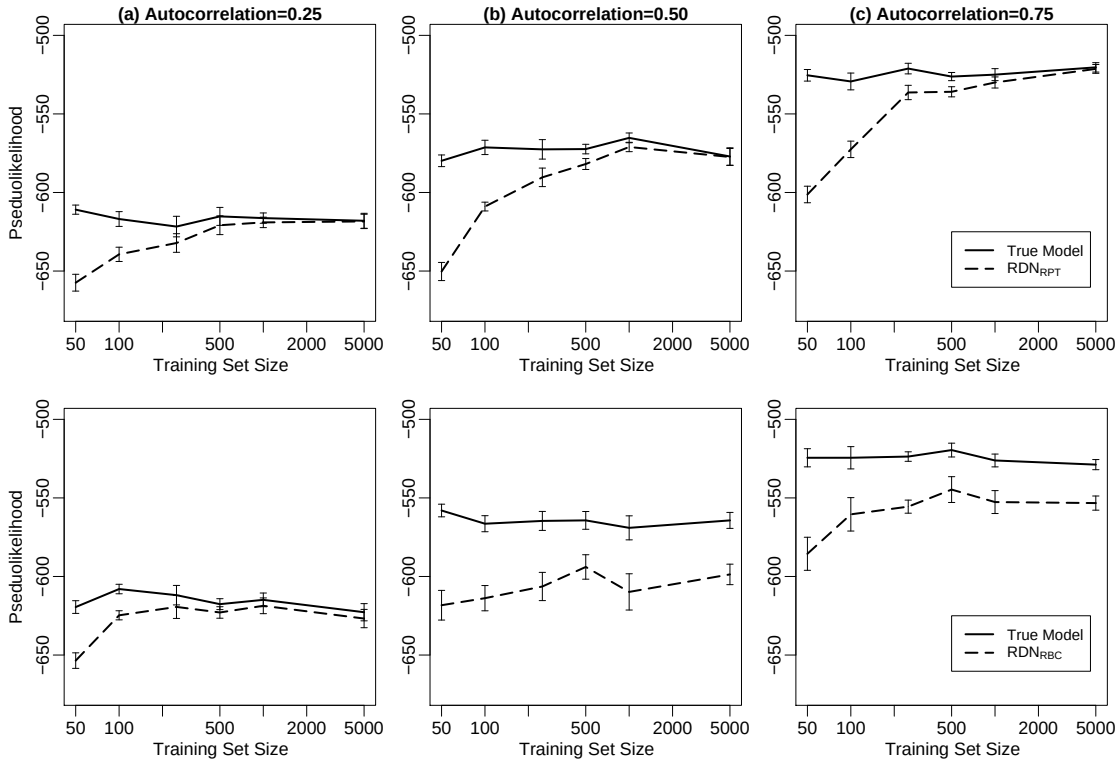

Figure 3.4. Evaluation of RDN_{RPT} (top row) and RDN_{RBC} (bottom row) learning.

These experiments show that the learned RDN_{RPT} is a good approximation to the true model by the time training-set size reaches 500, and that RDN_{RPT} learning is robust with respect to varying levels of autocorrelation.

There appears to be little difference between the RDN_{RPT} and RDN_{RBC} when autocorrelation is low, but otherwise the RDN_{RBC} needs significantly more data to estimate the parameters accurately. One possible source of error is variance due to lack of selectivity in the RDN_{RBC}(i.e., the model uses all available attributes), which necessitates the estimation of a greater number of parameters. However, there is little improvement even when we increase the size of the training sets to 10,000 objects. Furthermore, the discrepancy between the estimated model and the true model is greatest when autocorrelation is moderate. This indicates that the inaccuracies may be due to the naive Bayes independence assumption and its tendency to produce biased probability estimates [96].

3.3.1.2 RDN Inference

The second set of synthetic experiments evaluates the RDN inference procedure in a prediction context, where only a single attribute is unobserved in the test set. We generated data in the manner described above and learned models to predict X_1 using the intrinsic attributes of the object (X_2, X_3, X_4) as well as the class label and the attributes of directly related objects (X_1, X_2, X_3, X_4). At each autocorrelation level, we generated 10 training sets (size 500) to learn the models. For each training set, we generated 10 test sets (size 250) and used the learned models to infer marginal probabilities for X_1 on the test set instances. To evaluate the predictions, we report AUC results.[8] These experiments used the same levels of autocorrelation outlined above.

[8]Squared-loss results are qualitatively similar to the AUC results reported in Figure 3.5.

We compare the performance of four types of models. First, we measure the performance of RPTs and RBCs. These are *individual models* that represent each instance independently and do not use the class labels of related instances. Second, we measure the performance of the two RDNs described above: RDN_{RBC} and RDN_{RPT}. Third, we measure performance of the two RDNs while allowing the true labels of related instances to be utilized during inference. This demonstrates the level of performance possible if the RDNs could infer the true labels of related instances with perfect accuracy. We refer to these as *ceiling models*: RDN^{Ceil}_{RBC} and RDN^{Ceil}_{RPT}. Fourth, we measure the performance of two RMNs described below.

The first RMN is non-selective. We construct features from all the attributes available to the RDNs, defining clique templates for each pairwise combination of class label value and attribute value. More specifically, the available attributes consist of the intrinsic attributes of objects, and both the class label and attributes of directly related objects. The second RMN model, which we refer to as RMN_{Sel}, is a hybrid selective model—clique templates are only specified for the set of attributes selected by the RDN during learning. For both models, we used maximum-a-posteriori parameter estimation to estimate the feature weights, using conjugate gradient with zero-mean Gaussian priors, and a uniform prior variance of 5.[9] For RMN inference, we used loopy belief propagation [64].

We do not compare directly to RBNs because their acyclicity constraint prevents them from representing the autocorrelation dependencies in this domain. Instead, we include the performance of individual models, which also cannot represent the autocorrelation of X_1. Although RBNs and individual models cannot represent the autocorrelation directly, they can exploit the autocorrelation indirectly by using the observed attributes of related instances. For example, if there is a correlation be-

[9]We experimented with a range of priors; this parameter setting produced the best empirical results.

tween the words on a webpage and its topic, and the topics of hyperlinked pages are autocorrelated, then the models can exploit autocorrelation dependencies indirectly by modeling the contents of a webpage's neighboring pages. Recent work has shown that collective models (e.g., RDNs) are a low-variance means of reducing bias through direct modeling of the autocorrelation dependencies [42]. Models that exploit autocorrelation dependencies indirectly by modeling the observed attributes of related instances, experience a dramatic increase in variance as the number of observed attributes increases.

During inference we varied the number of known class labels in the test set, measuring performance on the remaining unlabeled instances. This serves to illustrate model performance as the amount of information seeding the inference process increases. We conjecture that performance will be similar when other information seeds the inference process—for example, when some labels can be inferred from intrinsic attributes, or when weak predictions about many related instances serve to constrain the system. Figure 3.5 graphs AUC results for each model as the proportion of known class labels is varied.

The data for the first set of experiments (top row) were generated with an RDN_{RPT}. In all configurations, RDN_{RPT} performance is equivalent, or better than, RPT performance. This indicates that even modest levels of autocorrelation can be exploited to improve predictions using an RDN_{RPT}. RDN_{RPT} performance is indistinguishable from that of RDN_{RPT}^{Ceil} except when autocorrelation is high and there are no labels to seed inference. In this situation, there is little information to constrain the system during inference so the model cannot fully exploit the autocorrelation dependencies. When there is no information to anchor the predictions, there is an identifiability problem—symmetric labelings that are highly autocorrelated, but with opposite values, appear equally likely. In situations where there is little seed informa-

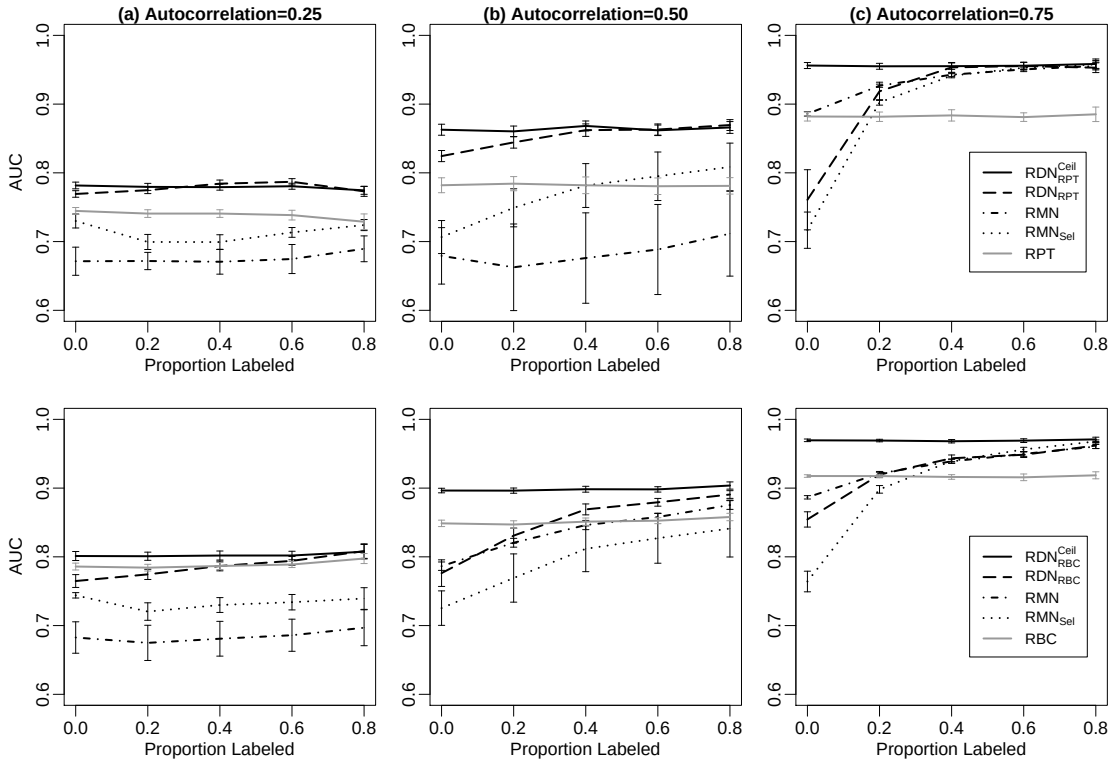

Figure 3.5. Evaluation of RDN_{RPT} (top row) and RDN_{RBC} (bottom row) inference.

tion, identifiability problems increase variance and bias RDN performance towards random.

When there is low or moderate autocorrelation, RDN_{RPT} performance is significantly higher than both RMN and RMN_{Sel}. In these situations, poor performance is likely due to a mismatch in feature space with the data generation model—if the RMN features cannot represent the data dependencies that are generated with aggregated features, the inferred probabilities will be biased. When there is high autocorrelation, RDN_{RPT} performance is indistinguishable from RMN, except when there are no labels to seed inference—the same situation where RDN_{RPT} fails to meet its ceiling. When autocorrelation is high, the mismatch in feature space is not a problem. In this situation, most neighbors share similar attribute values, thus the RMN features are able to accurately capture the data dependencies.

The data for the second set of experiments (bottom row) were generated with an RDN_{RBC}. The RDN_{RBC} feature space is roughly comparable to the RMN because the RDN_{RBC} uses multinomials to model individual neighbor attribute values. On these data, RDN_{RBC} performance is superior to RMN performance only when there is low autocorrelation. RMN_{Sel} uses fewer features than RMN and it has superior performance on the data with low autocorrelation, indicating that the RMN learning algorithm may be overfitting the feature weights and producing biased probability estimates. We experimented with a range of priors to limit the impact of weight overfitting, but the effect remained consistent.

RDN_{RBC} performance is superior to RBC performance only when there is moderate to high autocorrelation and sufficient seed information. When autocorrelation is low, the RBC is comparable to both the RDN_{RBC}^{Ceil} and RDN_{RBC}. Even when autocorrelation is moderate or high, RBC performance is still relatively high. Since the RBC is low-variance and there are only four attributes in our datasets, it is not surprising that the RBC is able to exploit autocorrelation to improve performance.

What is more surprising is that RDN_{RBC} requires substantially more seed information than RDN_{RPT} in order to reach ceiling performance. This indicates that our choice of model should take test-set characteristics (e.g., number of known labels) into consideration.

To investigate Gibbs sampling convergence, we tracked AUC throughout the RDN Gibbs sampling procedure. Figure 3.6 demonstrates AUC convergence on each inference task described above. We selected a single learned model at random from each task and report convergence from the trials corresponding to five different test sets. AUC improves very quickly, often leveling off within the first 250 iterations. This shows that the approximate inference techniques employed by the RDN may be quite efficient to use in practice. However, when autocorrelation is high, longer chains may be necessary to ensure convergence. There are only two chains that show a substantial increase in performance after 500 iterations and both occur in highly autocorrelated datasets. In addition, the RDN_{RBC} chains exhibit significantly more variance than the RDN_{RPT} chains, particularly when autocorrelation is high. This suggests that the use of longer Gibbs chains, or an approach that averages predictions obtained from multiple random restarts, would improve performance.

3.3.2 Empirical Data Experiments

We learned RDNs for five real-world relational datasets to illustrate the types of domain knowledge that can be learned, and we evaluated the models in a prediction context, where the values of a single attribute are unobserved.

We compared the models on five relational datasets (see appendix A.1.3 for a more detailed description of the data):

Gene: The data contain information about 1,243 genes and 1,734 interactions among their associated proteins. The class label was gene location (13 values).

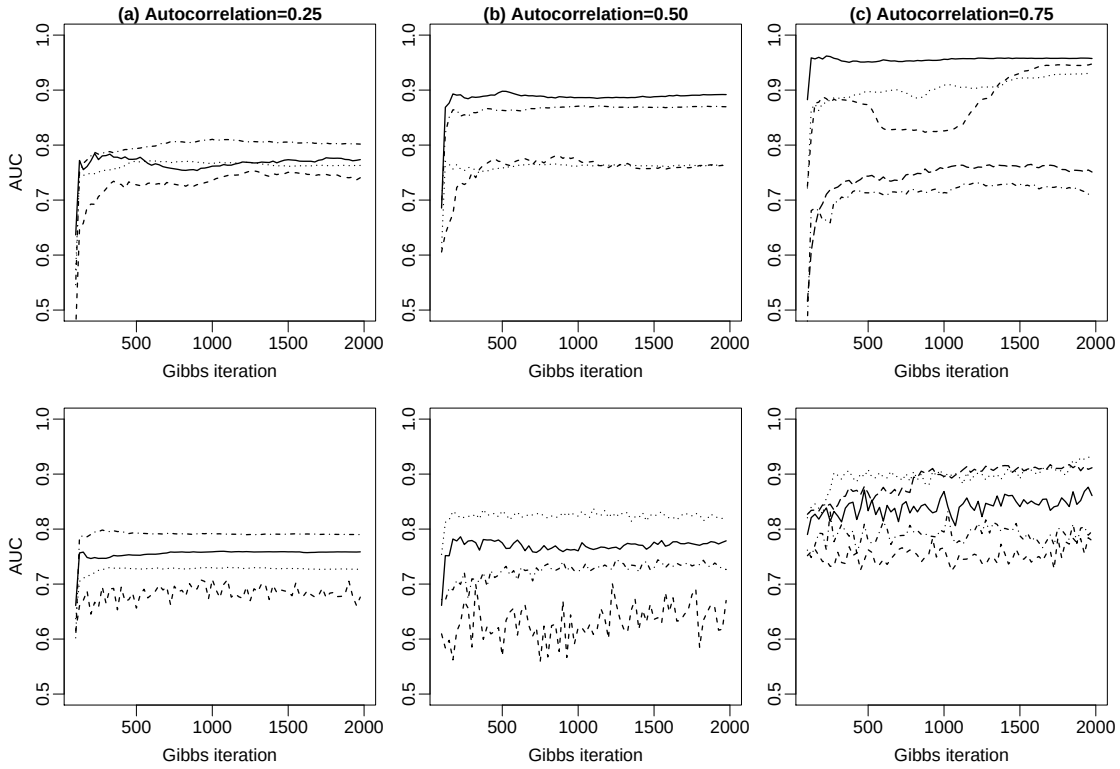

Figure 3.6. Gibbs convergence rates for five different trials of RDN_{RPT} (top row) and RDN_{RBC} (bottom row).

WebKB: The data comprise 3,877 web pages from four computer science departments. The class label was page category (five values).

IMDb: The data consist of a sample of 1,382 movies released in the U.S. between 1996 and 2001. In addition to movies, the data set contain objects representing actors, directors, and studios. The class label was opening weekend box-office receipts ($>$ and $\leq$ *$2million*).

Cora: The data consist of the sample of 4,330 machine-learning papers along with associated authors, cited papers, and journals. The class label was paper topic (seven values).

NASD: The data consist a sample of 10,000 brokers who were active in the years 1997-2001, along with approximately 12,000 associated branches, firms, and disclosures. The class label records whether the broker will be involved in fraud, or other serious misconduct, in the next calendar year (binary).

3.3.2.1 RDN Models

The *RDN*s in Figures 3.7-3.11 continue with the *RDN* representation introduced in Figure 2.3b. Each item type is represented by a separate plate. An arc from x to y indicates the presence of one or more features of x in the conditional model learned for y. Arcs inside a plate represent dependencies among the attributes of a single object. Arcs crossing plate boundaries represent dependencies among attributes of related objects, with edge labels indicating the underlying relations. When the dependency is on attributes of objects more than a single link away, the arc is labeled with a small rectangle to indicate the intervening related-object type. For example, in Figure 3.7 paper topic is influenced by the topics of other papers written by the paper's authors, so the arc is labeled with two *AuthoredBy* relations and a small A rectangle indicating an *Author* object.

In addition to dependencies among attribute values, relational learners may also learn dependencies between the structure of relations (edges in G_D) and attribute values. *Degree* relationships are represented by a small black circle in the corner of each plate—arcs from this circle indicate a dependency between the number of related objects and an attribute value of an object. For example, in Figure 3.7 author rank is influenced by the number of authors on the paper.

For each dataset, we learned an RDN_{RPT} with queries that included all neighbors up to two links away in the data graph. For example in Cora, when learning an RPT of a paper attribute, we considered the attributes of associated authors and journals, as well as papers related to those objects.

On the Cora data, we learned an RDN for seven attributes. Figure 3.7 shows the resulting RDN. The RDN learning algorithm selected 12 of the 139 dependencies considered for inclusion in the model. Four of the attributes—author rank, paper topic, paper type, and paper year—exhibit autocorrelation dependencies. In particular, the topic of a paper depends not only on the topics of other papers that it cites, but also on the topics of other papers written by the authors. This model is a good reflection of our domain knowledge about machine learning papers.

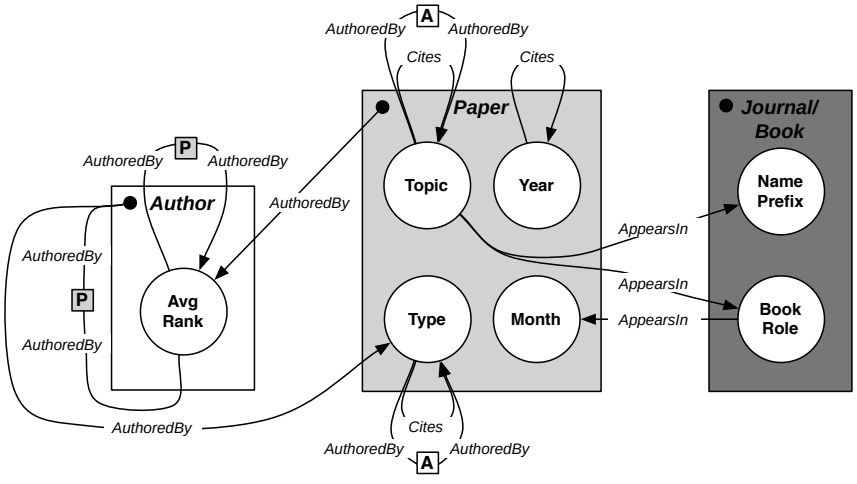

Figure 3.7. RDN for the Cora dataset.

Exploiting these types of autocorrelation dependencies has been shown to significantly improve classification accuracy of RMNs compared to RBNs, which cannot model cyclic dependencies [89]. However, to exploit autocorrelation, RMNs must be instantiated with the appropriate clique templates—to date there is no RMN algorithm for *learning* autocorrelation dependencies. RDNs are the first PRM capable of learning cyclic autocorrelation dependencies.

The Gene data contain attributes associated with both objects and links (i.e., interactions). We learned an RDN for seven attributes. Figure 3.8 shows the resulting RDN. The RDN learning algorithm selected 19 of the 77 dependencies considered for inclusion in the model. In these data, all the gene attributes exhibit autocorrelation—this is strong evidence that there are regularities among the genes whose proteins interact in the cell.

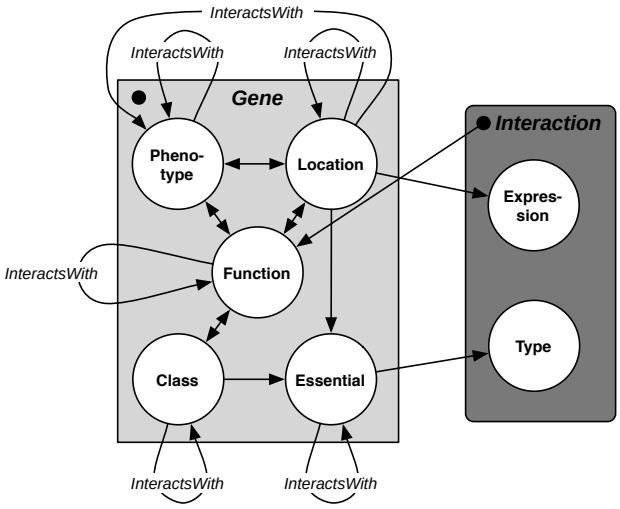

Figure 3.8. RDN for the Gene dataset.

On the IMDb data, we learned an RDN for ten discrete attributes. Figure 3.9 shows the resulting RDN. The RDN learning algorithm selected 29 of the 170 dependencies considered for inclusion in the model. Again, we see that four of the attributes exhibit autocorrelation. Movie receipts and genre each exhibit a number of autocor-

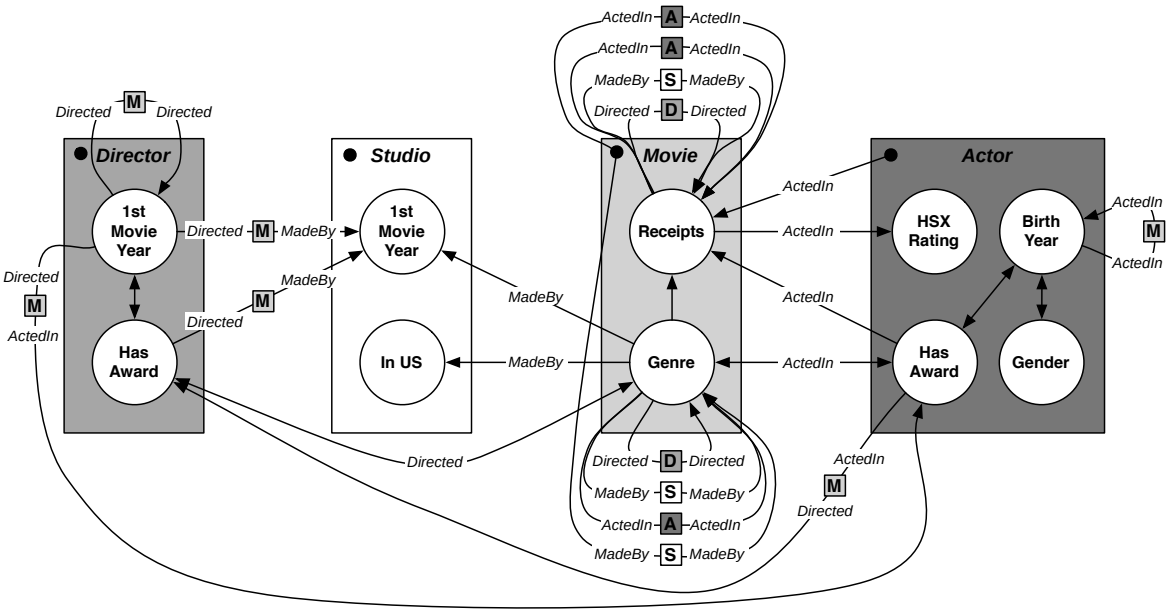

Figure 3.9. *RDN* for the IMDb dataset.

relation dependencies (through actors, directors, and studios), which illustrates the group structure of the Hollywood movie industry.

On the NASD data, we learned an *RDN* for eleven attributes. Figure 3.10 shows the resulting *RDN*. The *RDN* learning algorithm selected 32 of the 160 dependencies considered for inclusion in the model. Again, we see that four of the attributes exhibit autocorrelation. Subjective inspection by NASD analysts indicates that the *RDN* had automatically uncovered statistical relationships that confirm the intuition of domain experts. These include temporal autocorrelation of risk (past problems are indicators of future problems) and relational autocorrelation of risk among brokers at the same branch—indeed, fraud and malfeasance are usually social phenomena, communicated and encouraged by the presence of other individuals who also wish to commit fraud [11]. Importantly, this evaluation was facilitated by the interpretability of the *RDN*—experts are more likely to trust, and make regular use of, models they can understand.

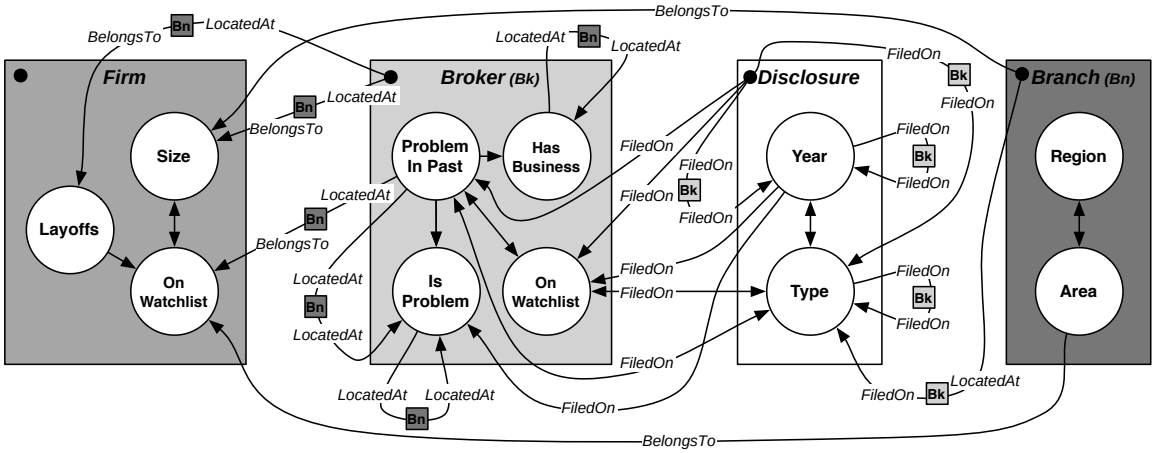

Figure 3.10. *RDN* for the NASD dataset.

On the WebKB data, we learned an *RDN* for four attributes. Figure 3.11 shows the resulting *RDN*. The *RDN* learning algorithm selected 9 of the 52 dependencies considered for inclusion in the model. All of the attributes exhibit autocorrelation in the WebKB data.

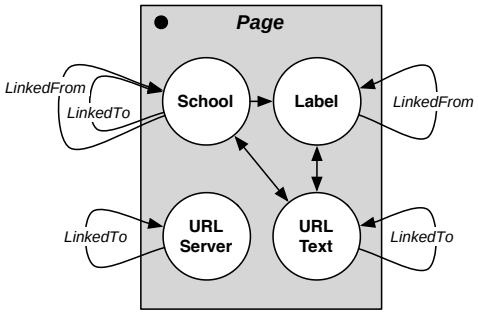

Figure 3.11. *RDN* for the WebKB dataset.

3.3.2.2 Prediction

We evaluated the learned models on prediction tasks in order to assess (1) whether autocorrelation dependencies among instances can be used to improve model accuracy, and (2) whether the *RDN*s, using Gibbs sampling, can effectively infer labels for a

network of instances. To do this, we compared the same four classes of models used in Section 3.3.1: individual models, RDNs, ceiling RDNs, and RMNs.

Figure 3.12 shows AUC results for the first three model types on the five prediction tasks. (We discuss RMN results below.) Figure 3.12a graphs the results of the RDN_{RPT}, compared to the RPT individual model. Figure 3.12b graphs the results of the RDN_{RBC}, compared to the RBC individual model. We used the following prediction tasks: movie receipts for IMDb, paper topic for Cora, page label for WebKB, gene location for Gene, and broker is-problem for NASD.

The graphs show AUC for the most prevalent class, averaged over a number of training/test splits. For Cora, IMDb, and NASD, we used temporal sampling where we learned models on one year of data and applied the models to the subsequent year. There were four temporal samples for IMDb and NASD, and five for Cora. For WebKB we used cross-validation by department, learning on three departments and testing on pages from the fourth, held-out department. For Gene there was no clear sampling choice, so we used ten-fold cross validation on random samples of genes. We used *interdependent sampling*—when there were links between the test and training sets, the class labels of the training set were made available to the RDN and RMNs for use during inference. We used two-tailed, paired t-tests to assess the significance of the AUC results obtained from the trials. The t-tests compare the RDN results to the individual and ceiling models, with a null hypothesis of no difference in the AUC. In Figure 3.12, asterisks denote model performance that is significantly different ($p < 0.10$) from RDN_{RPT} and RDN_{RBC}.

When using the RPT as the conditional learner (Figure 3.12a), RDN performance is superior to RPT performance on all tasks. The difference is statistically significant for three of the five tasks. This indicates that autocorrelation is both present in the data and identified by the RDNs. As mentioned previously, the RPT algorithm can sometimes use the observed attributes of related items to effectively reason with

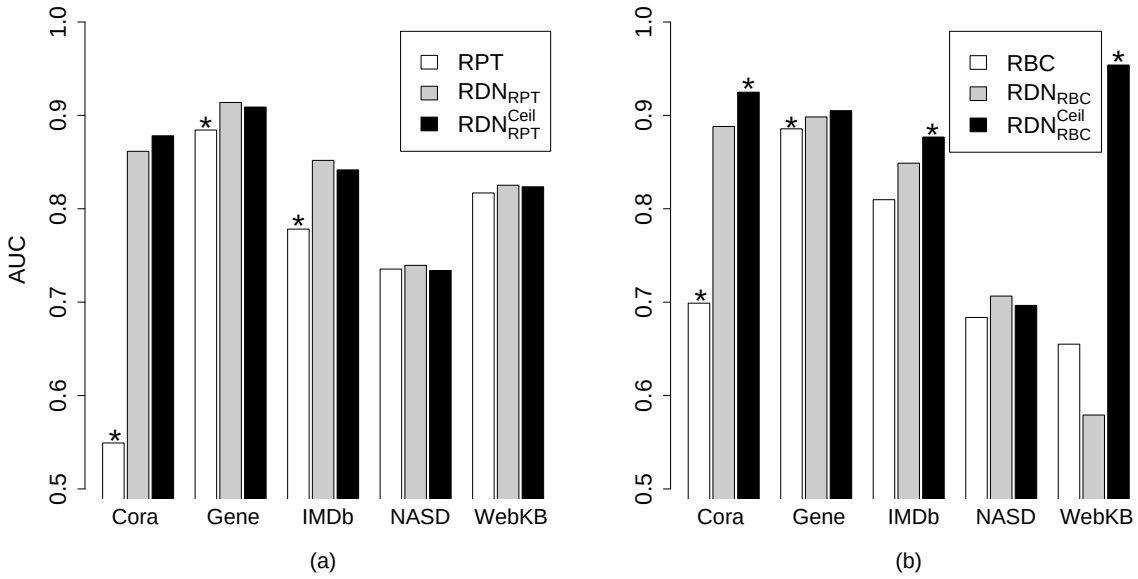

Figure 3.12. AUC results for (a) RDN_{RPT} and RPT and (b) RDN_{RBC} and RBC.

autocorrelation dependencies. However, in some cases the observed attributes contain little information about the class labels of related instances. This is the case for Cora—RPT performance is close to random because no other attributes influence paper topic, given the influence of related paper topics (see Figure 3.7). On all tasks, the RDNs achieve comparable performance to the ceiling models. This indicates that the RDN achieved the same level of performance as if it had access to the true labels of related objects. We note, however, that the ceiling model only represents a probabilistic ceiling—the RDN may perform better if an incorrect prediction for one object improves inferences about related objects. Indeed, on a number of the datasets, RDN performance is slightly higher than that of the ceiling model.

Similarly, when using the RBC as the conditional learner (Figure 3.12b), the performance of RDNs is superior to the RBCs on all but one task and statistically significant for two of the tasks. Notably, on the WebKB data RDN performance is worse than that of the RBC. However, the ceiling performance is significantly higher than RBC. This indicates that autocorrelation dependencies are identified by the

RDN but the model is unable to exploit those dependencies during Gibbs sampling. This effect is due to the amount of information available to seed the inference process. There is sparse information in the attributes other than page label, and because the departments are nearly disjoint, there are few labeled instances before inference. This leaves the RDN with little information to anchor its predictions, which results in marginal predictions closer to random. Similar behavior appeared in the synthetic data experiments, indicating that the RDN_{RBC} may need more information to seed the inference process.

The RDN_{RBC} achieves comparable performance to the ceiling models on only two of the five tasks. This may be another indication that RDNs combined with a non-selective conditional learner (e.g., RBCs) will experience increased variance during the Gibbs sampling process, and thus they may need more seed information during inference to achieve the near-ceiling performance. We should note that although the RDN_{RBC} does not significantly outperform the RDN_{RPT} on any of the tasks, the RDN^{Ceil}_{RBC} is significantly higher than RDN^{Ceil}_{RPT} for Cora and IMDb. This indicates that, when there is enough seed information, the RDN_{RBC} may achieve significant performance gains over the RDN_{RPT}.

Due to time and memory constraints, we were able to learn RMNs for only two of the real-world datasets. Recall that the RMN constructs its features from all the attributes available to the RDN and the RMN_{Sel} constructs its features from the attributes selected by the RDN. Table 3 reports model space information for each dataset—the number of attributes available to the RDN, the average number of attributes selected by the RDN, and the number of features constructed by the RMN and the RMN_{Sel}. Due to the size of the feature space considered by the non-selective RMNs, we were unable learn models for any of the datasets. We were able to successfully learn RMN_{Sel} for the Cora and IMDb datasets. The average AUC of the RMN_{Sel} was 74.4% for Cora and 60.9% for IMDb. This is far below the RDN results

	Num RDN attributes	**Num selected RDN attributes**	**Num RMN features**	**Num RMN_{Sel} features**
Cora	22	2.0	1029	98.0
Gene	19	3.1	3640	606.0
IMDb	15	5.0	234	90.5
NASD	16	5.7	526	341.5
WebKB	34	5.0	2478	270.0

Table 3.3. Number of attributes/features used by RDNs and RMNs.

reported in Figure 3.12. Note that previous RMN results [89] report accuracy of the most likely labeling for the entire dataset. In contrast, we are evaluating AUC of the marginal probabilities for each instance (inferred jointly). This indicates that RMN inference may produce biased marginal probability estimates when run in "loopy" relational networks, due to overfitting the clique weights. When skewed weights are applied to collectively infer the labels throughout the test set, the inference process may converge to extreme labelings (e.g., all positive labels in some regions of the graph, all negative labels in other regions), which would bias marginal probability estimates for many of the instances.

3.4 Related Work

There are three types of statistical relational models relevant to RDNs: probabilistic relational models, probabilistic logic models, and collective inference models. We discuss each of these below.

3.4.1 Probabilistic Relational Models

RDNs are a form of probabilistic relational model. As outlined in Section 2.5, learning and inference in PRMs involve a *data graph* G_D, a *model graph* G_M, and an *inference graph* G_I. All PRMs model data that can be represented as a graph (i.e.,

G_D) and although PRMs use different approximation techniques for inference in G_I, they all use a similar process for rolling out an inference graph G_I. Consequently, PRMs differ primarily with respect to the representation of the model graph G_M, how that model is learned, and the choice of inference algorithm.

Relational Bayesian Networks

RBNs [29] use a directed model graph $G_M = (V_M, E_M)$ and a set of conditional probability distributions P to represent a joint distribution over $\mathbf{X}$. Each node $v \in V_M$ corresponds to an $X_k^t \in \mathbf{X}$. The set P contains a conditional probability distribution for each variable given its parents, $p(x_k^t | pa_{x_k^t})$. Given (G_M, P), the joint probability for a set of values $\mathbf{x}$ is computed as a product over the item types T, the attributes of that type X^t, and the items of that type v, e:

$$p(\mathbf{x}) = \prod_{t \in T} \prod_{X_i^t \in X^t} \prod_{v:T(v)=t} p(x_{vi}^t | pa_{x_{vi}^t}) \prod_{e:T(e)=t} p(x_{ei}^t | pa_{x_{ei}^t})$$

The RBN learning algorithm for the most part uses standard Bayesian network techniques for parameter estimation and structure learning. One notable exception is that the learning algorithm must check for "legal" structures that are guaranteed to be acyclic when rolled out for inference on arbitrary data graphs. In addition, instead of exhaustive search of the space of relational dependencies, the structure learning algorithm uses greedy iterative-deepening, expanding the search in directions where the dependencies improve the likelihood.

The strengths of RBNs include understandable knowledge representations and efficient learning techniques. For relational tasks, with a huge space of possible dependencies, *selective* models are easier to interpret and understand than *non-selective* models. Closed-form parameter estimation techniques allow for efficient structure learning (i.e., feature selection). In addition, because reasoning with relational mod-

els requires more space and computational resources, efficient learning techniques make relational modeling both practical and feasible.

The directed acyclic graph structure is the underlying reason for the efficiency of RBN learning. As discussed previously, the acyclicity requirement precludes the learning of arbitrary autocorrelation dependencies and limits the applicability of these models in relational domains. RDNs enjoy the strengths of RBNs (namely, understandable knowledge representation and efficient learning) without being constrained by an acyclicity requirement.

Relational Markov Networks

RMNs [89] use a undirected model graph $U_M = (V_M, E_M)$ and a set of potential functions Φ to represent a joint distribution over $\mathbf{X}$. Again each node $v \in V_M$ corresponds to an $X_k^t \in \mathbf{X}$. RMNs use relational clique templates CT to specify the ways in which cliques are defined in U_M. Clique templates are defined over a set of item types, a boolean constraint on how the types must relate to each other in the data graph, and a set of attributes to consider on the matching items. Let $C(CT)$ be the set of cliques in the graph U_M that match a specific clique template CT. As with Markov networks, each clique $c \in C(CT)$ is associated with a set of variables X_c and a clique potential $\phi_c(x_c)$. Given (U_M, Φ), the joint probability for a set of values $\mathbf{x}$ is computed as a product over the clique templates CT and the matches to the clique template c:

$$p(\mathbf{x}) = \frac{1}{Z} \prod_{C_i \in CT} \prod_{c_j \in C_i} \phi_{c_j}(x_{c_j})$$

The RMN learning algorithm uses maximum-a-posteriori parameter estimation with Gaussian priors, modifying Markov network learning techniques. The algorithm assumes that the clique templates are pre-specified and thus does not search for the best structure. Because the user supplies a set of relational dependencies to consider

(i.e., clique templates), it simply optimizes the potential functions for the specified templates.

RMNs are not hampered by an acyclicity constraint, so they can represent arbitrary forms of autocorrelation. This is particularly important for reasoning in relational datasets where autocorrelation dependencies are nearly ubiquitous and often cannot be structured in an acyclic manner. However, the tradeoff for this increased representational capability is a decrease in learning efficiency. Instead of closed-form parameter estimation, RMNs are trained with conjugate gradient methods, where each iteration requires a round of inference. In large cyclic relational inference graphs, the cost of inference is prohibitively expensive—in particular, without approximations to increase efficiency, feature selection is intractable.

Similar to the comparison with RBNs, RDNs enjoy the strengths of RMNs but not their weaknesses. More specifically, RDNs are able to represent arbitrary forms of autocorrelation without being limited by efficiency concerns during learning. In fact, the pseudolikelihood estimation technique used by RDNs has been used recently to make feature selection tractable for conditional random fields [58] and Markov logic networks [48].

3.4.2 Probabilistic Logic Models

Within the class of PLMs, Markov logic networks (MLNs) [83] are most similar in nature to RDNs. In MLNs, each node is a grounding of a predicate in a first-order knowledge base, and features correspond to first-order formulae and their truth values. An MLN, unrolled over a set of objects in the domain, specifies an undirected Markov network. In this sense, they share the same strengths and weaknesses as RMNs—they are capable of representing cyclic autocorrelation relationships but suffer from decreased efficiency if full joint estimation is used during learning.

Recent work on structure learning for MLNs [48] has investigated the use of pseudolikelihood to increase learning efficiency. The MLN structure learning algorithm restricts the search space by limiting the number of distinct variables in a clause, and then uses beam search, with a weighted pseudolikelihood scoring function, to find the best clauses to add to the network.

Although both RDNs and MLNs use pseudolikelihood techniques to learn model structures efficiently, they each employ a different representational formalism. In particular, MLNs use weighted logic formulae while RDNs use aggregate features in CPDs. Our future work will investigate the performance tradeoffs between RDN and MLN representations when pseudolikelihood estimation is used for learning.

3.4.3 Ad hoc Collective Models

An alternative approach to collective inference combines local individual classification models (e.g., RBCs) with a joint inference procedure (e.g., relaxation labeling). Examples of this technique include iterative classification [67], link-based classification [54], and probabilistic relational neighbor models [55, 56]. These approaches to collective inference were developed in an ad hoc procedural fashion, motivated by the observation that they appear to work well in practice. RDNs formalize this approach in a principled framework—learning models locally (maximizing pseudolikelihood) and combining them with a global inference procedure (Gibbs sampling) to recover a full joint distribution. In this work, we have demonstrated that autocorrelation is the reason behind improved performance in collective inference (see Jensen et al. [42] for more detail) and explored the situations under which we can expect this type of approximation to perform well.

3.5 Conclusion

In this chapter, we presented relational dependency networks, a new form of probabilistic relational model. We showed the *RDN* learning algorithm to be a relatively simple method for learning the structure and parameters of a probabilistic graphical model. In addition, *RDN*s allow us to exploit existing techniques for learning conditional probability distributions of relational datasets. Here we have chosen to exploit our prior work on *RPT*s, which construct parsimonious models of relational data, and *RBC*s, which are simple and surprisingly effective non-selective models. We expect the general properties of *RDN*s to be retained if other approaches to learning conditional probability distributions are used, given that those approaches learn accurate local models.

The primary advantage of *RDN*s is the ability to efficiently learn autocorrelation dependencies. Autocorrelation is a nearly ubiquitous phenomenon in relational datasets and the resulting dependencies are often cyclic in nature. If a dataset exhibits autocorrelation, an *RDN* can learn the associated dependencies and then exploit those dependencies to improve overall inferences by collectively inferring values for the entire set of instances simultaneously. The real and synthetic data experiments in this chapter show that collective inference with *RDN*s can offer significant improvement over individual approaches when autocorrelation is present in the data. Except in cases when there are few test set labels, the performance of *RDN*s approaches the performance that would be possible if all the class labels of related instances were known. Furthermore, our experiments show that inference with *RDN*s is comparable, or superior, to *RMN* inference over a range of conditions, which indicates that pseudolikelihood estimation can be used effectively to learn an accurate approximation of the full joint distribution.

We also presented learned *RDN*s for a number of real-world relational domains, demonstrating another strength of *RDN*s—their understandable and intuitive knowl-

edge representation. Comprehensible models are a cornerstone of the knowledge discovery process, which seeks to identify novel and interesting patterns in large datasets. Domain experts are more willing to trust, and make regular use of, understandable models—particularly when the induced models are used to support additional reasoning. Understandable models also aid analysts' assessment of the utility of the additional relational information, potentially reducing the cost of information gathering and storage and the need for data transfer among organizations—increasing the practicality and feasibility of relational modeling.

CHAPTER 4

LATENT GROUP MODELS

Our recent work investigating how collective inference improves classification has illustrated the effect of model representation on performance in relational domains [42]. More specifically, we showed that modeling the direct dependencies among class labels of related instances is a low-variance means of reducing model bias when autocorrelation is present. An alternative approach is to model the dependencies among class labels indirectly through their association with the observed attributes of related instances, but this approach experiences a dramatic increase in variance as the number of observed attributes increases.

In this work, we have shown that direct modeling with *RDN*s can lead to significant improvements in performance over individual models in domains with even modest amounts of autocorrelation. However, this approach fails to capture a frequent characteristic of autocorrelated data—the presence of underlying groups, conditions, or events that are correlated with the attributes on a set of entities. Models that represent the underlying group structure and the association between unobserved group properties and observed attribute values and links may be able to express the joint distribution more accurately and compactly than approaches that only model direct dependencies among class labels.

Recall the fragment of the NASD database, where brokers exhibit autocorrelation with respect to their fraud status. For reference, we include the graphic again in Figure 4.1(a). The autocorrelation in this example can be represented through the underlying group structure of the data. In Figure 4.1(b), groups of brokers that work

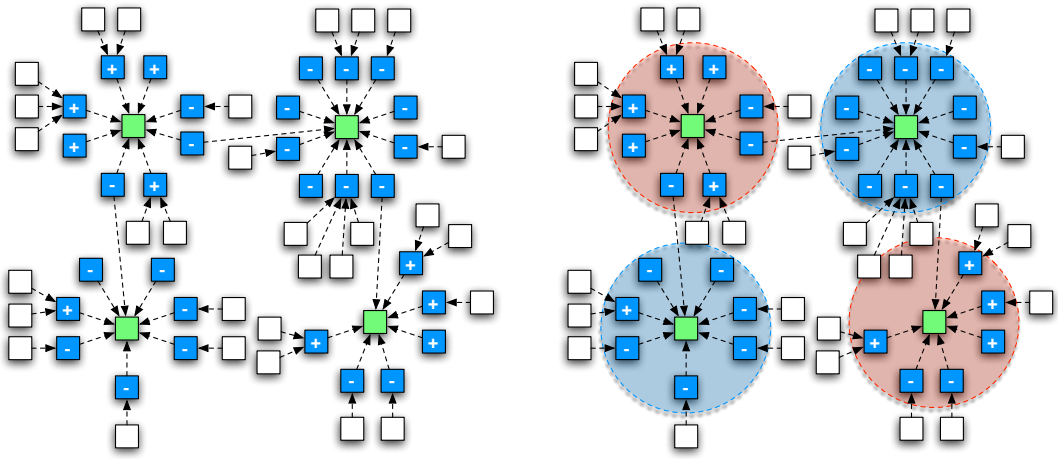

(a) Data fragment (b) Group structure

Figure 4.1. Example NASD database fragment and group structure.

together at a branch are likely to share similar attribute values. In this example, the branch object is a *coordinating object* that connects the group members (i.e., brokers). Branches where many of the brokers are involved in fraud may be encouraging malfeasance; other branches appear to be focusing on legitimate business since few of the brokers have been identified as fraudulent.

Another example of underlying group structure is illustrated in Figure 4.2 with example data from the World Wide Web. In this case, the objects are web pages and the links are hyperlinks among the pages. The pages are labeled according to a binary topic variable. Similar to fraud status, page topic also exhibits autocorrelation and the autocorrelation can be represented through the underlying group structure. However, in this case there are no coordinating objects that serve to connect the group members. Instead, the groups can be identified by the pattern of linkage among the pages. Individual webpages belong to *communities*—sets of pages that discuss common topics, referencing other pages in their community more often than pages external to their community (e.g., alternative energy sites point to documents discussing solar and wind power).

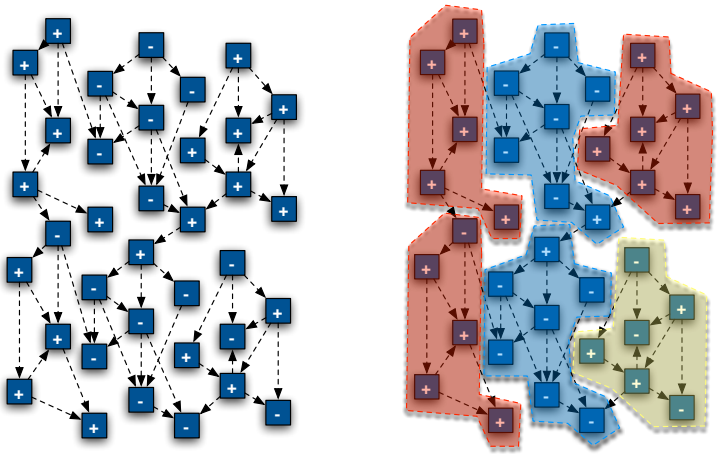

(a) Data fragment (b) Group structure

Figure 4.2. Example WebKB fragment and group structure.

Modeling these underlying group structures is a third approach to representing autocorrelation dependencies. Group structure can be used to model autocorrelation dependencies that arise due to a number of causes. Membership in the group may cause the correlation among object attribute values. For example, the purchases of book club members will be correlated. Alternatively, the group may be formed through associations among objects with similar attribute values. For example, demographic information will be correlated among students in the same school. In either case, the *identity* and *properties* of the group can be utilized to characterize the dependencies among the class labels of member instances indirectly. In interdependent data samples, there may be enough data to reason about each group in the training set independently through the use of identifiers [80]. For example, once we have training data on a sufficient number of brokers at a branch, we can accurately reason about the risk of an additional employee independent of other branches. However, when there is limited data for each group, or when the samples are independent, modeling the properties of the groups (e.g., corrupt branches) will offset the limited data and allow for generalization across groups.

In this chapter, we describe latent group models (LGMs). LGMs represent a joint probability distribution over both the attributes and links of a relational dataset, incorporating link existence uncertainty and hierarchical latent variables. LGMs posit groups of objects in the data—membership in these groups influences the observed attributes of the objects, as well as the existence of links among the objects. LGMs address a number of weaknesses of current collective inference models. First, LGMs extend recent PRM representations to model link structure and autocorrelation dependencies indirectly through the hidden group structures. These group structures enable the incorporation of link information into PRMs in a more tractable way than PRMs with link uncertainty [30] because group membership decouples attribute and link dependencies. Second, the group structures can capture dependencies among neighboring but unlinked instances (e.g., transitive relationships), allowing information to propagate in a more elaborate manner during inference than with models that restrict their consideration to dependencies among closely linked instances. Group models are a natural way to extend PRM representations to improve model performance without fully representing the $O(N^2)$ dependencies between all pairs of instances. Third, LGMs generalize about the properties of groups. This is in contrast to recent work modeling specific groups and objects in the training set to improve classification performance in interdependent samples [81, 80]. Consequently, learned LGMs can be applied to prediction tasks in both interdependent and independent samples. Finally, LGMs recover the underlying group structure, which can be examined to improve domain understanding and inform development of additional modeling techniques.

We start by discussing the latent group model representation and then describe a specific implementation that we utilize throughout the thesis. We evaluate LGM inference on synthetic datasets, showing that LGMs outperform RDNs and RMNs in a range of conditions, particularly when there are moderate-sized clusters with

low linkage. Next, we present empirical evaluation of *LGM*s on three real-world prediction tasks to demonstrate the capabilities of the model, showing that *LGM*s can outperform models that ignore latent groups, particularly when there is little known information with which to seed the inference process. Finally, we discuss related work and conclude.

4.1 Latent Group Models

Latent group models specify a generative probabilistic model for the attributes and link structure of a relational dataset. The model posits groups of objects in the data of various types. Membership in these groups influences the observed attributes of objects, as well as the existence of relations (links) among objects.

4.1.1 LGM Representation

The *LGM* extends the *PRM* representation outlined in Section 2.5 to model a joint distribution over both the attributes and links of a relational dataset. To model link uncertainty, we include an augmented edge set E' that contains an edge for every pair of objects in the data ($\forall v_i, v_j \in V_D \;\; e_{ij} \in E'$) with a binary link variable X_L to indicate whether a relation exists between the incident objects.[1] In addition to the objects and links in the data, we also model a set of groups G. As with objects and links, each group is associated with a type, $T(g_i) = t_{g_i}$ and a set of attributes based on that type $\mathbf{X}_{\mathbf{g_i}}^{\mathbf{t_{g_i}}}$. Each object $v_i \in V_D$ belongs to a set of groups $\mathbf{g_{v_i}} = (g_{v_i 1}, ..., g_{v_i k})$. Group membership and properties (i.e., attributes) can influence the values of object attributes, link attributes, and link existence. An *LGM* represents a joint distribution over the values of the attributes in the data, $\mathbf{x} = \{\mathbf{x}_{\mathbf{v_i}}^{\mathbf{t_{v_i}}} : v_i \in V_D \; s.t. \; T(v_i) = t_{v_i}\} \cup \{\mathbf{x}_{\mathbf{e_j}}^{\mathbf{t_{e_j}}} : e_j \in E_D \; s.t. \; T(e_j) = t_{e_j}\} \cup \{x_{e_k L} : e_k \in E'\} \cup \{\mathbf{x}_{\mathbf{g_l}}^{\mathbf{t_{g_l}}} : g_l \in G \; s.t. \; T(g_l) = t_{g_l}\}$.

[1] We assume binary links and at most one link between any pair of objects. However, it is relatively straightforward to extend the model to accommodate deviations from these assumptions.

There are two steps to incorporating groups and their properties into PRMs. First, we need to detect the underlying group structure. When the groups are identified by a *coordinating object* (e.g., branch), detection is a relatively easy task—we can identify groups through high degree nodes and their immediate neighbors. When groups consist of *communities*, group detection is more difficult. However, if intra-community links are more frequent than inter-community links, the existing relations can be used as evidence of the underlying community structure, and group membership can be inferred from the patterns of relations.

Next, we need to infer the latent group properties and model their influence on the attributes and relations of group members. When the groups are observable, we can model the latent attributes with a relatively simple application of the expectation-maximization (EM) algorithm [15]. A similar approach is used in information retrieval where latent-unigram models represent each document as a *group* of word occurrences[2] that are conditionally independent given the *topic* of the document [6].

When groups are unobserved, group membership and properties must be jointly inferred from the observed relations and attributes. To continue the document retrieval metaphor, it is as if we have word occurrence information (attribute values) and noisy indicators of word co-occurrence within documents (link information) but we do not know the document boundaries or the topic distributions. In these situations, an iterative procedure may be necessary to recover group membership and infer latent group properties.

For our initial investigation of LGMs, we make several simplifying assumptions about the data. We assume a unipartite relational data graph (i.e., single object and link type) and that there are no link attributes other than X_L. We also assume there is one group type with one attribute and that each object belongs to a single group.

[2]However, the "vocabulary" is much smaller in relational domains—we generally have fewer than ten class values, whereas documents have thousands of unique words.

Furthermore, in this work we limit consideration to a specific model structure. In particular, we assume there is a fixed number of groups and that object class labels and link existence are conditionally independent given group membership and properties. We also assume additional object attributes are only influenced by the object's class label. Our *LGM* implementation[3] models the following generative process for a dataset with N_O objects and N_G groups:

1. For each group g, $1 \leq g \leq N_G$:
   (a) Choose a group attribute value x_g from $p(X_g)$, a multinomial probability with k values.
2. For each object i, $1 \leq i \leq N_O$:
   (a) Choose a group g_i uniformly from the range $[1, N_G]$.
   (b) Choose a class value c_i from $p(C|X_g)$, a multinomial probability conditioned on the object's group attribute x_{g_i}.
   (c) For each object attribute $A \in \mathbf{A_M}$:
      i. Choose a value for a_i from $p(A|C)$, conditioned on the object's class label c_i.
3. For each object j, $1 \leq j \leq N_O$:
   (a) For each object k, $j < k \leq N_O$:
      i. Choose an edge value e_{jk} from $p(E|G_j == G_k)$, a Bernoulli probability conditioned on whether the two objects are in the same group.

This generative process specifies the joint distribution of a dataset G_D as follows:

[3]From this point forward, references to *LGM*s will pertain to this specific implementation.

$$p(G_D) = \prod_{g \in G} p(x_g) \prod_{v_i \in V_D} p(c_i|x_{g_i}) \prod_{A \in \mathbf{A}} p(a_i|c_i) \cdot \prod_{j,k:(v_i,v_j) \in E_D} p(e_{jk}{=}1|g_j{=}{=}g_k) \prod_{j,k:(v_i,v_j) \notin E_D} p(e_{jk}{=}0|g_j{=}{=}g_k)$$

See Figure 4.3 for a graphical representation of the model. The template consists of four plates, which represent replicates of groups, objects, attributes, and potential binary links among objects. Groups each have an attribute X. Objects have a group membership G, a class label C, and attributes $A_1, ..., A_M$. E is a binary variable indicating link existence among all $\binom{N_O}{2}$ pairs of objects. The conditions on the arcs constrain the manner in which the model is *rolled out* for inference[4]—each E is influenced by two G variables and each C is influenced by a single X variable in the unrolled Bayes net.

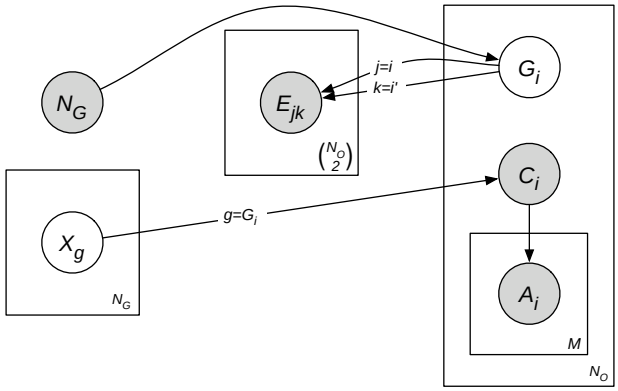

Figure 4.3. *LGM* graphical representation.

4.1.2 LGM Learning

Learning an *LGM* consists of learning the parameters of the distribution and inferring the latent variables on both objects (group membership) and groups (group attributes). Ideally, we would learn the model using a straightforward application

[4]We use *contingent Bayesian network* [62] notation to denote context-specific independence.

of the EM algorithm—iterating between inferring the latent variables (E-step) and estimating the parameters (M-step). Unfortunately, there are difficulties with this approach.

When group membership is unknown, each of the C variables depends on all the X variables and each of the E variables depends on all the G variables—there is no longer context-specific independence to exploit and each E-step will require inference over a large, complex, rolled-out Bayes net where objects' group memberships are all interdependent given the link observations. Although approximate inference techniques (e.g., loopy belief propagation) may allow accurate inference in each E-step, given the number of latent variables and their dependency on sparse link information ($L \ll \binom{N_O}{2}$), we conjecture that EM will not converge to a reasonable solution due to many local (suboptimal) maxima in the likelihood function. Also when using EM to learn the entire model, there are N_O latent group membership variables with N_G possible values and N_G latent group attribute values with k possible values. If the average group size is small ($N_G = O(N_O)$), we conjecture that EM will be very sensitive to the start state.

We note however, that if group membership is known, then exact inference is not only feasible but is also much more efficient. This is because the objects and observed links are conditionally independent given the underlying group structure. For this reason we propose a sequential learning procedure that decouples group identification from the remainder of the estimation process. Our algorithm is motivated by the observation that collective models improve performance by propagating information only on existing links. This indicates that autocorrelated groups should have more intra-group links than inter-group links and as such, graph clustering techniques should be able to identify groups from the link structure alone. Accordingly, we utilize the following approximate learning algorithm:

1. Hypothesize group membership for objects based on the observed link structure.

2. Use EM to infer group attributes and estimate the remaining parameters of the model.

A hard clustering approach in the first step, which assigns each object to a single group, greatly simplifies the estimation problem in the second step—we only need to infer the latent group attribute values and estimate the parameters of $p(X)$, $p(C|X)$, and $p(A_i|C)$ for $1 \leq i \leq m$. To this end, we employ a recursive spectral decomposition algorithm with a norm-cut objective function [86] to cluster the objects into groups with high intra-group and low inter-group linkage.

Spectral clustering techniques partition data into disjoint clusters using the eigenstructure of a similarity matrix. We use the divisive, hierarchical clustering algorithm of [86] on the relational graph formed by the observed links in the data. The algorithm recursively partitions the graph as follows: Let $\mathbf{E}_{N\times N} = [E(i,j)]$ be the adjacency matrix and let $\mathbf{D}$ be an $N \times N$ diagonal matrix with $d_i = \sum_{j\in V} E(i,j)$. Solve the eigensystem $(\mathbf{D}-\mathbf{E})\mathbf{x} = \lambda\mathbf{D}\mathbf{x}$ for the eigenvector $\mathbf{x}_1$ associated with the 2^{nd} smallest eigenvalue λ_1. Consider m uniform values between the minimum and maximum value in $\mathbf{x}_1$. For each value m: bipartition the nodes into (A, B) such that $\forall v_a \in A\ x_{1a} < m$, and calculate the NCut value for the partition, $NCut(A,B) = \frac{\sum_{i\in A, j\in B} E(i,j)}{\sum_{i\in A} d_i} + \frac{\sum_{i\in A, j\in B} E(i,j)}{\sum_{j\in B} d_j}$. Partition the graph into the (A, B) with minimum *NCut*. If $stability(A,B) \leq c$, recursively repartition A and B.[5]

Once we have identified the groups with spectral clustering, we use EM to infer values for X and estimate the parameters of $P(X)$ and $P(C|X)$. We iterate the following steps until the probability distributions have converged to within a tolerance of 0.001:

E-step $t+1$**:** Infer values for X^{t+1} with $P^{t+1}(x_g|\mathbf{c_g}) = \prod_{c_i:g=G_i} \frac{P^t(c_i|x_g)P^t(x_g)}{P(c_i)}$

[5]We use the stability threshold proposed in [86] where the stability value is the ratio of the minimum and maximum bin sizes, after the values of $\mathbf{x}_1$ are binned by value into m bins. Unless otherwise noted, we use $m = \lceil log_2(N) + 1 \rceil$ and $c = 0.06$.

M-step $t+1$**:** Calculate maximum likelihood estimates for $P^{t+1}(X)$ and $P^{t+1}(C|X)$ using the inferred values of X^{t+1}

In addition, we estimate the parameters of $P(A_i|C)$ for $1 \leq i \leq m$. Because the object attributes are conditionally independent of the group attributes given the objects' class labels, we do not need to use EM to estimate these CPDs.

As we show in Section 4.2, our sequential learning approach appears to work well in practice. However, refinements to iterate the clustering and EM steps, or to incorporate soft clusterings, may improve results even further.

4.1.3 LGM Inference

When applying an LGM for prediction, the class labels C, group membership G, and group attributes X are all unobserved and must be inferred. Our inference algorithm is similar to the sequential learning procedure:

1. Hypothesize group membership for objects based on the observed link structure.
2. Use belief propagation to infer group attributes and object class labels jointly.

We begin by using spectral clustering to identify the groups using the observed links. This simplifies inference by partitioning the objects into disjoint sets and fixing their group memberships. Then inference can be decomposed into disjoint subtasks, one for each group. Within each group, the class labels are conditionally independent given the group attribute values so exact inference is possible. We use standard belief propagation [78] to jointly infer group attributes and class labels.

4.2 Experimental Evaluation

The experiments in this section demonstrate the utility of latent group models in relational domains. First, we use synthetic datasets to explore the conditions under which LGMs improve performance over comparable collective models. We vary the

clustering and linkage of the data, showing that LGMs improve performance when intra-group linkage is sparse or when there is little information to seed inference. Next, we evaluate LGMs on three real-world prediction tasks, showing that LGMs can leverage autocorrelation to improve model accuracy. Again, we show that LGMs achieve significant performance gains when there is less information available to seed the inference process.

LGMs can be used for prediction tasks in both interdependent and independent samples. In interdependent samples there may be enough information about the class distribution associated with the groups in the training set for group membership to improve inference without inferring group attributes. There are a number of relational learning approaches [87, 81, 80] that use group identities in the training set to improve inference in these situations. In independent samples, it is necessary to generalize about group properties to improve performance. LGMs are the first prediction model to generalize about group properties, thus we expect LGMs will be most useful for prediction tasks in independent samples. For this reason, we focus our evaluation primarily in this context. Independent samples reflect a number of relevant relational domains. For example, independent samples can be used to develop models of web pages on localized sites for application on the broader World Wide Web. Alternatively, independent samples can be used to develop fraud detection models on data from a single city for application on branches and brokers in the remainder of the country. Finally, independent samples can be used to develop gene prediction models on a genome from a single organism for application on other related organisms.

4.2.1 Synthetic Data Experiments

To explore the effects of graph structure on LGM inference, we generated homogeneous data graphs with an autocorrelated class label and linkage due to the underlying group structure. Each object has four boolean attributes: X_1, X_2, X_3

and X_4. We varied linkage and group size and learned models to predict X_1. See appendix A.1.2 for a detailed description of the data generation process.

More specifically, we generated data with small and large groups sizes, and high and low levels of linkage. The first set of data have small group size and low linkage, thus we expect it will be difficult to exploit the autocorrelation in the data due to low connectivity. The second set of data have small group size but high linkage, thus we expect it will be easier to exploit neighbor information but that it may be difficult to identify the underlying groups. The third set of data have large group size and low linkage. We expect the LGMs will be more accurate on data with large group sizes because they can incorporate information from a wider neighborhood than RDNs and RMNs, which use only local neighbor information. The fourth set of data have large group size and high linkage—we expect that models will be able to exploit autocorrelation dependencies most effectively in these data, due to the high connectivity and clustering.

Figure 4.4 graphs a sample synthetic dataset with small group size and high linkage. The final datasets are homogeneous—there is only one object type and one link type, and each object has four attributes. After the groups are used to generate the data, we delete them from the data—the groups are not available for model learning or inference.

We compare the performance of LGMs to five different models. The first two models are RDNs and RMNs. These models use the intrinsic attributes of objects, the observed attributes of directly related objects, and the class labels of directly related objects to predict X_1.

The third model (RDN_{Grp}) is a modification of the RDN, which incorporates the groups discovered in the LGM clustering. More specifically, we augment the dataset so that each pair of group members are directly linked before we learn an RDN_{Grp}. This model demonstrates the utility of propagating information among distant group

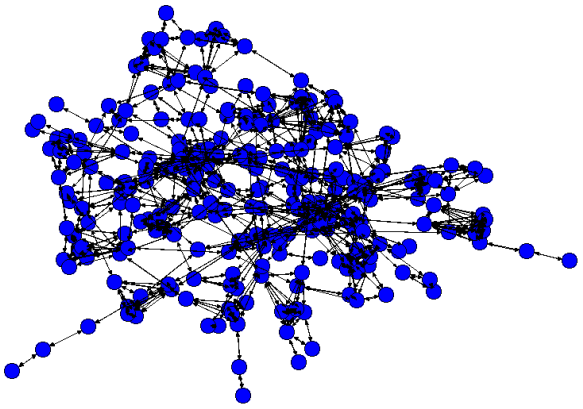

Figure 4.4. Sample synthetic dataset.

members in an RDN. In addition to the attributes used by the RDN and the RMN, the RDN_{Grp} also uses the class labels and observed attributes of group members to model X_1.

The fourth model (LGM_{Rand}) is a modification of the LGM, which uses random groups rather than the groups discovered by the spectral clustering component. We include LGM_{Rand} to illustrate the utility of the identified groups.

The fifth model ($wvRN$) is a weighted-vote relational neighbor classifier [55, 56]. $wvRN$ is an iterative collective model that estimates an object's class probabilities using the weighted mean of the class-membership probabilities of the object's neighbors. We include $wvRN$ as a baseline autocorrelation model that uses only the class labels in the data graph.

Figure 4.5 shows AUC results for each of the models on the four different types of data. During inference, we varied the number of known class labels available to seed the inference process by randomly labeling a portion ($\{0.0, 0.3, 0.6\}$) of the test set instances. We expect performance to be similar when other information serves to seed the inference process—either when some labels can be inferred from intrinsic attributes, or when weak predictions about many related instances serve to constrain the system. At each level of labeling, we generated five test sets. For each test set, we

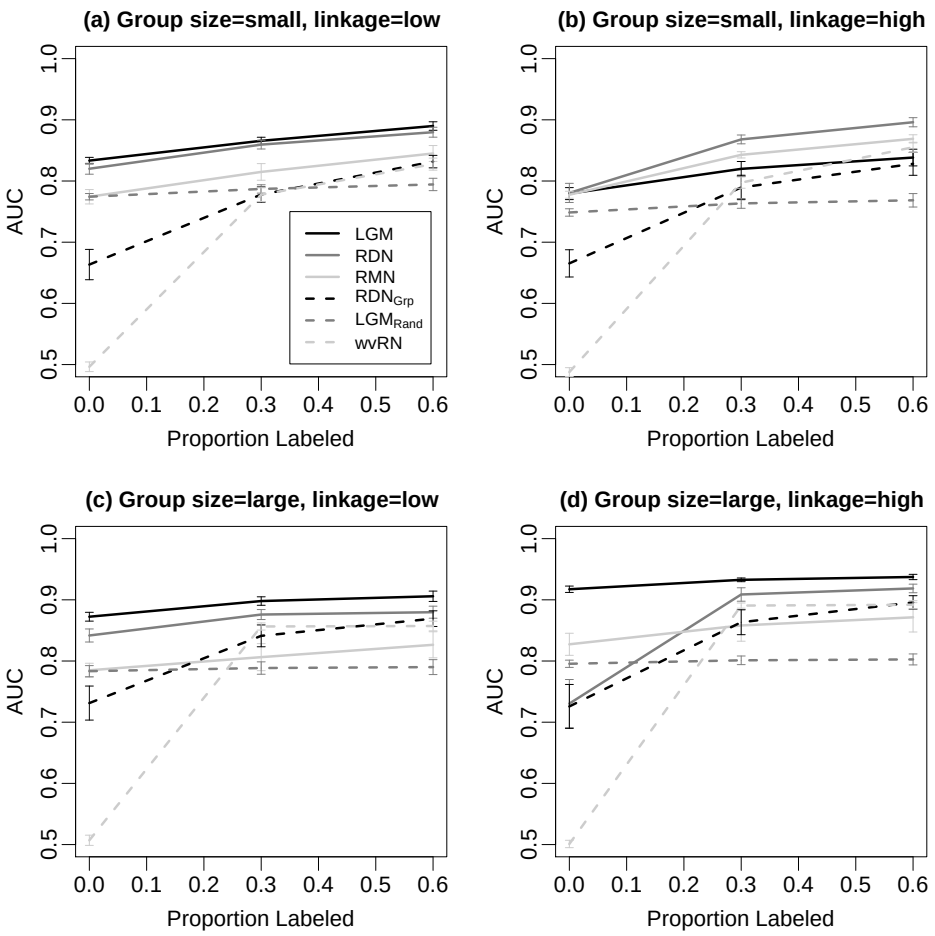

Figure 4.5. Evaluation of *LGM* inference.

generated five training sets and learned the models. For each training/test split, we ran five trials of inference at each level of labeling. The inference trials measure the variability of performance within a particular sample, given the random labeling. The error bars indicate the standard error of the AUC estimates for a single training/test split, averaged across the training/test splits.

Across all datasets, *LGM*s perform significantly better than the two baseline models LGM_{Rand} and $wvRN$. This indicates that *LGM*s are identifying groupings that are useful for exploiting autocorrelation information beyond objects' immediate neighbors. Surprisingly the performance of RDN_{Grp} is significantly lower than all but the $wvRN$. This indicates that *LGM* improvements are not simply from the

linking up of distant neighboring objects in the data. The model representation (e.g., conditional independence of class given group) must also contribute to the performance gains.

When group size is small and linkage is low, LGMs perform only slightly better than RDNs, which indicates that the groups are too small for the LGM to significantly capitalize on group information.

When group size is small and linkage is high, LGMs are outperformed by both RDNs and RMNs when the test set is at least partially labeled. The LGMs' poor performance on these data is due to the learning algorithm's inability to identify the latent group structure. When the density of linkage between groups is relatively high compared to the average group size, it is difficult for the spectral clustering algorithm to correctly identify the fine grained underlying group structure.

When group size is large, LGMs outperform the other models regardless of linkage. In these data, the larger groups allow LGMs to propagate information farther in the graph than RDNs and RMNs, which use only local neighbor information. The most significant improvement is when linkage is high and there are no labeled instances in the test set. This indicates that LGMs can aggregate sparse attribute information across wide neighborhoods to offset the lack of class label information.

4.2.2 Empirical Data Experiments

We present results for two LGM variations. The first variation, LGM_k, sets the number of group attribute values to the number of class label values, $k = |C|$ (e.g., for binary tasks, $k = 2$); the second variation, LGM_{2k}, sets $k = 2|C|$. We compare the LGM to four alternative models. The first two are individual inference models: the RPT and the RBC. The third model is an RDN_{RPT}. The fourth model (RDN^{Ceil}_{RPT}) is a probabilistic ceiling for the RDN_{RPT}, where we allow the true labels of related instances to be used during inference. This model shows the level of performance

possible if the RDN_{RPT} could infer the true labels of related instances with perfect accuracy.

The first set of experiments considers the restricted task of predicting class labels using only the class labels of related instances and/or the group membership. This limits confounding effects due to feature construction and model selection. The models do not have equivalent feature spaces, nor do they all perform feature selection, but the differences are minimized when the models are restricted to consider a small number of attributes (i.e., class label and/or group membership). A second set of experiments includes object attributes in each of the models to evaluate the impact of intrinsic attribute information on performance.

For the RPTs and RBCs, we clustered the training and test sets together and used cluster ID as the sole attribute in the model. The performance of these models illustrates the baseline utility of clustering without typing the groups and serves as a comparison to previous work [81], which clusters the data to generate additional features for prediction. For the LGM, RDN_{RPT} and RDN_{RPT}^{Ceil}, we used the class label of related instances as the sole attribute available for modeling. When possible we used exact inference, but for RDNs, which require approximate inference, we used Gibbs with chains of length 500 and burn-in of 100. (At this length, accuracy and AUC had seemingly converged.) During inference we again varied the number of known class labels available to seed the inference process.

We compared the six models on three relational datasets (see appendix A.1.3 for a more detailed description of the data):

WebKB: We considered the unipartite co-citation web graph. The class label was page category (five values). As in previous work on this dataset, we do not try to predict the category *Other*; we remove them from the data after creating the co-citation graph.

IMDb: We considered a unipartite graph of 1,382 movies released in the U.S. between 1996 and 2001, where links indicate movies that are made by a common studio. The class label was opening weekend box-office returns (binary).

Cora: We considered the unipartite co-citation graph of 4,330 machine-learning papers. The class label was paper topic (seven values).

Figure 4.6 shows AUC results for each of the models on the three prediction tasks when the models do not use additional attributes. The graph shows AUC for the most prevalent class, averaged over the training/test splits.[6] For WebKB, we used cross-validation by department, learning on three departments and testing on the fourth. For IMDb, we used *snowball sampling* [32] to bipartition the data into five disjoint training/test samples. For Cora, we used five temporal samples where we learned the model on one year and applied the model to the subsequent year. For each training/test split we ran 10 trials at each level of labeling, except for the RDNs where we ran 5 trials due to relative inefficiency of RDN inference. The error bars indicate the standard error of the AUC estimates for a single training/test split, averaged across the training/test splits. This illustrates the variability of performance within a particular sample, given the random initial labeling.

On WebKB and IMDb, LGM performance quickly reaches performance levels comparable to RDN_{RPT}^{Ceil} at less than 40% known labels. Note that RDNs and LGMs cannot be expected to do better than random at 0% labeled. This indicates that the LGM is able to exploit group structure when there is enough information to accurately infer the group attribute values. RDN_{RPT} performance doesn't converge as quickly to the ceiling. There are two explanations for this effect. First, when there are few constraints on the labeling space (e.g., fewer known labels), RDN inference may not be able to fully explore the space of labelings. Although we saw performance

[6] Accuracy results, over all classes, show similar behavior.

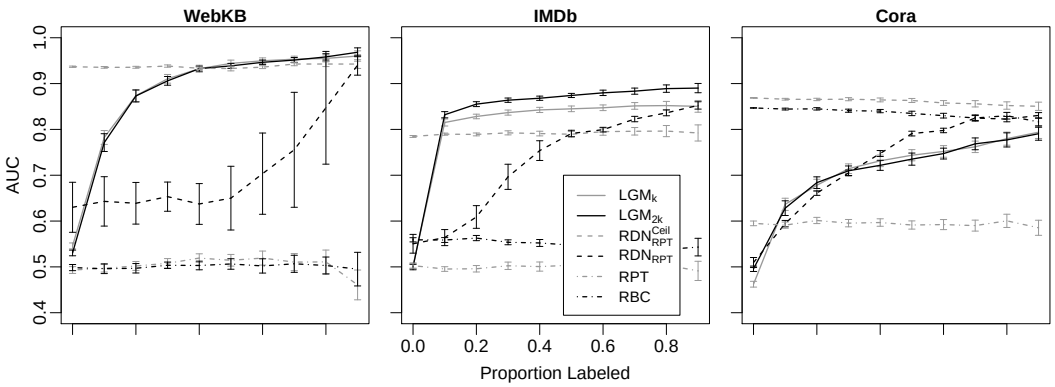

Figure 4.6. *LGM* performance when the class label is the only available attribute.

plateau for Gibbs chains of length 500-2000, it is possible that longer chains, or alternative inference techniques, could further improve *RDN* performance [56]. The second explanation is that joint models are disadvantaged by the data's sparse linkage. When there are few labeled instances, influence may not be able to propagate to distant objects over the existing links in the data. In this case, a group model that allow influences to propagate in more elaborate ways can exploit the seed information more successfully.

RPT performance is near random on all three datasets. This is because the *RPT* algorithm uses feature selection and only a few cluster IDs show significant correlation with the class label. This indicates there is little evidence to support generalization about cluster identities themselves. The *RBC* does not perform feature selection and uses cluster IDs without regard to their support in the data. On Cora, the *RBC* significantly outperforms all other models. However, Cora is the one dataset where the test set instances link into the training set. This indicates that the *RBC* approach may be superior for prediction tasks on interdependent samples.

LGM performance does not reach that of RDN_{RPT}^{Ceil} in Cora. Although the *LGM* outperforms the RDN_{RPT} when there is little know information, eventually the RDN_{RPT} takes over as it converges to RDN_{RPT}^{Ceil} performance. We conjecture that this effect is due to the quality of the clusters recovered in Cora. When the clus-

ter stopping threshold is more conservative, the clustering algorithm returns fewer, larger-sized clusters. In this case, the model will be able exploit group structure with fewer labeled instances. However, when we use a less conservative threshold, the clustering algorithm returns a greater number of smaller-sized clusters. In this case, the model has the potential to make more accurate predictions but only when there is a large number of labeled instances to identify the group attribute values accurately. A technique that allows information to propagate outside the clusters (e.g., soft clustering) may be more robust in this situation.

Figure 4.7 shows average AUC results for each of the three prediction tasks when we include attributes in the models. For the WebKB task, we included three page attributes: *school, url-server, url-text*; for IMDb, we included eight movie *genre* attributes; for Cora, we included three paper attributes: *type, year, month*. In all three datasets, the attributes improve LGM performance when there are fewer known labels. This is most pronounced in the IMDb, where LGM achieves ceiling performance with no class label information, indicating that movie genre is predictive of group attribute. In contrast, the RDN_{RPT} is not able to exploit the attribute information as fully. In particular, in the WebKB task, the attributes significantly impair RDN_{RPT} performance. This is due to the RDN_{RPT} feature selection process, which selects biased page attributes over the pairwise autocorrelation features in this restricted tack. However, in the other two domains where this is not a problem, the RDN_{RPT} still does not propagate the attribute information as effectively as the LGM when there are less than 40% known class labels.

4.3 Related Work

There are two types of relational models relevant to LGMs: those that model coordinating objects and their properties, and those that model communities and their properties.

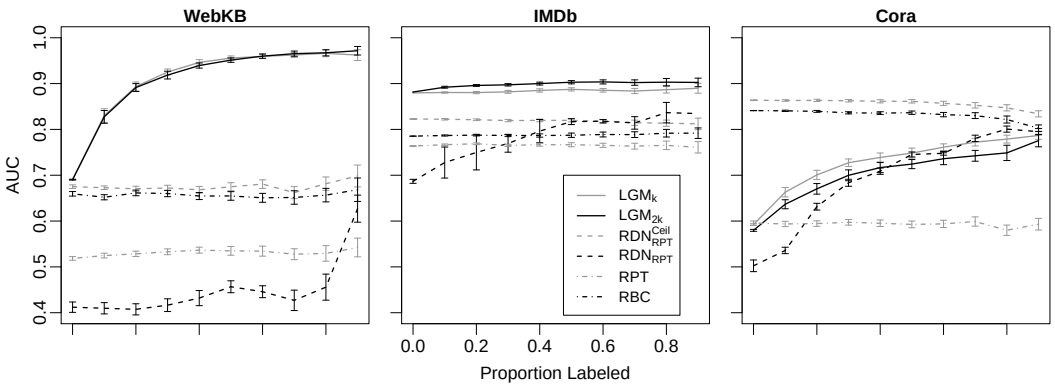

Figure 4.7. *LGM* performance when additional attributes are included.

4.3.1 Modeling Coordinating Objects

Slattery and Mitchell [87] use an approach based on the *HITS* algorithm [47] to identify coordinating objects in the data. This approach exploits autocorrelation dependencies by propagating information through these objects, but it does not generalize about group properties.

ACORA [80] is a relational learning system that uses novel aggregation function to capture information in high-dimensional attributes. The *ACORA* aggregation functions can be used to model coordinating objects through identifier attributes (e.g., object IDs). *ACORA*'s aggregation functions can also be used to model communities indirectly. The aggregated features can be used to model the distribution of an item's neighboring objects (e.g., a paper's reference IDs)—and items in the same community should have similar distributions. Indeed, this approach has achieved significant gains in classification accuracy compared to *RBN*s in the Cora domain [80]. However, *ACORA* features do not generalize about group properties, consequently this approach must be applied to interdependent samples.

The social networks community provides latent variable models that cluster objects based on their link structure [77, 36, 94, 44]. These approaches are primarily used for clustering rather than for prediction. The models use the patterns of relations to identify which *roles* the objects play in the data. Although these models

often incorporate richer representations for the relational link structure (e.g., [94]), they typically do not incorporate attributes into the model. One exception is the ART model, where the textual content of email documents is used to moderate pairwise interactions among individuals and thus refine the process of role discovery to reflect latent link types [59].

*RBN*s have been used to cluster the objects in relational datasets [90]. The approach, which uses latent variables on a subset of object types, will be useful in situations where the coordinating objects are fixed and known. For example in the cinematic domain, an *RBN* with a latent variable on studios could be used to represent the autocorrelation among movie returns. However, this approach does not posit group structures. Furthermore, the dependencies among the latent variables, as with the other dependencies in *RBN*s, must be structured to be acyclic.

4.3.2 Modeling Communities

Popescul and Ungar [81] cluster relational database tables using standard k-means clustering algorithms and then use the cluster IDs as features in individual inference models. This approach has been shown to improve prediction performance, but it can only be employed in situations where the test set instances link into the clusters used during training because the features use the identity of the clusters rather than generalizing over the properties of the groups.

Kubica, Moore, Schneider and Yang [50] use a latent variable model to cluster objects into groups based on their attribute values and link structure. Their approach is geared toward clustering data with multiple transactional links (e.g., phone calls, email) where the link patterns are homogeneous with respect to the groups. In other words, it is assumed that all groups have the same distribution of intra- and inter-group linkage. A situation where the patterns of linkage differ among groups is, however, easy to imagine. For example, consider machine learning papers: Reinforce-

ment learning papers tend to cite papers in optimization, operations research, and theory, but genetic algorithm papers cite primarily other genetic algorithm papers. Allowing the link probabilities to vary among groups will be important for modeling group structures in large heterogeneous domains.

4.3.3 Discussion

Consider the case where there are k group attribute values, $|C|$ class values, and each object has a latent group variable. There is a spectrum of group models ranging from $k = |C|$ to $k = N_G$. PRMs that model autocorrelation with global parameters, reason at one end of the spectrum ($k = |C|$) by implicitly using $|C|$ groups. Techniques that cluster the data for features to use in individual models (e.g., [81]), reason at the other end of the spectrum ($k = N_G$) by using the identity of each cluster. The approach of Kubica et al. [50] uses $k = 1$ in the sense that it ties the parameters of intra- and inter-group link probabilities across all groups.

When group size is large, there may be enough data to reason about each group independently (i.e., use $k = N_G$). For example, once a studio has made a sufficient number of movies, we can accurately reason about the likely returns of its next movie independently. However, when group size is small, modeling all groups with the same distribution (i.e., use $k = |C|$) will offset the limited data available for each group. A model that can vary k may be thought of as a backoff model, with the ability to smooth to the background signal when there is not enough data to accurately estimate a group's properties in isolation. LGMs offer a principled framework within which to explore this spectrum.

One of the primary advantages of LGMs is that influence can propagate between pairs of objects that are not directly linked but are close in graph space (e.g., in the same group). In RMNs and RDNs, the features of an object specify its Markov blanket. This limits influence propagation because features are generally constructed

over the attributes of objects one or at most two links away in the data. Influence can only propagate farther by influencing the probability estimates of attribute values on each object in a path sequentially. An obvious way to address this issue is to model the $O(N_O^2)$ dependencies among all pairs of objects in the data, but dataset size and sparse link information makes this approach infeasible for most datasets. PRMs with link uncertainty [54] are the only current models that consider the full range of dependencies and their influence on observed attributes. Because LGMs can aggregate influence over an extended local neighborhood, they are a natural way to expand current representations while limiting the number of dependencies to model.

4.4 Conclusion

In this chapter, we presented latent group models, a PRM extension that models attribute and link structure jointly, using latent groups to improve reasoning in relational domains. To date, work on statistical relational models focused primarily on models of attributes conditioned on the link structure (e.g., [89]), or on models of link structure conditioned on the attributes (e.g., [54]). Our initial investigation has shown that modeling the interaction among links and attributes can improve model generalization when there is natural clustering in the data.

Latent group models are a natural means to model the attribute and link structure simultaneously. The groups decouple the link and attribute structure, thereby offering a way to learn joint models tractably. Our analysis has shown that group models outperform other collective models when there is little information to seed inference. This is likely because a smaller amount of information is needed to infer group properties than is needed to propagate information throughout sparse relational graphs. This suggests *active inference* as an interesting new research direction—where techniques choose which instances to label based on estimated improvement to the collective predictions.

Latent group models extend the manner in which collective models exploit autocorrelation to improve model performance. One of the reasons collective inference approaches work is that the class labels are at the "right" level of abstraction—they *summarize* the attribute information that is relevant to related objects [42]. Group models also summarize the information but at higher level of abstraction (i.e., group membership and properties). Positing the existence of groups decouples the search space into a set of biased abstractions and could be considered a form of predicate invention [88]. This allows the model to consider a wider range of dependencies to reduce bias while limiting potential increases in variance. Indeed, the results we report for LGMs using only the class labels and the link information achieve nearly the same level of performance reported by relational models in the recent literature.

CHAPTER 5

BIAS/VARIANCE ANALYSIS

Our evaluation of model performance herein has demonstrated that each model reacts differently to various relational data characteristics—graph structure, level of autocorrelation, and the amount of seed information available for inference. To quantify the effects of data characteristics on performance more formally, we outline a bias/variance framework for relational datasets.

Bias/variance analysis is a useful tool for investigating the performance of machine learning algorithms. Conventional analysis decomposes loss into errors due to aspects of the learning process, but in relational and network applications, the inference process introduces an additional source of error. Collective inference techniques introduce additional error both through the use of approximate inference algorithms and through variation in the availability of test set information. To date, the impact of *inference* error on model performance has not been investigated. In this chapter, we outline a new bias/variance framework that decomposes loss into errors due to both the *learning* and *inference* processes. We evaluate performance of a number of relational models on synthetic data and utilize the framework to investigate hypotheses regarding the mechanisms behind poor model performance (e.g., identifiability problems increase *RDN* inference variance). With this understanding, we propose a number of algorithmic modifications to explore to improve model performance.

5.1 Conventional Approach

Bias/variance analysis [25, 16] has been used for a number of years to investigate the mechanisms behind model performance. This analysis is based on the fundamental understanding that prediction error has three components (bias, variance, and noise) and that there is a tradeoff between bias and variance when learning statistical models. Searching over a larger model space, to estimate a more complex model, can decrease bias but often increases variance. On the other hand, very simple models can sometimes outperform complex models due to decreased variance, albeit with higher bias (e.g., [37]).

Conventional bias/variance analysis decomposes loss into errors due to aspects of learning procedures. Loss is decomposed into three factors: bias, variance and noise. In the traditional decomposition, bias and variance measure estimation errors in the learning technique. For example, the Naive Bayes classifier typically has high bias due to the assumption of independence among features, but low variance due to the use of a large sample (i.e., entire training set) to estimate the conditional probability distribution for each feature [17].

The assumption underlying the conventional decomposition is that there is no variation in model predictions due to (1) the inference process, and (2) the available information in the test set. Classification of relational data often violates these assumptions when *collective inference* techniques are used. Collective inference often requires the use of approximate inference techniques, which can introduce variation in model predictions for a single instance. For example, final predictions for an instance may depend on the initial (random) start state used during inference, thus multiple runs of inference may result in different predictions. In addition, relational models are often applied to classify a partially labeled test set, where the known class labels serve to seed the collective inference process. Current methods for evaluating relational learning techniques typically assume that labeling different nodes in the

test set have equivalent impact. However, the heterogeneity of the relational graph may allow some instances to have more of an impact on neighbor predictions than others—thus, *which* instances are labeled in the test set may cause additional variation in the predictions. Finally, relational models are generally learned on a fully labeled training set (i.e., the class labels of all neighbors are known), but then applied to an unlabeled, or partially labeled, test set. This mismatch between training and test set information may impact the final model predictions.

To date, the impact of *inference* error on model performance has not been investigated. In this chapter, we propose a new bias/variance framework that decomposes marginal squared-loss error into components of both the learning and inference processes. We evaluate the performance of a number of relational models on synthetic data and use the framework to understand the reasons for poor model performance. Each of the models exhibits a different relationship between error and dataset characteristics. For example, RMNs have higher inference bias in densely connected networks; RDNs have higher inference variance when there is little information to seed the inference process; LGMs have higher learning bias when the underlying group structure is difficult to identify from the network structure. Using this understanding, we propose a number of algorithmic modifications to improve model performance.

5.2 Relational framework

In conventional bias/variance analysis, loss is decomposed into three factors: bias, variance and noise [25, 16]. Given an example x, a model that produces a prediction $f(x) = y$, and a true value for x of t, squared loss is defined as: $L(t, y) = (t - y)^2$. The expected loss for an example x can be decomposed into bias, variance, and noise components. Here the expectation is over training sets D—the expected loss is measured with respect to the variation in predictions for x when the model is learned on different training sets: $E_{D,t}[L(t, y)] = B(x) + V(x) + N(x)$.

Bias is defined as the loss incurred by the mean prediction y_m relative to the optimal prediction y_*: $B(x) = L(y_*, y_m)$. Variance is defined as the average loss incurred by all predictions y, relative to the mean prediction y_m: $V(x) = E_D[L(y_m, y)]$. Noise is defined as the loss that is incurred independent of the learning algorithm, due to noise in the data set: $N(x) = E_t[L(t, y_*)]$.

Bias and variance estimates are typically calculated for each test set example x using models learned from a number of different training sets. This type of analysis decomposes model error to associate it with aspects of *learning*, not aspects of *inference*. The technique assumes that exact inference is possible and that the training and test sets have the same available information. However, in relational datasets there can be additional variation due to the use of approximate inference techniques and due to the availability of test set information. In order to accurately ascribe errors to learning *and* inference, we have extended the conventional bias/variance framework to incorporate errors due to the inference process.

For relational data, we first define the expected *total* loss for an instance x as an expectation over training sets D_{tr} and test sets D_{te}. Following the standard decomposition for loss as described in [27], we can decompose *total* loss into *total* bias, variance, and noise:

$$
\begin{aligned}
& E_{Dtr,Dte,t}[L(t,y)] \\
&\quad = \; E_{Dtr,Dte,t}[(t-y)^2] \\
&\quad = \; E_t[(t-E[t])^2] + E_{Dtr,Dte}[(y-E[t])^2] \\
&\quad = \; N_T(x) + E_{Dtr,Dte}[(y - E_{Dtr,Dte}[y] + E_{Dtr,Dte}[y] - E[t])^2] \\
&\quad = \; N_T(x) + E_{Dtr,Dte}[(y - E_{Dtr,Dte}[y])^2 + (E_{Dtr,Dte}[y] - E[t])^2 + \\
&\qquad\; 2(y - E_{Dtr,Dte}[y]) \cdot (E_{Dtr,Dte}[y] - E[t])] \\
&\quad = \; N_T(x) + E_{Dtr,Dte}[(y - E_{Dtr,Dte}[y])^2] + (E_{Dtr,Dte}[y] - E[t])^2 \\
&\quad = \; N_T(x) + V_T(x) + B_T(x)
\end{aligned}
$$

In this decomposition the total bias $B_T(x)$, and total variance $V_T(x)$ are calculated with respect to variation in model predictions due to both the learning and inference algorithms.

Then we define the *learning* loss as an expectation over training sets D_{tr} alone, using a fully labeled test set for inference. For example, when predicting the class label for instance x_i, the model is allowed to use the class labels (and attributes) of all other instances in the dataset ($X - \{x_i\}$). This enables the application of exact inference techniques and ensures that the test set information most closely matches the information used during learning. Note that this part of the analysis mirrors the conventional approach to bias/variance decomposition, isolating the errors due to the learning process. For this reason, we will refer to the components as *learning* bias, variance, and noise:

$$
\begin{aligned}
& E_{Dtr,t}[L(t,y)] \\
&= E_{Dtr,t}[(t-y)^2] \\
&= E_t[(t-E[t])^2] + E_{Dtr}[(y-E[t])^2] \\
&= N_L(x) + E_{Dtr}[(y-E_{Dtr}[y]+E_{Dtr}[y]-E[t])^2] \\
&= N_L(x) + E_{Dtr}[(y-E_{Dtr}[y])^2 + (E_{Dtr}[y]-E[t])^2 + \\
&\quad 2(y-E_{Dtr}[y])\cdot(E_{Dtr}[y]-E[t])] \\
&= N_L(x) + E_{Dtr}[(y-E_{Dtr}[y])^2] + (E_{Dtr}[y]-E[t])^2 \\
&= N_L(x) + V_L(x) + B_L(x)
\end{aligned}
$$

Once we have measured the *total* and *learning* bias/variance, we can define *inference* bias/variance as the difference between the total error and the error due to the learning process alone:

$$B_I(x) = B_T(x) - B_L(x)$$

$$V_I(x) = V_T(x) - V_L(x)$$

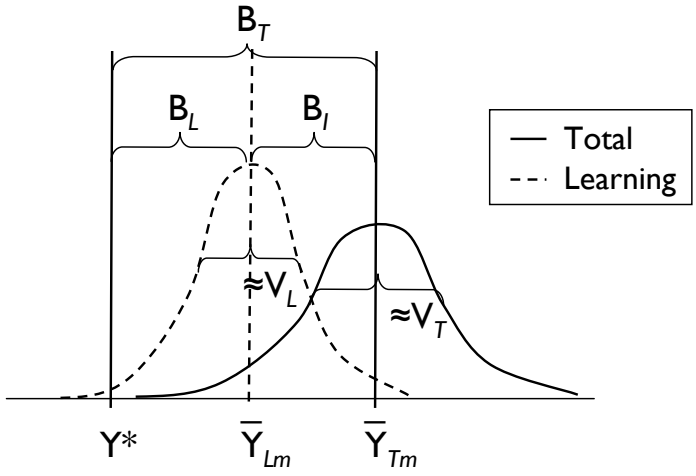

Figure 5.1. Distributions of model predictions.

For example, consider the distributions of model predictions in Figure 5.1. We measure the variation of model predictions for an instance x in the following ways. First, when we generate synthetic data we record the data generation probability as the optimal prediction y^*. Next, we record the marginal predictions for x inferred with models learned on different training sets, allowing the class labels of related instances to be used during inference. These predictions form the *learning* distribution, with a mean *learning* prediction of y_{Lm}. Finally, we record predictions for x inferred with models learned on different training sets, where each learned model is applied a number of times on a single test set. These predictions form the *total* distribution, with a mean *total* prediction of y_{Tm}. The model's *learning* bias is calculated as the difference between y^* and y_{Lm}; the *inference* bias is calculated as the difference between y_{Lm} and y_{Tm}. The model's *learning* variance is calculated from the spread of the *learning* distribution; the *inference* variance is calculated as the difference between the *total* variance and the *learning* variance.

5.3 Experimental Evaluation

To explore the effects of relational graph and attribute structure on model performance, we used the *RDN* and *LGM* data generation procedures described in chapters 3 and 4. The details of the synthetic data generation procedures are outlined in appendices A.1.1 and A.1.2.

Our experiments evaluate model performance in a prediction context, where only a single attribute is unobserved in the test set. We generated disjoint training and test sets and learned models to predict X_1 using the intrinsic attributes of the object (X_2, X_3, X_4) as well as the class label and the attributes of directly related objects (X_1, X_2, X_3, X_4). During inference we varied the number of known class labels in the test set, measuring performance on the remaining unlabeled instances. To evaluate model performance, we measured squared loss and decomposed it into bias and variance components for each model.

To measure, and decompose, the expected loss over training and test sets, we used the following procedure:

1. For each outer trial $i = [1, 5]$:
   (a) Generate test set.
   (b) For each learning trial $j = [1, 5]$:
      i. Generate training set, record optimal predictions.
      ii. Learn model of X_1 on the training set.
      iii. Infer marginal probabilities for test set with fully labeled test data (i.e., $\mathbf{X} - \{X_i\}$), record *learning* predictions.
      iv. For each inference trial $k = [1, 5]$ and proportion labeled p= $[0.0, 0.3, 0.6]$:
         A. Randomly label p% of test set.
         B. Infer marginal probabilities for unlabeled test instances, record *total* predictions.

C. Measure squared loss.

(c) Calculate *learning* bias and variance from distributions of *learning* predictions.

(d) Calculate *total* bias and variance from distributions of *total* predictions.

2. Calculate average model loss.

3. Calculate average *learning* bias and variance.

4. Calculate average *total* bias and variance.

5.3.1 RDN Analysis

The first set of bias/variance experiments evaluates the data and models from Section 3.3.1. More specifically, we compare the performance of three models: RDN, RMN, and RMN_{Sel}.

Figure 5.2 graphs the squared loss decomposition for each model on data generated with an RDN_{RPT}. Again, we vary the level of autocorrelation and the proportion of labeled instances in the test set. The first column graphs overall loss; the second column graphs *total* and *learning* bias; the third column graphs *total* and *learning* variance. *Inference* bias (variance) is calculated as the difference between total bias (variance) and learning bias (variance).

On the low autocorrelation data (row a), both the RMN and the RMN_{Sel} have higher loss than the RDN. This is primarily due to high learning bias of the RMN and RMN_{Sel}. Recall that we had hypothesized that since the data were generated with an RDN_{RPT}, an RMN would not be able to represent the data dependencies as well as an RDN when autocorrelation is less extreme (due to incompatible feature spaces). The high learning bias for RMNs supports this hypothesis. In contrast, the RDN has very low learning bias across all experiments—which is to be expected because the data were generated with an RDN.

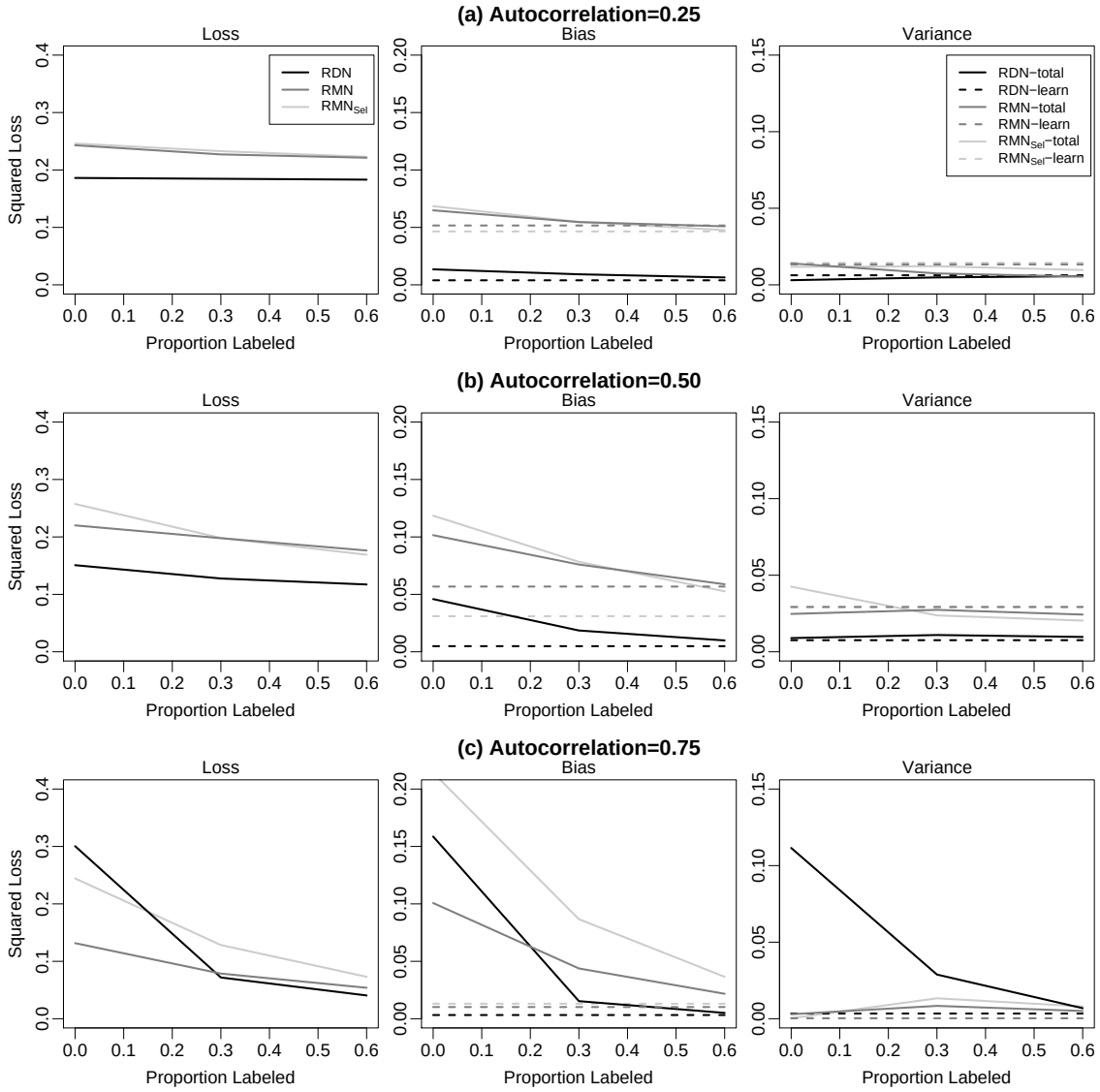

Figure 5.2. Bias/variance analysis on RDN_{RPT} synthetic data.

On the high autocorrelation data (row c), all three models have low learning bias. This indicates that the models have nearly equivalent representational power for the dependencies in these data. All three models also have high inference bias. (Note the difference between total bias and learning bias.) However, the models each react differently to the amount of labeled data in the test set. *RDN*s have higher inference bias when there are 0% labeled instances but lower inference bias when the test set is at least partially labeled. Inference bias in this case is due to an identifiability problem. When there is no information to anchor the predictions, symmetric labelings that are highly autocorrelated, but with opposite values, will appear equally likely. Marginalizing over these opposite labelings biases a model's probability estimates towards random. When there are 0% labeled, it appears that *RMN*s are better able to exploit the sparse attribute information to accurately anchor its predictions. However, when there are 30% or 60% labeled, it appears that *RDN*s are better able to exploit the available class labels to accurately anchor its predictions.

*RDN*s also experience high inference variance on these data when there are 0% labeled. (Note the difference between *RDN* total variance and learning variance.) The combination of *RDN* feature selection and Gibbs sampling inference are the likely cause of *RDN* high inference bias and variance in this situation. Recall that the Gibbs sampling process is seeded with a random labeling over the test set instances. When there is high autocorrelation, the *RDN* learning algorithm often selects the class label in lieu of other observed attributes in the data. When such an *RDN* is applied with Gibbs sampling to a test set with few labeled instances, the inference process can be unduly influenced by the initial random labeling and remain in a localized area of labeling space during inference. Thus, the initial random labeling can increase the variance of predictions over multiple runs of inference and the overall bias of the predictions. The loopy belief propagation inference procedure used by *RMN*s does

not use an initial random labeling, and consequently it is not as susceptible to this problem.

On the earlier experiments in Section 3.3.1, RMN_{Sel} significantly outperformed the RMN on data with low and medium autocorrelation. However, when we measure squared-loss the RMN has significantly lower loss than the RMN_{Sel} on data with medium levels of autocorrelation. On these data, the RMN_{Sel} has higher learning bias than the RMN, which indicates that learning bias can skew probability estimates in RMNs without necessarily affecting the overall ranking of the estimates.

Figure 5.3 graphs the squared loss decomposition for each model on data generated with an RDN_{RBC}. Recall that the RMN feature space is more comparable to data generated by an RDN_{RBC} because both models represent the dependencies among all neighbor values individually, instead of aggregating related values into a single value before modeling dependencies, as the RDN_{RPT} does.

As expected, because the features spaces are more comparable, RMN learning bias is similar to RDN on all but the low autocorrelation data. It is this difference in learning bias that accounts for the RMN's inferior performance on the low autocorrelation data. This indicates that minor incompatibilities in representation have more effect in noisy data.

On the medium autocorrelation data (row b), RDNs have higher squared loss compared to the RMN. However, our previous experiments in Section 3.3.1 showed RDNs have higher AUC on the same data. This indicates that the RDNs produce better rankings of the inferred probability estimates but the estimates themselves are not as accurate. The squared-loss decomposition shows that the inaccuracies are due to high inference variance. The RDN_{RBC} has higher inference variance on the medium autocorrelation data than on the high autocorrelation data, particularly on the trials with 0% labeled instances. This indicates that a small amount of information may unduly influence the RDN_{RBC} which models each of an object's neighbors

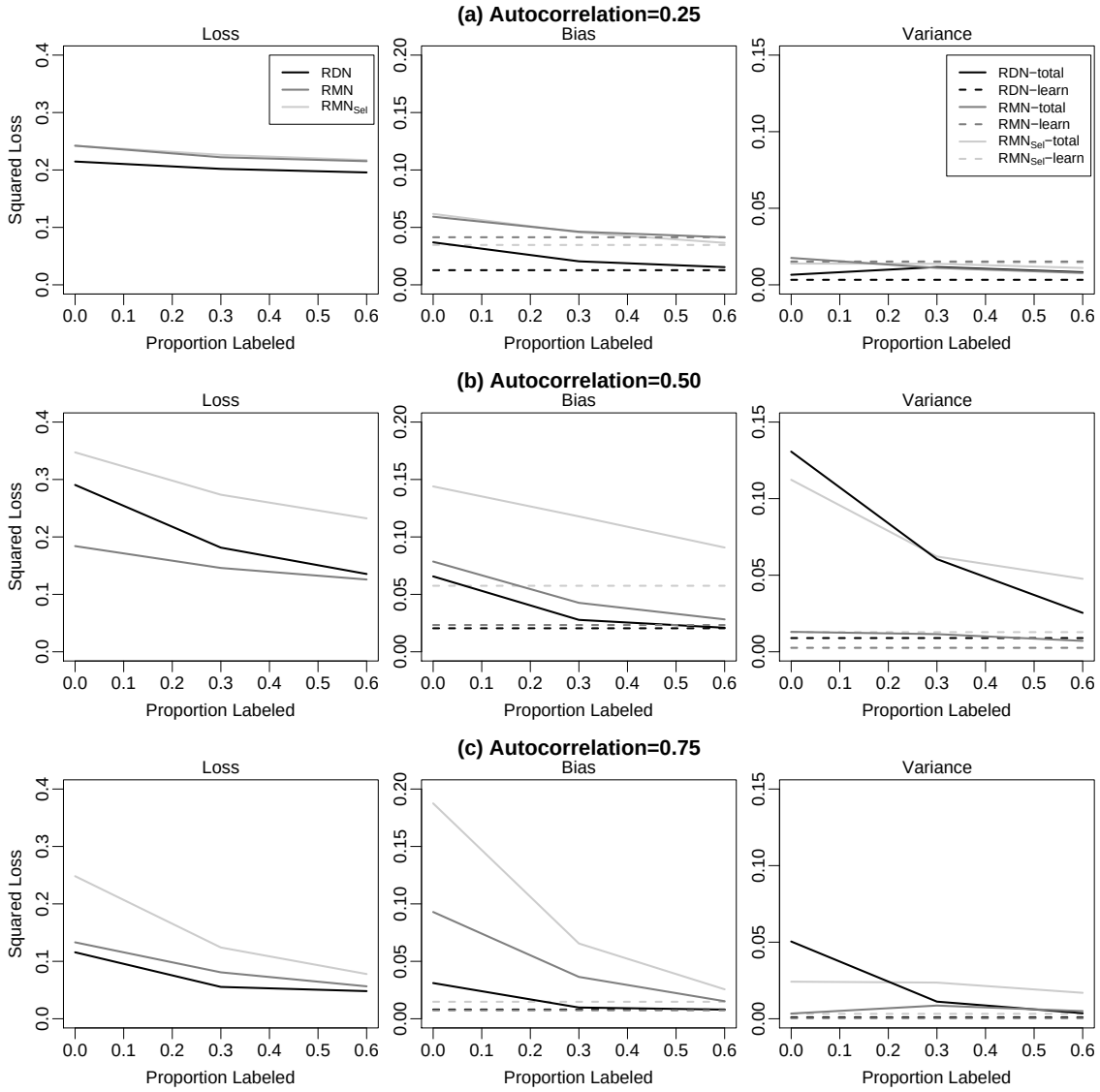

Figure 5.3. Bias/variance analysis on RDN_{RBC} synthetic data.

individually. On the low autocorrelation data, there is not enough information in the neighbor attributes to drive the model to extreme labelings; on the high autocorrelation data, there is enough information to keep the inference process from converging to such extremes.

On the high autocorrelation data (row c), where identifiability issues are more of a problem, RDN performance is somewhat better than RMNs. This suggests that RDN inference variance has less of an effect than RMN inference bias on performance. This may indicate that marginalizing over the set of labelings that are easily reached through finite Gibbs sampling is more effective than marginalizing over all possible labelings.

5.3.2 LGM Analysis

The second set of bias/variance experiments evaluates the data and models from Section 4.2.1. More specifically, we compare the performance of four models: LGM, RDN, RMN, and RDN_{Grp}.

Figure 5.4 graphs performance on the four different types of LGM data, with small/large group sizes and high/low linkage. Again, we graph the squared loss decomposition for each model as the level of test-set labeling is varied. We investigated performance for different levels of autocorrelation, however we only report results for medium autocorrelation because varying autocorrelation does not alter the relative performance of the models—lower levels of autocorrelation weaken the effects, higher levels strength the effects.

When group size is small and linkage is high (row b), the LGM is outperformed by the RDN when the test data are at least partially labeled. The bias/variance decomposition shows that poor LGM performance is due to high learning bias. This is due to the LGM algorithm's inability to identify the latent group structure when group size is small and linkage is high. When density of linkage between groups is

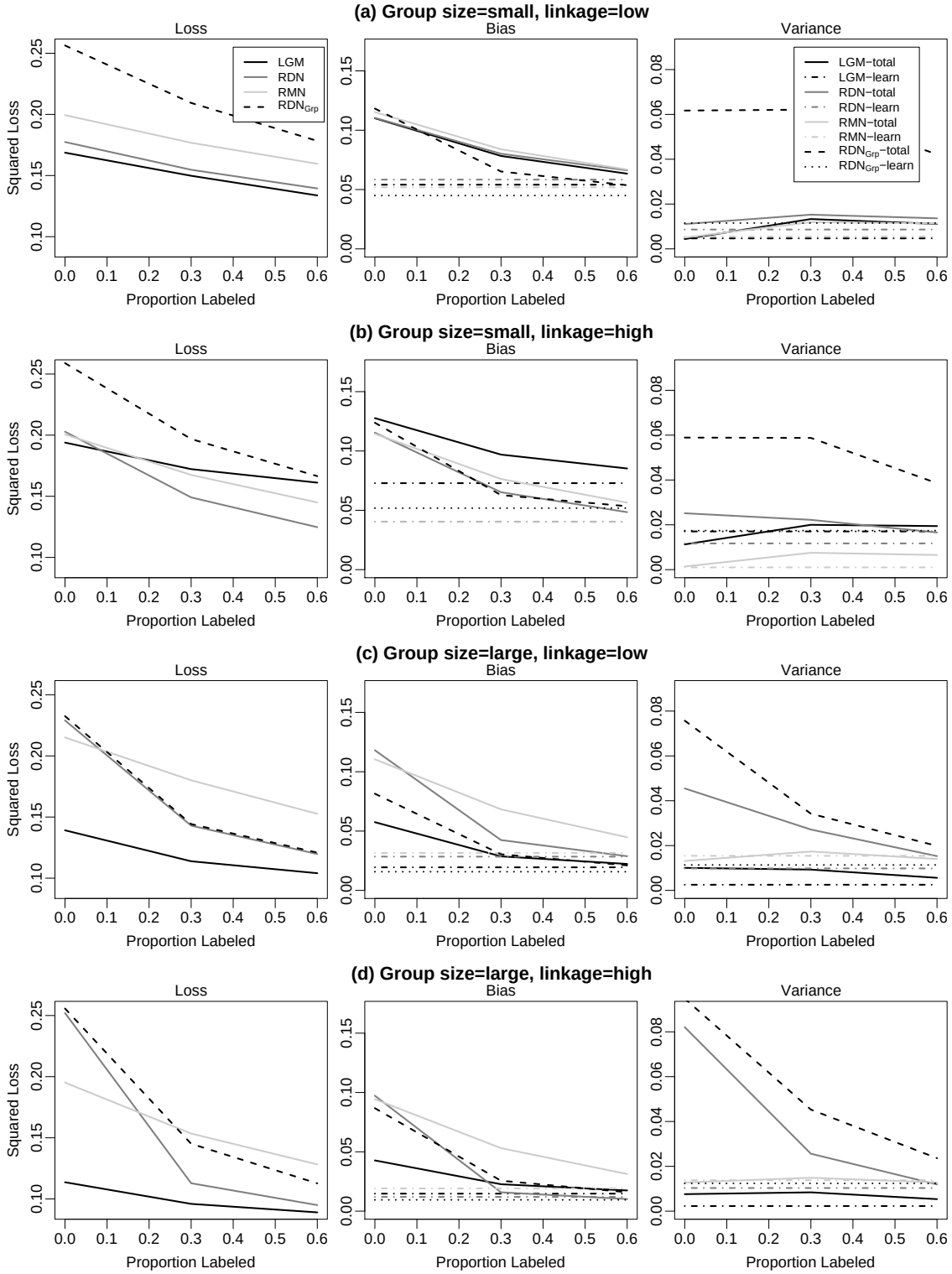

Figure 5.4. Bias/variance analysis on *LGM* synthetic data.

relatively high compared to group size it is difficult for the LGM spectral clustering algorithm to correctly identify the fine grained underlying group structure, and this in turn will bias the learned model. When we allow LGMs to utilize the true underlying group structure, this bias disappears.

When group size is large (row c and d), the LGM significantly outperforms the RDN. The bias/variance decomposition shows that poor RDN performance is due to bias and variance in the inference process. This indicates that LGMs are less susceptible to identifiability problems than other PRMs when the data exhibit clustering. LGMs use link structure to exploit information from more distant but related parts of the data graph and this additional information may be enough to anchor the predictions in a sparsely labeled dataset. Notice that the RDN does not suffer from high inference variance in data with small groups. This suggests that the Gibbs sampling is less likely to be influenced by the initial labeling when the underlying group structures are small—larger groups may prevent the Gibbs chain from mixing well.

When group size is large, both the LGM and the RDN significantly outperform the RMN, provided the test set is at least partially labeled. In these cases, the bias/variance decompositions show that poor RMN performance is due to high inference bias. In fact, RMN total bias is similar across all four types of data, but RMN learning bias is lower when group size is large. This indicates that RMN inference bias is always high, perhaps due to a bias in loopy belief propagation when it is run in a densely connected network. This could also be a result of the RMN algorithm learning skewed clique weights when the network has large underlying groups. When these weights are applied with loopy belief propagation to collectively infer the labels throughout the test set, the inference process may converge to extreme labelings when the graph is very "loopy" (i.e., densely connected). We experimented with a wide range of priors to limit to the impact of weight overfitting but the effect remained consistent.

On the previous experiments in Section 4.2.1, we showed the RDN always outperforms the RDN_{Grp}. The bias/variance decompositions show that poor RDN_{Grp} performance is due to extremely high inference variance. This indicates that the additional group links make the Gibbs sampling inference procedure even more susceptible to variance due to the initial labelings by preventing the Gibbs chain from mixing well. In addition, the RDN_{Grp} has much higher variance than the RDN in the data with small groups (row a and b). When the LGM learning procedure is biased, the identified groups (and thus links added to RDN_{Grp}) are less accurate. These "noisy" links allow the Gibbs initial labeling to influence a wider relational neighborhood and make it more likely that the RDN_{Grp} inference procedure will only explore states near the initial labeling.

5.4 Conclusion

This chapter presents a new bias/variance framework that decomposes squared-loss error into aspects of both the *learning* and *inference* processes. To date, work on relational models focused primarily on the development of models and algorithms rather than the analysis of mechanisms behind model performance. In particular, the impact of collective inference techniques applied to graphs of various structure has not been explored. This work has demonstrated the effects of graph characteristics on relational model performance, illustrating the situations in which we can expect each model to perform well. These experiments also help us understand model limitations and suggest a number of ways to improve the design of relational learning/inference algorithms.

To improve LGM performance, we need to improve the identification of clusters when inter-group linkage drowns out a weak intra-group signal. This may be achieved by the use of alternative clustering techniques in the LGM learning approach, or

through the development of a joint learning procedure that clusters for groups while simultaneously estimating the attribute dependencies in the model.

To improve *RDN* performance, we need to improve inference when there are few labeled instances in the test set. This may be achieved through the use of non-random initial labeling to seed the Gibbs sampling procedure. We have started exploring the use *RPT*s, learned on the observed attributes in the data, to predict class labels for use in the initial Gibbs labeling. Preliminary results indicate that this modification to the inference procedure reduces *RDN* loss by $10-15\%$ when there is 0% test set labeling. Alternatively, we could improve the *RDN* learning algorithm by using meta-knowledge about the test set to bias the feature selection process. For example, if we know that the model will be applied to an unlabeled test set, then we can bias the selective learning procedure to prefer attributes that will be known with certainty during the inference process.

Finally, to improve *RMN* performance, we need to improve inference when connectivity is high, either when there are large clusters or when overall linkage is dense. This may be achieved through the use of approximate inference techniques other than loopy belief propagation, or through the use of aggregate features in clique templates (that summarize cluster information) rather than using redundant pairwise features. Alternatively, when using pairwise clique templates in a densely connected dataset, it may be helpful to downsample the links in the graph to reduce inference bias.

CHAPTER 6

CONCLUSION

In this chapter, we summarize the contributions of this work and discuss areas for future work, including model extensions and new directions.

6.1 Contributions

In this thesis, we investigated the connections between autocorrelation and improvements in inference due to the use of probabilistic relational models and collective inference procedures. In particular, we explored the effects of data characteristics and representation choices on inference accuracy and investigated the mechanisms behind model performance.

First, we developed *RDN*s to model the joint distribution of attribute values in relational datasets. *RDN*s use pseudolikelihood estimation techniques to approximate the full joint distribution. This approximation enables a relatively simple approach to parameter estimation and structure learning in relational domains. We demonstrated the quality of the *RDN* approximation empirically over a range of data conditions, showing that if the models are learned from moderate to large datasets, the approximation is accurate. Furthermore, we proved that in the limit as dataset size grows to infinity, the pseudolikelihood approximation will be an unbiased estimate of the full joint distribution. *RDN* learning techniques offer a number of advantages over comparable *PRM*s. First, *RDN* learning is more efficient than both *RBN*s and *RMN*s. Second, *RDN* learning offers the first tractable means to learn relational au-

tocorrelation dependencies. Finally, *RDN* learning techniques can be used to learn parsimonious models, which improve inference efficiency and model interpretability.

Next, we developed *LGM*s to model the joint distribution of attributes and links in relational datasets. *LGM*s posit the existence of an underlying group structure to decouple attribute and link dependencies. The group structures are a low variance approach to modeling the dependencies among neighboring but unlinked instances (e.g., transitive relationships [36]), which improves performance by allowing sparse information to propagate in a more elaborate manner during inference. We demonstrated empirically that *LGM*s achieve superior performance over a range of data conditions, particularly when there is little information to seed the inference process.

Our analysis has explored the use of alternative approaches to representing and reasoning with relational autocorrelation dependencies. The experiments have demonstrated a unique property of relational data—there are a number of nearly equivalent representational choices for relational dependencies that exhibit different performance characteristics. This indicates that properties other than attribute correlation structure should be considered when choosing a model for relational datasets. Individual models (e.g., *RPT*s and *RBC*s) represent autocorrelation indirectly through the observed attributes of related instances. This approach will perform well when a single observed attribute is highly correlated with the class, otherwise it will difficult for the algorithms to cope with the increased dimensionality during learning. *RDN*s represent autocorrelation directly through the class labels of related instances. This approach will perform well when at least a portion of the test set is labeled—to anchor the model predictions so the remainder can be easily inferred with collective inference. *LGM*s represent autocorrelation indirectly through the properties of higher-level group structures, which connect members with autocorrelated labels. This approach will perform well when there is sparse test set information and the data exhibit clustering or long-range dependencies. In this case, the link structure

can be exploited to propagate the sparse information throughout the graph during collective inference.

Finally, we extended conventional bias/variance analysis to relational domains. Our bias/variance framework decomposes loss into aspects of both the learning and the inference processes to account for the additional error due to the use of collective inference techniques. We compared model performance on synthetic datasets with different graph characteristics and levels of autocorrelation, varying the availability of test set information. We demonstrated empirically that collective inference accounts for a significant portion of model error and that relative model performance varies significantly across different types of data graphs.

More specifically, our bias/variance analysis has shown the relational data characteristics that can impact model performance. Graph structure, autocorrelation dependencies, and amount of test set labeling, all affect relational model performance. *LGM*s are more robust to sparse labeling and perform well when graph clustering is high. When the underlying groups are small and linkage is low, *LGM*s experience high learning bias due to poor cluster identification. *RDN*s, applied with Gibbs sampling, experience high variance on test data with sparse labeling, but perform well across a wide range of graph structures. *RMN*s, applied with loopy belief propagation, have higher bias on densely connected graphs, but are more robust to sparse test set labeling. Our analysis has demonstrated the error introduced by the use of collective inference techniques and how that error varies across models and datasets. This suggests a number of directions to pursue to improve model performance—either by incorporating properties of the inference process into learning or through modification of the inference process based on properties of learning.

Overall, this work provides better models and tools for studying relational datasets—from the World Wide Web to biological domains; from fraud detection to citation analysis. Relational data offer unique opportunities to boost model accuracy and

improve decision-making quality if the algorithms can learn effectively from the additional information the relationships provide. A better understanding of probabilistic relational models, both in theoretical and practical terms, will enable improvements to the robustness, efficiency, and interpretability of relational models. Through this, we can extend the range, applicability, and performance gains of all relational models.

6.2 Future Work

There are a number of interesting avenues for future work that modify and extend the ideas presented in this thesis. We outline immediate areas of future study for each component first and then discuss farther reaching directions inspired by this thesis.

Our future work on *RDN*s will investigate modifications to the learning and inference procedures suggested by the bias/variance analysis. Bagging techniques [7] may be a means of reducing the variance of the RDN_{RPT} Gibbs sampling procedure. Calibration techniques [96] may improve the RDN_{RBC} probability estimates and reduce inference variance. In addition, averaging the estimates of multiple Gibbs chains may reduce variance while only incurring a moderate increase in computational cost. Future work will also compare *RDN*s to Markov logic networks in order to evaluate the performance tradeoffs for using pseudolikelihood approximations in structure learning techniques for different relational representations.

Our future work on *LGM*s will also investigate modifications and extensions suggested by the bias/variance analysis. In particular, alternative clustering techniques or an iterative sequential learning procedure may reduce the *LGM* learning bias on data where spectral clustering does not identify the best groupings. Also, to improve learning bias, we will investigate approaches to estimating the latent group structure and parameters jointly, perhaps incorporating a hierarchical Dirichlet process [91] to estimate k. However, a joint learning approach may increase both learning and inference variance due to the increased size of the model space. In addition, an evaluation

in the context of *interdependent samples* will compare LGMs and the use of identifiers attributes in *ACORA* [80]. We will evaluate the relative performance gains of each model when the samples have varying degrees of overlap and explore the utility of generalizing about group properties in these domains.

There are two directions that we will explore to improve on our initial work with the bias/variance framework. First, we intend to broaden our analysis to real data sets and evaluate algorithm modifications in these domains. This will lead towards a full characterization of the situations in which we can expect relational models to achieve superior performance. Next, we plan to extend the framework to analyze additional aspects of model performance. In particular, the analysis of alternative loss functions (e.g., zero-one) and analysis of errors when estimating the full joint (rather than marginals), will increase our understanding of model performance over a wider range of conditions. Also, examining interaction effects between learning and inference errors may help to inform the design of joint learning and inference procedures, which could significantly extend the performance gains of relational models.

In broader ranging future work, we plan to continue investigating the behavior of relational learning techniques, while developing new models and algorithms. A better understanding of the underlying principles of relational learning will drive the design of practical models and algorithms for a broad spectrum of tasks, changing the face of analysis in fields from homeland security to healthcare informatics.

One area of research suggested by the findings in this work, is the interaction between learning and inference in relational domains. To date, the majority of learning algorithms have been developed independently of inference algorithms.[1] However, we have shown there are multiple methods of representing the same relational dependencies. The choice of representation can impact performance through different aspects

[1]The recent work of Wainwright [92] is a notable exception.

of learning and inference. This indicates a potential interaction between the choice of representation for learning and the effectiveness of subsequent inference. A novel iterative procedure, where measures of inference accuracy and efficiency are used to bias the learning process, may improve relational model performance and broaden their applicability. Our bias-variance framework will facilitate the development of such techniques.

Another area for future work, is the use of underlying group structures to correct for biases in feature selection in relational data. Prior work has shown that features of instances with high degree and autocorrelation will have feature score distributions with increased variance due to lower effective sample sizes [40]. However, our work on *LGM*s also indicates that there is a connection between effective sample size and the underlying groups in the data, particularly when autocorrelation is high. This connection can be exploited to develop an efficient technique for unbiased feature selection that is appropriate for all likelihood-based relational models, by explicitly accounting for group structure in a graph-based resampling technique. This will enable efficient estimation of the variance of feature scores, which can be used to calculate the difference between *expected* and *observed* variance and then incorporated into an unbiased model selection framework.

6.3 Conclusion

In conclusion, this thesis has explored the connections between autocorrelation and improvements in inference due to the use of probabilistic relational models and collective inference procedures. We have examined autocorrelation as an exemplar of complex relational dependencies—involving cycles, redundant representations, and long-ranging correlations. We have shown that there are a number of ways to incorporate autocorrelation dependencies into *PRM*s in a tractable manner. The efficiency gains we obtain with the *RDN* pseudolikelihood approximation and the *LGM* decou-

pling of attribute and link dependencies will make relational modeling both practical and feasible in large, relational datasets where current methods are computationally intensive, if not intractable. We have also explored the performance characteristics of various relational models, attributing their errors to aspects of the models' learning and inference procedures. This is a first step towards a generalization of PRM characteristics—an investigation of the mechanisms behind performance and a determination of which situations additional complexity is warranted will lead towards a better theory of relational learning.

APPENDIX

A.1 Datasets

A.1.1 RDN Synthetic Data

Our RDN synthetic datasets are homogeneous data graphs with an autocorrelated class label and linkage due to an underlying (hidden) group structure. Each object has four boolean attributes: X_1, X_2, X_3 and X_4. We used the following generative process for a dataset with N_O objects and N_G groups:

For each object i, $1 \leq i \leq N_O$:

Choose a group g_i uniformly from the range $[1, N_G]$.

For each object j, $1 \leq j \leq N_O$:

For each object k, $j < k \leq N_O$:

Choose whether the two objects are linked from $p(E|G_j == G_k)$, a Bernoulli probability conditioned on whether the two objects are in the same group.

For each object i, $1 \leq i \leq N_O$:

Randomly initialize the values of $\mathbf{X} = \{X_1, X_2, X_3, X_4\}$ from a uniform prior distribution.

Update the values of $\mathbf{X}$ with 500 iterations of Gibbs sampling using the specified RDN.

The data generation procedure for $\mathbf{X}$ uses a simple RDN where X_1 is autocorrelated (through objects one link away), X_2 depends on X_1, and the other two attribute

have no dependencies. To generate data with autocorrelated X_1 values, we used manually specified conditional models for $p(X_1|\mathbf{X_1}_R, X_2)$. $RPT_{0.5}$ refers to the RPT CPD that is used to generate data with autocorrelation levels of 0.5. $RBC_{0.5}$ refers to the analogous RBC CPD. Detailed specifications of these models follow. Unless otherwise specified, the experiments use the settings below:

$$
\begin{aligned}
N_O &= 250 \\
N_G &= \frac{N_O}{10} \\
p(E|G_j{=}G_k) &= \{p(E{=}1|G_j{=}G_k) = 0.50;\ p(E{=}1|G_j{\neq}G_k) = \frac{1}{N_O}\} \\
RDN &=: [\, p(X_1|\mathbf{X_1}_R, X_2) = RPT_{0.5} \textit{ or } RBC_{0.5}; \\
&\qquad p(X_2|X_1) = \{p(X_2{=}1|X_1{=}1) = p(X_2{=}0|X_1{=}0) = 0.75\}; \\
&\qquad p(X_3 = 1) = p(X_4 = 1) = 0.50\,]
\end{aligned}
$$

We detail the manually specified conditional models used in Section 3.3.1. Specifically, there are three RBCs and three RPTs. Each one is designed to generate data with low, medium, or high levels of autocorrelation (0.25, 0.50, 0.75). The RBCs are specified below and the RPTs are specified in Figures A.1-A.3.

$$
\begin{aligned}
RBC :=\quad & p(X_1|\mathbf{X_1}_R, X_2) \propto \prod_R p(X_{1R}|X_1) \cdot p(X_2|X_1) \\
RBC_{0.25} :\quad & p(X_{1R}|X_1) := p(X_{1R}{=}1|X_1{=}1) = p(X_{1R}{=}0|X_1{=}0) = 0.5625 \\
& p(X_2|X_1) := p(X_2{=}1|X_1{=}1) = p(X_2{=}0|X_1{=}0) = 0.75 \\
RBC_{0.50} :\quad & p(X_{1R}|X_1) := p(X_{1R}{=}1|X_1{=}1) = p(X_{1R}{=}0|X_1{=}0) = 0.6250 \\
& p(X_2|X_1) := p(X_2{=}1|X_1{=}1) = p(X_2{=}0|X_1{=}0) = 0.75 \\
RBC_{0.75} :\quad & p(X_{1R}|X_1) := p(X_{1R}{=}1|X_1{=}1) = p(X_{1R}{=}0|X_1{=}0) = 0.6875 \\
& p(X_2|X_1) := p(X_2{=}1|X_1{=}1) = p(X_2{=}0|X_1{=}0) = 0.75
\end{aligned}
$$

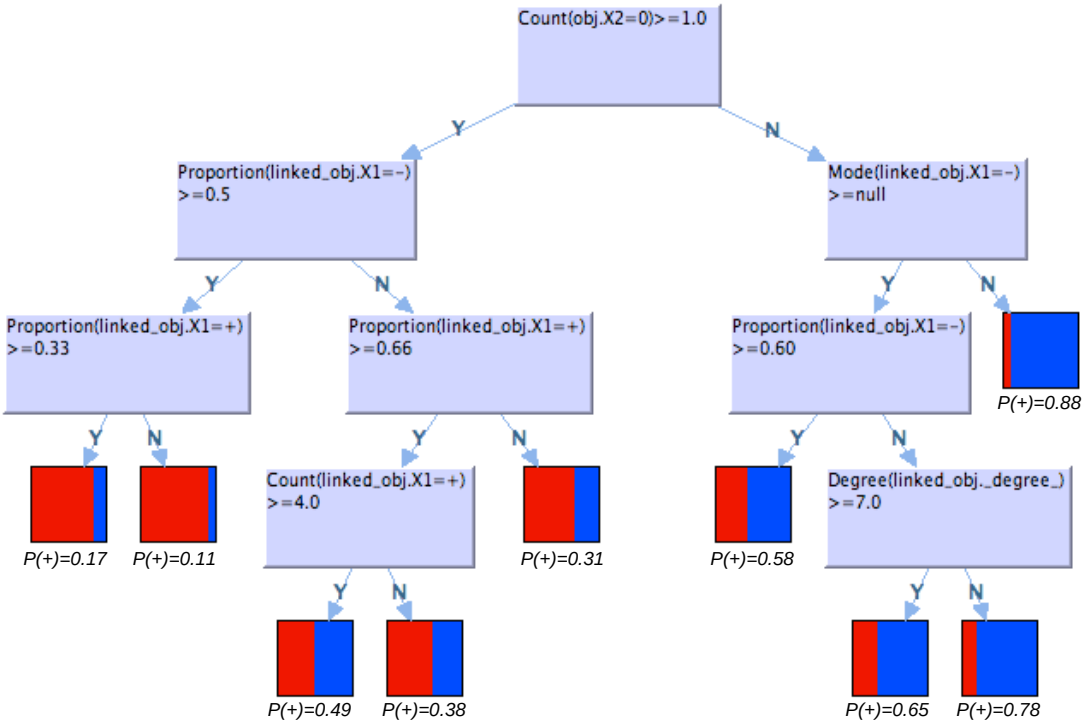

Figure A.1. $RPT_{0.25}$ used for synthetic data generation with low autocorrelation.

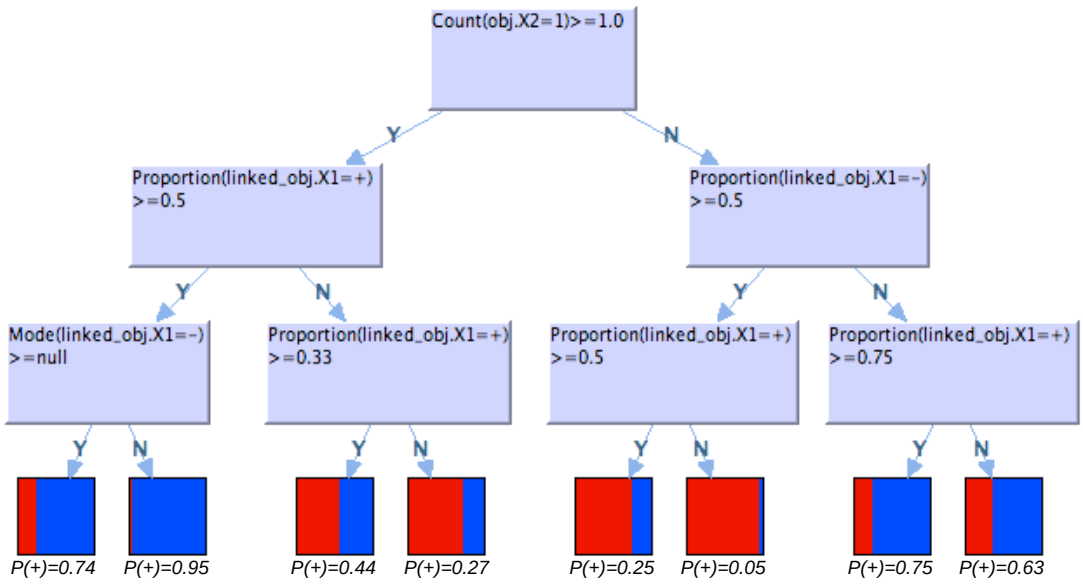

Figure A.2. $RPT_{0.50}$ used for synthetic data generation with medium autocorrelation.

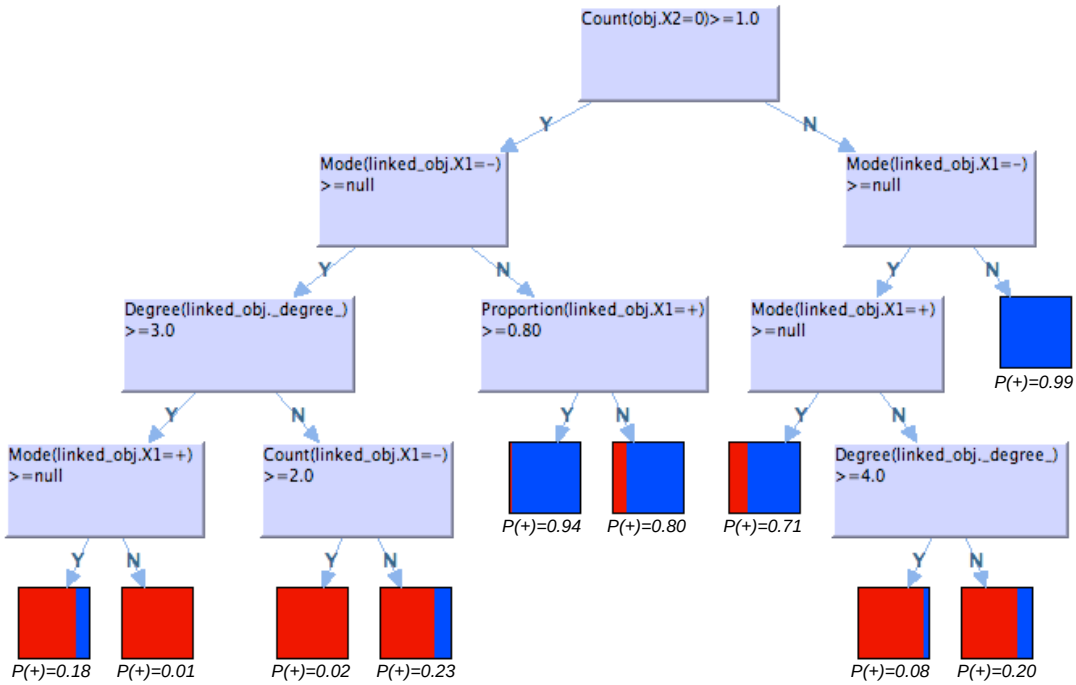

Figure A.3. $RPT_{0.75}$ used for synthetic data generation with high autocorrelation levels.

A.1.2 LGM Synthetic Data

Our *LGM* synthetic datasets are homogeneous data graphs with autocorrelation due to an underlying (hidden) group structure. Each object has a group G and four boolean attributes: X_1, X_2, X_3 and X_4. Each group has an associated attribute X_g. We used the following generative process to generate a dataset with N_O objects and G_S average group size:

For each group g, $1 \leq g \leq (N_G = N_O/G_S)$:

Choose a value for group attribute x_g from $p(X_g)$.

For each object i, $1 \leq i \leq N_O$:

Choose a group g_i uniformly from the range $[1, N_G]$.

Choose a class value X_{1i} from $p(X_1|X_g)$.

Choose a value for X_{2i} from $p(X_2|X_1)$.

Choose a value for X_{3i} from $p(X_3)$.

Choose a value for X_{4i} from $p(X_4)$.

For each object j, $1 \leq j \leq N_O$:

For each object k, $j < k \leq N_O$:

Choose whether the two objects are linked from $p(E|G_j == G_k)$.

The procedure uses a simple model where X_1 has an autocorrelation level of 0.5, X_2 depends on X_1, and the other two attributes have no dependencies. Unless otherwise specified, the experiments use the settings specified below.

$$
\begin{aligned}
N_O &= 250 \\
p(X_g) &= \{p(X_g{=}1) = 0.50; p(X_g{=}0) = 0.50\} \\
p(X_1|X_g) &= p(X_1{=}1|X_g{=}1){=}0.90; \\
&\quad\ p(X_1{=}0|X_g{=}0){=}0.90. \\
p(X_2|X_1) &= p(X_2{=}1|X_1{=}1){=}0.75; \\
&\quad\ p(X_2{=}0|X_1{=}0){=}0.75. \\
p(X_3{=}1) &= 0.50 \\
p(X_4{=}1) &= 0.50
\end{aligned}
$$

We generated data with two different groups sizes and levels of linkage:

$$
\begin{aligned}
G_S &: small = 5;\ large = 25 \\
L_{low}|G_S = small &: p(E{=}1|G_j{=}G_k) = 0.50;\ p(E{=}1|G_j{\neq}G_k) = 0.0008. \\
L_{high}|G_S = small &: p(E{=}1|G_j{=}G_k) = 0.80;\ p(E{=}1|G_j{\neq}G_k) = 0.004. \\
L_{low}|G_S = large &: p(E{=}1|G_j{=}G_k) = 0.20;\ p(E{=}1|G_j{\neq}G_k) = 0.0008. \\
L_{high}|G_S = large &: p(E{=}1|G_j{=}G_k) = 0.30;\ p(E{=}1|G_j{\neq}G_k) = 0.004.
\end{aligned}
$$

A.1.3 Real World Datasets

Figure A.4 depicts the objects and relations in each real-world dataset.

The first dataset is drawn from Cora, a database of computer science research papers extracted automatically from the web using machine learning techniques [60]. We selected the set of 4,330 machine-learning papers along with associated authors, cited papers, and journals. The resulting collection contains approximately 13,000

objects and 26,000 links. For classification, we sampled the 1669 papers published between 1993 and 1998.

On the Cora data, we learned an *RDN* for seven attributes. Author rank records ordering in paper authorship (e.g., first author, second author). Paper type records category information (e.g., PhD thesis, technical report); topic records content information (e.g., genetic algorithms, reinforcement learning); year and month record publication dates. Journal name-prefix records the first four title letters (e.g., IEEE, SIAM); book-role records type information (e.g., workshop, conference).

The second data set (Gene) is a relational data set containing information about the yeast genome at the gene and the protein level.[1] The data set contains information about 1,243 genes and 1,734 interactions among their associated proteins.

The Gene data contain attributes associated with both objects and links (i.e., interactions). We learned an *RDN* for seven attributes. Gene function records activities of the proteins encoded by the genes; location records each protein's localization in the cell; phenotype records characteristics of individuals with a mutation in the gene/protein; class records the protein type (e.g., transcription factor, protease); essential records whether the gene is crucial to an organism's survival. Interaction expression records the correlation between gene expression patterns for pairs of interacting genes; type records interaction characteristics (e.g., genetic, physical).

The third dataset is drawn from the Internet Movie Database (IMDb).[2] We collected a sample of 1,382 movies released in the United States between 1996 and 2001, with their associated actors, directors, and studios. In total, this sample contains approximately 42,000 objects and 61,000 links.

On the IMDb data, we learned an *RDN* for ten discrete attributes. First-movie-year records the date of the first movie made by a director or studio; has-award records

[1]See http://www.cs.wisc.edu/∼dpage/kddcup2001/.

[2]See http:// www.imdb.com.

whether a director or actor has won an Academy award; in-US records whether a studio is located in the US; receipts records whether a movie made more than $2 million in the opening weekend box office; genre records a movie's type (e.g., drama, comedy); hsx-rating records an actor's value on the Hollywood Stock Exchange (www.hsx.com); birth-year and gender record demographic information.

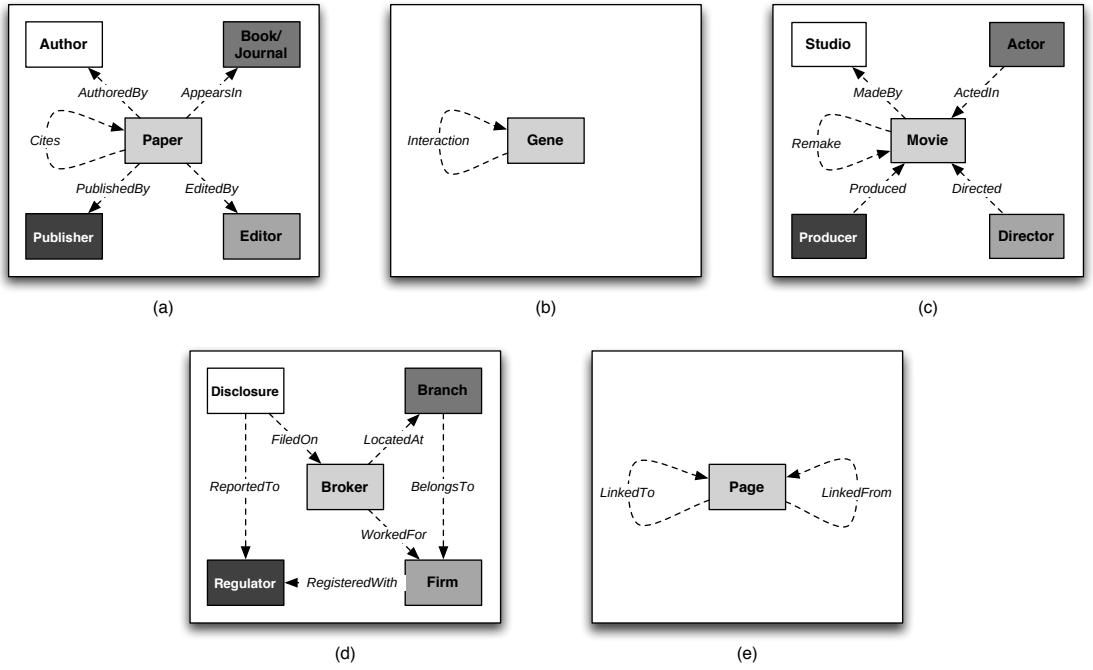

Figure A.4. Data schemas for (a) Cora, (b) Gene, (c) IMDb, (d) NASD, and (e) WebKB.

The fourth dataset is from the National Association of Securities Dealers (NASD) [66]. It is drawn from NASD's Central Registration Depository (CRD©) system, which contains data on approximately 3.4 million securities brokers, 360,000 branches, 25,000 firms, and 550,000 disclosure events. Disclosures record disciplinary information on brokers, including information on civil judicial actions, customer complaints, and termination actions. Our analysis was restricted to small and moderate-size firms with fewer than 15 brokers, each of whom has an approved NASD registration. We

selected a set of approximately 10,000 brokers who were active in the years 1997-2001, along with 12,000 associated branches, firms, and disclosures.

On the NASD data, we learned an *RDN* for eleven attributes. Firm size records the number of employed stockbrokers each year; layoffs records the number of terminations each year. On-watchlist records whether a firm or broker is under heightened supervision. Broker is-problem and problem-in-past record whether a broker is, or has been, involved in serious misconduct; has-business records whether a broker owns a business on the side. Disclosure type and year record category (e.g., customer complaint) and date information regarding disciplinary events (filed on brokers). Region and area record location information about branches.

The fifth data set was collected by the WebKB Project [12]. The data comprise 3,877 web pages from four computer science departments. The web pages have been manually labeled with the categories course, faculty, staff, student, research project, or other. The collection contains approximately 8,000 hyperlinks among the pages.

On the WebKB data, we learned an *RDN* for four attributes. School records page location (e.g., Cornell, Washington); label records page type (e.g., student, course); URL-server records the first portion of the server name following *www* (e.g., cs, engr); URL-text records the name of the first directory in the URL path (e.g., UTCS, department).

BIBLIOGRAPHY

[1] Anselin, L. *Spatial Econometrics: Methods and Models*. Kluwer Academic Publisher, The Netherlands, 1998.

[2] Bernstein, A., Clearwater, S., and Provost, F. The relational vector-space model and industry classification. In *Proceedings of the IJCAI-2003 Workshop on Learning Statistical Models from Relational Data* (2003), pp. 8–18.

[3] Besag, J. Spatial interaction and the statistical analysis of lattice systems. *Journal of the Royal Statistical Society, Series B 36*, 2 (1974), 192–236.

[4] Besag, J. Statistical analysis of non-lattice data. *The Statistician 24*, 3 (1975), 179–195.

[5] Blau, H., Immerman, N., and Jensen, D. A visual query language for relational knowledge discovery. Tech. Rep. 01-28, University of Massachusetts Amherst, Computer Science Department, 2001.

[6] Blei, D., Ng, A., and Jordan, M. Latent Dirichlet allocation. *Journal of Machine Learning Research 3* (2003), 993–1022.

[7] Breiman, L. Bagging predictors. *Machine Learning 24*, 2 (1996), 123–140.

[8] Casella, G., and Berger, R., Eds. *Statistical Inference*. Druxbury, 2002.

[9] Chakrabarti, S., Dom, B., and Indyk, P. Enhanced hypertext categorization using hyperlinks. In *Proceedings of the ACM SIGMOD International Conference on Management of Data* (1998), pp. 307–318.

[10] Comets, F. On consistency of a class of estimators for exponential families of Markov random fields on the lattice. *The Annals of Statistics 20*, 1 (1992), 455–468.

[11] Cortes, C., Pregibon, D., and Volinsky, C. Communities of interest. In *Proceedings of the 4th International Symposium of Intelligent Data Analysis* (2001), pp. 105–114.

[12] Craven, M., DiPasquo, D., Freitag, D., McCallum, A., Mitchell, T., Nigam, K., and Slattery, S. Learning to extract symbolic knowledge from the World Wide Web. In *Proceedings of the 15th National Conference on Artificial Intelligence* (1998), pp. 509–516.

[13] Cressie, N. *Statistics for Spatial Data.* John Wiley and Sons, Inc, New York, 1993.

[14] Davidson, D. The logical form of action sentences. In *The Logic of Decision and Action*, N. Rescher, Ed. University of Pittsburgh Press, 1967.

[15] Dempster, A., Laird, N., and Rubin, D. Maximum likelihood from incomplete data via the EM algorithm. *Journal of the Royal Statistical Society, Series B 39*, 1 (1977), 1–38.

[16] Domingos, P. A unified bias-variance decomposition for zero-one and squared loss. In *Proceedings of the 17th National Conference on Artificial Intelligence* (2000), pp. 564–569.

[17] Domingos, P., and Pazzani, M. On the optimality of the simple bayesian classifier under zero-one loss. *Machine Learning 29* (1997), 103–130.

[18] Domingos, P., and Richardson, M. Mining the network value of customers. In *Proceedings of the 7th ACM SIGKDD International Conference on Knowledge Discovery and Data Mining* (2001), pp. 57–66.

[19] Doreian, P. Network autocorrelation models: Problems and prospects. In *Spatial Statistics: Past, Present, and Future.* Ann Arbor Institute of Mathematical Geography, 1990, ch. Monograph 12, pp. pp. 369–389.

[20] Dzeroski, S., and Lavrac, N., Eds. *Relational Data Mining.* Springer-Verlag, 2001.

[21] Fawcett, T. ROC graphs: Notes and practical considerations for data mining researchers. Tech. Rep. HPL-2003-4, Hewlett-Packard Labs, 2003.

[22] Fawcett, T., and Provost, F. Adaptive fraud detection. *Data Mining and Knowledge Discovery 1*, 3 (1997), 291–316.

[23] Fayyad, U., Piatetsky-Shapiro, G., Smyth, P., and Uthurusamy, R., Eds. *Advances in Knowledge Discovery and Data Mining.* M.I.T. Press, 1996.

[24] Flach, P., and Lachiche, N. 1BC: A first-order Bayesian classifier. In *Proceedings of the 9th International Conference on Inductive Logic Programming* (1999), pp. 92–103.

[25] Friedman, J. On bias, variance, 0/1-loss, and the curse-of-dimensionality. *Data Mining and Knowledge Discovery 1*, 1 (1997), 55–77.

[26] Friedman, N., Getoor, L., Koller, D., and Pfeffer, A. Learning probabilistic relational models. In *Proceedings of the 16th International Joint Conference on Artificial Intelligence* (1999), pp. 1300–1309.

[27] Geman, S., Bienenstock, E., and Doursat, R. Neural networks and the bias/variance dilemma. *Neural Computation 4* (1992), 1–58.

[28] Geman, S., and Graffine, C. Markov random field image models and their applications to computer vision. In *Proceedings of the 1986 International Congress of Mathematicians* (1987), pp. 1496–1517.

[29] Getoor, L., Friedman, N., Koller, D., and Pfeffer, A. Learning probabilistic relational models. In *Relational Data Mining*. Springer-Verlag, 2001, pp. 307–335.

[30] Getoor, L., Friedman, N., Koller, D., and Taskar, B. Learning probabilistic models with link uncertainty. *Journal of Machine Learning Research 3* (2002), 679–707.

[31] Gidas, B. Consistency of maximum likelihood and pseudolikelihood estimators for Gibbs distributions. In *Proceedings of the Workshop on Stochastic Differential Systems with Applications in Electrical/Computer Engineering, Control Theory, and Operations Research* (1986), pp. 129–145.

[32] Goodman, L. Snowball sampling. *Annals of Mathematical Statistics 32* (1961), 148–170.

[33] Heckerman, D., Chickering, D., Meek, C., Rounthwaite, R., and Kadie, C. Dependency networks for inference, collaborative filtering and data visualization. *Journal of Machine Learning Research 1* (2000), 49–75.

[34] Heckerman, D., Meek, C., and Koller, D. Probabilistic models for relational data. Tech. Rep. MSR-TR-2004-30, Microsoft Research, 2004.

[35] Hill, S., Provost, F., and Volinsky, C. Network-based marketing: Identifying likely adopters via consumer networks. *Statistical Science 22*, 2 (2006).

[36] Hoff, P., Raftery, A., and Handcock, M. Latent space approaches to social network analysis. *Journal of the American Statistical Association 97* (2002), 1090–1098.

[37] Holte, R. Very simple classification rules perform well on most commonly used datatsets. *Machine Learning 11* (1993), 63–91.

[38] Jaeger, M. Relational Bayesian networks. In *Proceedings of the 13th Conference on Uncertainty in Artificial Intelligence* (1997), pp. 266–273.

[39] Jensen, D., and Neville, J. Autocorrelation and linkage cause bias in evaluation of relational learners. In *Proceedings of the 12th International Conference on Inductive Logic Programming* (2002), pp. 101–116.

[40] Jensen, D., and Neville, J. Linkage and autocorrelation cause feature selection bias in relational learning. In *Proceedings of the 19th International Conference on Machine Learning* (2002), pp. 259–266.

[41] Jensen, D., and Neville, J. Avoiding bias when aggregating relational data with degree disparity. In *Proceedings of the 20th International Conference on Machine Learning* (2003), pp. 274–281.

[42] Jensen, D., Neville, J., and Gallagher, B. Why collective inference improves relational classification. In *Proceedings of the 10th ACM SIGKDD International Conference on Knowledge Discovery and Data Mining* (2004), pp. 593–598.

[43] Jordan, M. Graphical models. *Statistical Science 19* (2004), 140–155.

[44] Kemp, C., Griffiths, T., and Tenenbaum, J. Discovering latent classes in relational data. Tech. Rep. AI Memo 2004-019, Massachusetts Institute of Technology, 2004.

[45] Kersting, K. Representational power of probabilistic-logical models: From upgrading to downgrading. In *IJCAI-2003 Workshop on Learning Statistical Models from Relational Data* (2003), pp. 61–62.

[46] Kersting, K., and Raedt, L. De. Basic principles of learning Bayesian logic programs. Tech. Rep. 174, Institute for Computer Science, University of Freiburg, 2002.

[47] Kleinberg, J. Authoritative sources in a hyperlinked environment. In *Proceedings of the 9th ACM SIAM Symposium on Discrete Algorithms* (1998), pp. 25–27.

[48] Kok, S., and Domingos, P. Learning the structure of Markov logic networks. In *Proceedings of the 22nd International Conference on Machine Learning* (2005), pp. 441–448.

[49] Kramer, S., Lavrac, N., and Flach, P. Propositionalization approaches to relational data mining. In *Relational Data Mining*. Springer-Verlag, 2001, pp. 262–291.

[50] Kubica, J., Moore, A., Schneider, J., and Yang, Y. Stochastic link and group detection. In *Proceedings of AAAI/IAAI 2002* (2002), pp. 798–806.

[51] Lafferty, J., McCallum, A., and Pereira, F. Conditional random fields: Probabilistic models for segmenting and labeling sequence data. In *Proceedings of the 18th International Conference on Machine Learning* (2001), pp. 282–289.

[52] Lauritzen, S., and Sheehan, N. Graphical models for genetic analyses. *Statistical Science 18*, 4 (2003), 489–514.

[53] Lehmann, E., and Casella, G. *Theory of Point Estimation*. Springer-Verlag, New York, 1998.

[54] Lu, Q., and Getoor, L. Link-based classification. In *Proceedings of the 20th International Conference on Machine Learning* (2003), pp. 496–503.

[55] Macskassy, S., and Provost, F. A simple relational classifier. In *Proceedings of the 2nd Workshop on Multi-Relational Data Mining, KDD2003* (2003), pp. 64–76.

[56] Macskassy, S., and Provost, F. Classification in networked data: A toolkit and a univariate case study. Tech. Rep. CeDER-04-08, Stern School of Business, New York University, 2004.

[57] Marsden, P., and Friedkin, N. Network studies of social influence. *Sociological Methods and Research 22*, 1 (1993), 127–151.

[58] McCallum, A. Efficiently inducing features of conditional random fields. In *Proceedings of the 19th Conference on Uncertainty in Artificial Intelligence* (2003), pp. 403–410.

[59] McCallum, A., Corrada-Emmanuel, A., and Wang, X. Topic and role discovery in social networks. In *Proceedings of the 19th International Joint Conference on Artificial Intelligence* (2005), pp. 786–791.

[60] McCallum, A., Nigam, K., Rennie, J., and Seymore, K. A machine learning approach to building domain-specific search engines. In *Proceedings of the 16th International Joint Conference on Artificial Intelligence* (1999), pp. 662–667.

[61] McPherson, M., Smith-Lovin, L., and Cook, J. Birds of a feather: Homophily in social networks. *Annual Review of Sociology 27* (2001), 415–445.

[62] Milch, B., Marthi, B., Sontag, D., Russell, S., Ong, D., and Kolobov, A. Approximate inference for infinite contingent Bayesian networks. In *Proc. of the 10th International Workshop on Artificial Intelligence and Statistics* (2005), pp. 238–245.

[63] Mirer, T. *Economic Statistics and Econometrics*. Macmillan Publishing Co, New York, 1983.

[64] Murphy, K., Weiss, Y., and Jordan, M. Loopy belief propagation for approximate inference: An empirical study. In *Proceedings of the 15th Conference on Uncertainty in Artificial Intelligence* (1999), pp. 467–479.

[65] Neal, R. Probabilistic inference using Markov chain Monte Carlo methods. Tech. Rep. CRG-TR-93-1, Dept of Computer Science, University of Toronto, 1993.

[66] Neville, J., Şimşek, O., Jensen, D., Komoroske, J., Palmer, K., and Goldberg, H. Using relational knowledge discovery to prevent securities fraud. In *Proceedings of the 11th ACM SIGKDD International Conference on Knowledge Discovery and Data Mining* (2005), pp. 449–458.

[67] Neville, J., and Jensen, D. Iterative classification in relational data. In *Proceedings of the Workshop on Statistical Relational Learning, 17th National Conference on Artificial Intelligence* (2000), pp. 42–49.

[68] Neville, J., and Jensen, D. Supporting relational knowledge discovery: Lessons in architecture and algorithm design. In *Proceedings of the Data Mining Lessons Learned Workshop, ICML2002* (2002), pp. 57–64.

[69] Neville, J., and Jensen, D. Collective classification with relational dependency networks. In *Proceedings of the 2nd Multi-Relational Data Mining Workshop, KDD2003* (2003), pp. 77–91.

[70] Neville, J., and Jensen, D. Dependency networks for relational data. In *Proceedings of the 4th IEEE International Conference on Data Mining* (2004), pp. 170–177.

[71] Neville, J., and Jensen, D. Leveraging relational autocorrelation with latent group models. In *Proceedings of the 4th Multi-Relational Data Mining Workshop, KDD2005* (2005).

[72] Neville, J., and Jensen, D. Leveraging relational autocorrelation with latent group models. In *Proceedings of the 5th IEEE International Conference on Data Mining* (2005), pp. 322–329.

[73] Neville, J., and Jensen, D. Bias/variance analysis for network data. In *Proceedings of the Workshop on Statistical Relational Learning, 23rd International Conference on Machine Learning* (2006).

[74] Neville, J., and Jensen, D. Relational dependency networks. *Journal of Machine Learning Research* (2006), to appear.

[75] Neville, J., Jensen, D., Friedland, L., and Hay, M. Learning relational probability trees. In *Proceedings of the 9th ACM SIGKDD International Conference on Knowledge Discovery and Data Mining* (2003), pp. 625–630.

[76] Neville, J., Jensen, D., and Gallagher, B. Simple estimators for relational Bayesian classifers. In *Proceedings of the 3rd IEEE International Conference on Data Mining* (2003), pp. 609–612.

[77] Nowicki, K., and Snijders, T. Estimation and prediction for stochastic blockstructures. *Journal of the American Statistical Association 96* (2001), 1077–1087.

[78] Pearl, J., Ed. *Probabilistic Reasoning In Intelligent Systems: Networks of Plausible Inference*. Morgan Kaufmann, 1988.

[79] Perlich, C., and Provost, F. Aggregation-based feature invention and relational concept classes. In *Proceedings of the 9th ACM SIGKDD International Conference on Knowledge Discovery and Data Mining* (2003), pp. 167–176.

[80] Perlich, C., and Provost, F. Acora: Distribution-based aggregation for relational learning from identifier attributes. *Machine Learning 62*, 1/2 (2006), 65–105.

[81] Popescul, A., and Ungar, L. Cluster-based concept invention for statistical relational learning. In *Proceedings of the 10th ACM SIGKDD International Conference on Knowledge Discovery and Data Mining* (2004), pp. 665–670.

[82] Popescul, A., Ungar, L., Lawrence, S., and Pennock, D. Statistical relational learning for document mining. In *Proceedings of the 3rd IEEE International Conference on Data Mining* (2003), pp. 275–282.

[83] Richardson, M., and Domingos, P. Markov logic networks. *Machine Learning 62* (2006), 107–136.

[84] Sachs, L. *Applied Statistics*. Springer-Verlag, 1992.

[85] Sanghai, S., Domingos, P., and Weld, D. Dynamic probabilistic relational models. In *Proceedings of the 18th International Joint Conference on Artificial Intelligence* (2003), pp. 992–1002.

[86] Shi, J., and Malik, J. Normalized cuts and image segmentation. *IEEE Transactions on Pattern Analysis and Machine Intelligence 22*, 8 (2000), 888–905.

[87] Slattery, S., and Mitchell, T. Discovering test set regularities in relational domains. In *Proceedings of the 17th International Conference on Machine Learning* (2000), pp. 895–902.

[88] Stahl, I. Predicate invention in inductive logic programming. In *Advances in Inductive Logic Programming*. 1996, pp. 34–47.

[89] Taskar, B., Abbeel, P., and Koller, D. Discriminative probabilistic models for relational data. In *Proceedings of the 18th Conference on Uncertainty in Artificial Intelligence* (2002), pp. 485–492.

[90] Taskar, B., Segal, E., and Koller, D. Probabilistic classification and clustering in relational data. In *Proceedings of the 17th International Joint Conference on Artificial Intelligence* (2001), pp. 870–878.

[91] Teh, Y., Jordan, M., Beal, M., and Blei, D. Hierarchical Dirichlet processes. *Journal of the American Statistical Association* (2006), to appear.

[92] Wainwright, M. Estimating the "wrong" Markov random field: Benefits in the computation-limited setting. In *Advances in Neural Information Processing Systems* (2005).

[93] White, H. *Estimation, Inference and Specification Analysis*. Cambridge University Press, New York, 1994.

[94] Wolfe, A., and Jensen, D. Playing multiple roles: Discovering overlapping roles in social networks. In *Proceedings of the Workshop on Statistical Relational Learning, 21st International Conference on Machine Learning* (2004).

[95] Yang, Y., Slattery, S., and Ghani, R. A study of approaches to hypertext categorization. *Journal of Intelligent Information Systems 18*, 2-3 (2002), 219–241.

[96] Zadrozny, B., and Elkan, C. Obtaining calibrated probability estimates from decision trees and naive Bayesian classifiers. In *Proceedings of the 18th International Conference on Machine Learning* (2001), pp. 609–616.